



**CZECH TECHNICAL UNIVERSITY IN PRAGUE**

---

**Faculty of Transportation Sciences  
Department of Mechanics and Materials**

**NUMERICAL SIMULATION OF IMPACT WITH BARRIERS**

Master's Thesis

Study Programme: Intelligent Transport Systems

Thesis supervisor: doc. Ing. Michal Micka, CSc.

**Raissa Likhonina**

---

**Prague, 2015**



**K618 ..... Ústav mechaniky a materiálů**

**ZADÁNÍ DIPLOMOVÉ PRÁCE**  
(PROJEKTU, UMĚLECKÉHO DÍLA, UMĚLECKÉHO VÝKONU)

Jméno a příjmení studenta (včetně titulů):

**Raissa Likhonina**

Kód studijního programu a studijní obor studenta:

**N 3710 – IS – Inteligentní dopravní systémy**

Název tématu (česky): **Numerická simulace nárazu do svodidla**

Název tématu (anglicky): Numerical simulation of impact with the barriers

**Zásady pro vypracování**

Při zpracování diplomové práce se řiďte osnovou uvedenou v následujících bodech:

- V obecné části uvést přehled svodidel používaných v ČR, uvést základní technické podmínky pro jejich používání a příklady technického řešení.
- Uvést způsoby numerické simulace chování svodidla při nárazu dopravním prostředkem a použité programy pro pružnoplastický výpočet pro kvazistatické zatížení a výpočet pro zatížení rázem.
- Vypracovat geometrický model jednoho pole svodidla a provést analýzu rázového děje při nárazu tělesa na svodidlo. Pro simulaci děje použít programy ANSYS a LS DYNA.
- Provést rozbor výsledků

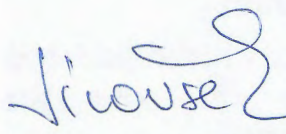

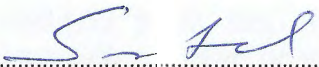
- Rozsah grafických prací: dle potřeby v textu nebo v příloze
- Rozsah průvodní zprávy: minimálně 55 stran textu (včetně obrázků, grafů a tabulek, které jsou součástí průvodní zprávy)
- Seznam odborné literatury: ČSN EN 1317-2 Část 2: Svodidla a mostní svodidla  
ČSN EN 1317-3 Část 3: Tlumiče nárazu  
ČSN EN 1317-+A1 Část 5: Požadavky na výrobky a posuzování shody zachytných systémů pro vozidla  
ANSYS Users manual  
LS DYNA Pre-post manual

Vedoucí diplomové práce: **doc. Ing. Michal Micka, CSc.**

Datum zadání diplomové práce: **9. června 2014**  
(datum prvního zadání této práce, které musí být nejpozději 10 měsíců před datem prvního předpokládaného odevzdání této práce vyplývajícího ze standardní doby studia)

Datum odevzdání diplomové práce: **31. května 2015**

- a) datum prvního předpokládaného odevzdání práce vyplývající ze standardní doby studia a z doporučeného časového plánu studia  
b) v případě odkladu odevzdání práce následující datum odevzdání práce vyplývající z doporučeného časového plánu studia

    
.....  
prof. Ing. Ondřej Jiroušek, Ph.D. prof. Dr. Ing. Miroslav Svítek  
vedoucí děkan fakulty  
Ústavu mechaniky a materiálů

Potvrzuji převzetí zadání diplomové práce.

  
.....  
Rassa Likhonina  
jméno a podpis studenta

V Praze dne..... 9. června 2014

**Declaration:**

I do not have a compelling reason against the use of this school work within the intention of §60 of the Act No. 121/2000 Coll., on Copyright and Rights Related to Copyright and on Amendment to Certain Acts (Copyright Act).

Hereby I declare that I have elaborated this thesis independently under the supervision of my supervisor, using information sources listed in the bibliography in accordance with Ethical guidelines for writing the master's theses.

In Prague \_\_\_\_\_

Name \_\_\_\_\_

**Acknowledgement:**

I would like to express my gratitude to my supervisor doc. Ing. Michal Micka, CSc. for his useful comments, valuable advices and engagement through the learning process of this master thesis. I would also like to thank my family for their support during my study.

In Prague \_\_\_\_\_

Name \_\_\_\_\_

**NÁZEV:**

Numerická simulace nárazu do svodidla

**AUTOR:**

Bc. Raissa Likhonina

**KATEDRA (ÚSTAV):**

Ústav mechaniky a materiálů, K618

**VEDOUCÍ PRÁCE:**

doc. Ing. Michal Micka, CSc.

**Abstrakt:**

Hlavním cílem dané práce je provedení numerické simulace v programovém prostředí ANSYS LS-DYNA. Pro tyto účely byly zvoleny dva typy silničních svodidel s úrovní zadržení H2: JSNH4/H2 a JSAM-2/H2. Cíl dané práce úzce souvisí s dílčími úkoly, mezi kterými je sestavení výpočtových modelů, nastavení příslušných parametrů modelů, provedení výpočtů, vyhodnocení a porovnání dosažených výsledků. V dané práci byly použity programy ANSYS Workbench a LS-DYNA. Na základě stanovené síly nárazu, výsledného průhybu jednotlivých částí konstrukce a vypočtené vnitřní energie bylo provedeno vyhodnocení výsledků.

**Klíčová slova:**

metoda konečných prvků, nelineární vlastnosti, výpočtový model, okrajové podmínky, pružně-plastická deformace, úroveň zadržení, pracovní šířka, dynamický průhyb, pracovní diagram, Workbench, LS-DYNA

**TITLE:**

Numerical simulation of impact with barriers

**AUTHOR:**

Bc. Raissa Likhonina

**DEPARTMENT:**

Department of Mechanics and Materials, K618

**SUPERVISOR:**

doc. Ing. Michal Micka, CSc.

**Abstract:**

The main aim of the present master's thesis is to perform numerical simulation in ANSYS LS-DYNA. For these purposes two types of safety barriers are used: JSNH4/H2 and JSAM-2/H2. The aim is closely connected with such objectives as safety barrier geometrical model creation, setting parameters of crash tests, calculation performance, data analysis and results evaluation. In this work ANSYS Workbench and LS-DYNA have been used. On the basis of impact forces, body displacement and internal energy obtained during numerical simulation the results evaluation is fulfilled.

**Keywords:**

finite element method, non-linear characteristics, numerical model, boundary conditions, elastic and plastic deformation, containment level, working width, dynamic deflection, stress-strain curve, Workbench, LS-DYNA

# Content

Content.....	6
List of abbreviations.....	7
List of symbols.....	9
1. Introduction.....	10
2. Theoretical part.....	17
2.1. General information.....	17
2.1.1. Classification of road restraint systems.....	17
2.1.2. Basic parameters.....	27
2.1.3. Steel safety barriers.....	36
2.1.3.1. History.....	36
2.1.3.2. Steel safety barriers installation on road infrastructure.....	39
2.2. Numerical simulation and selected types of road safety barriers.....	47
2.2.1. Numerical simulation.....	47
2.2.1.1. Crash tests, calculations and numerical simulation.....	47
2.2.1.2. ANSYS Workbench and LS-DYNA.....	50
2.2.2. Types of safety barriers under analysis.....	52
2.2.2.1. Safety barrier JSNH4/H2.....	52
2.2.2.2. Safety barrier JSAM-2/H2.....	63
3. Practical part.....	72
3.1. Creation of geometrical models in ANSYS Workbench.....	73
3.2. Definition of geometrical model properties and numerical simulation parameters in LS-DYNA PrePost.....	87
3.3. Calculation in LS-DYNA and evaluation of obtained results.....	104
3.4. Comparison of obtained results for JSNH4/H2 and JSAM-2/H2.....	141
4. Conclusion.....	145
Bibliography.....	147
List of terminology.....	154
List of figures.....	157
List of tables.....	162



# List of abbreviations

Abbreviation	Definition
AMDS CR	ArcelorMittal Distribution Solutions Czech Republic s.r.o.
APDL	ANSYS Parametric Design Language
ASI	Acceleration Severity Index
CAD model	Computer-Aided Design model
BSORT	number of cycles between Bucket sorts
BT	Birth Time
DAGG	maximum aggregate size
DC	exponential Decay Coefficient
DOF	Degrees Of Freedom
DT	Death Time
ERF	European Union Road Federation
FD	dynamic coefficient of friction
FEM	Finite Element Method
FPC	unconfined compression strength
FRCFRQ	number of cycles between contact force updates
FS	static coefficient of friction
FSF	Coulomb friction scale factor
FTYPE	formulation flag
HGV	Heavy Goods Vehicles
HSLA	High Strength Low Alloy
INCRE	maximum strain increment for subincrementation
ITRETRC	cap retraction
LCIDAB	load curve ID defining airbag thickness
MAXPAR	maximum parametric coordinate in segment search
MBOXID	master segments within specified box
MPR	master side forces
MST	optional thickness for master surface
MSTYP	Master Segment Type
PHD index	Post-impact Head Deceleration index
PRED	pre-existing damage
SBOPT	segment-based contact option
SBOXID	slave segments within specified box

<b>SFM</b>	master penalty stiffness
<b>SFMT</b>	scale factor for master surface thickness
<b>SFS</b>	slave penalty stiffness
<b>SFST</b>	scale factor for slave surface thickness
<b>SOFT</b>	soft constraint option
<b>SOFSCCL</b>	scale factor for constraint forces of soft constraint option
<b>SST</b>	optional thickness for slave surface
<b>SPR</b>	slave side forces
<b>SSTYP</b>	<b>Slave Segment Type</b>
<b>THIV</b>	<b>Theoretical Head Impact Velocity</b>
<b>TKP</b>	Technical Quality Conditions ( <b>T</b> echnické <b>K</b> valitativní <b>P</b> odmínky)
<b>TP</b>	Technical Conditions ( <b>T</b> echnické <b>P</b> odmínky)
<b>TZÚS</b>	Technical and Test Institute for Construction in Prague ( <b>T</b> echnický a <b>Z</b> kušební <b>Ú</b> stav <b>S</b> tavební Praha)
<b>VCDI</b>	<b>Vehicle Cockpit Deformation Index</b>
<b>VC</b>	coefficient for viscous friction
<b>VDC</b>	viscous damping coefficient
<b>VEC</b>	vectorization flag
<b>VSF</b>	viscous friction scale factor

# List of symbols

Symbol	Definition	Units of measurement
<b>a</b>	vehicle acceleration	[m/s <sup>2</sup> ]
<b>D<sub>m</sub></b>	dynamic deflection	[m]
<b>E<sub>k</sub></b>	kinetic energy	[kJ]
<b>E</b>	Young modulus	[Pa]
<b>E<sub>s</sub></b>	kinetic energy of a vehicle obtained while solving symmetric task	[kJ]
<b>E<sub>t</sub></b>	total kinetic energy of a vehicle	[kJ]
<b>F<sub>s</sub></b>	impact force	[kN]
<b>G</b>	initial shear modulus	[Pa]
<b>h</b>	height	[m]
<b>L<sub>0</sub></b>	minimum elongation	[%]
<b>m</b>	vehicle mass	[kg]
<b>M<sub>m</sub></b>	measured total weight	[kg]
<b>M<sub>t</sub></b>	specified total weight	[kg]
<b>r</b>	radius	[m]
<b>ReH</b>	minimum yield strength	[MPa]
<b>Rm</b>	tensile strength	[MPa]
<b>S<sub>0</sub></b>	area	[m <sup>2</sup> ]
<b>v<sub>ct</sub></b>	initial calculated test speed	[m/s]
<b>v<sub>st</sub></b>	speed specified in standards	[m/s]
<b>V</b>	volume	[m <sup>3</sup> ]
<b>V<sub>I<sub>m</sub></sub></b>	vehicle deflection	[m]
<b>V<sub>t</sub></b>	specified speed	[m/s]
<b>V<sub>m</sub></b>	measured speed	[m/s]
<b>W<sub>m</sub></b>	working width	[m]
<b>W<sub>u</sub></b>	non-deformed width of the system	[m]
<b>α<sub>m</sub></b>	measured angle	[°]
<b>α<sub>t</sub></b>	specified angle	[°]
<b>ε</b>	plastic strain	[-]
<b>ρ</b>	mass density	[kg/m <sup>3</sup> ]
<b>σ</b>	stress	[MPa]

# 1. Introduction

In our century of a rapid development of automotive industry and increasing number of vehicles the issues of all road users' safety become more and more acute.

For the majority of people the vehicles have become an integral part of their lives. It is not surprising as it is conditioned by the peculiarities of our epoch, which demands from us to be faster, more flexible and "moving", to use our time more efficiently. We need our "steel friends" (both public and individual means of transportation) to take us to and from school, work or some recreational places and we cannot imagine our life without them.

People are used to using public transport and cannot manage without it. On the other hand more and more people can afford themselves to have their own vehicles, which mean greater comfort and flexibility. Moreover, currently many families have more than one vehicle and the number of such families is growing. With all benefits this fact brings with it there are several problems needed to be solved. Among them there are traffic jams, air pollution and traffic accidents, which result in injuries and fatal cases.

Day by day engineers try to find the ways to decrease the number of accidents and to mitigate their causes. Thus, safety systems aimed at preventing accidents (active safety systems) and aimed at eliminating the causes of accidents (passive safety systems) become more and more sophisticated. Owing to it though with vast motorization the number of traffic accidents is growing their severity has experienced a relative decrease.

It is worth to mention that the credit for vehicles becoming safer should be paid to new methods applied while designing and testing technical innovations. Nowadays numerical simulation using finite element methods (FEM) is commonly and widely used in automotive industry [23]. These simulations can distinctly help when there is a need, for example, to define deformation areas of cars and their safety elements able to eliminate fatal injuries when accidents take place.

Unfortunately, application of numerical simulation, which is proved to be successful in automobile sphere, is not so common for passive safety systems on the roads themselves, i.e. for road safety restraint systems. One of the problem is that there is no unique methodology, how to use numerical simulation in this particular area [23]. Currently all safety barriers for permanent and repeat usage on the roads have to be tested in real crash tests [20]. The methods and all corresponding specifications in preparing, performing crash tests

and evaluating obtained results are specified in ČSN EN 1317 standards. It is clear enough that test preparation and testing itself is both expensive and time consuming. According to relevant standards each type of a safety barrier is required to be tested with several types of crash tests. Moreover, we should remember that during real crash tests it is not possible to take into account all parameters and situations, which could occur. It is well known that there will be always some deviations from test to test. Therefore, numerical simulation with application of highly sophisticated programmes using FEM analysis can present a very powerful tool and be of a great support for performing real crash tests, thus, contributing in correct and accurate design and construction of safety barriers. Then using numerical simulation we will be able to some degree to predict the behavior of a certain type of a safety barrier subject to test and even more - using results of one crash test we will be able to simulate a wide range of impacts with different parameters (e.g. different angles of an impact, velocity etc.) and various types of cars.

Due to mentioned advantages numerical simulation can bring the interest to this method is increasing. There exists a wide range of different literature, which describes the numerical simulation using LS-DYNA programme and based on FEM principles. These papers are really different as far as their subjects of investigation and main objectives are concerned. Some of them, for example, are devoted to testing of new types of safety barriers, which are made of a new material and which are not used on real roads yet [31], [61]. Other works describe simulation of impacts on bridge barriers or even on rockfall barriers [59]. In this connection we would like to mention only several papers studying the problem of numerical simulation of a vehicle impact on a safety barrier.

One of the earliest publications in this area is a work by Gruber K., Herrmann M. and Pitzer M., where already in 1991 the authors described a computer simulation of a side impact using different mobile barriers [29]. They tried to prove that the numerical simulation of crash processes and explicit finite element codes like DYNA3D could provide an efficient and promising tool for the analysis of deformation behavior of structural components and permit profound studies of different variants at early stages of the design process [29]. But at this time the idea did not seem to be much realistic, because computers were not powerful enough and simulation programmes were not sophisticated enough for these particular purposes.

The situation has changed since then and it results in growing number of different publications in this field.

One of the most recent papers is a work by Mr. Borovinšek from Slovenia, who uses simulation for designing optimal reinforcement of an existing crash barrier common in Slovenia [15]. He uses explicit finite element program LS-DYNA. Simulation has proved to be quite a success, because, as the author writes, it gives almost the same results as real crash test held on [15].

Another example is a publication by Mr. Ulker and Mr. Rahman, "Traffic Barriers under Vehicular Impact from Computer Simulation to Design Guidelines", where the problem of a vehicular impact on a portable concrete barrier is investigated [56]. The achievement of this work is in the fact, that the results from FE simulation and the rigid body model are found to be consistent and in good agreement with the full-scale crash test. Therefore, the charts, which are made from the obtained results and aimed for assessing the barrier displacement, are claimed to be useful for the purpose of design of crash barriers of this type.

Zike S., Kalkins K., Ozolins O. apply finite element code LS-DYNA for other purposes. In their work they consider the application of composite materials in road safety barriers with the help of a numeric model of a glass fiber/polymer composite [61].

Another interesting work concerning safety enhancement of a water-filled road safety barrier using interaction of composite materials is presented by Thiyahiddini M. I. M., Thambiratnam D., Gu Y. T. and Gover R. [55].

Borkowski W., Hryciów Z., Rybak P., Wysocki J. and Wisniewski A. use numerical simulation in LS-DYNA to evaluate the effectiveness of the innovative road safety system equipped with prototype component segments composed of a body made of a plastic filled with reinforced concrete. They assess test results of simulation on the basis of ASI, THIV and PHD index and conclude that a new system meets the normative requirements [14].

Similar investigations are made all round the world: in Italy [13], in Korea [31], in China [30], in the USA [19], [18], in Romania [25] and so on. And the authors of such publications have come to a similar conclusion, that the numerical simulation is a very helpful tool for design and construction as well as testing of crash barriers.

At this point we afford ourselves to mention one more interesting work, which has been held in Czech Republic and authored by Ing. J. Drozda and doc. Ing. T. Rotter from Czech Technical University in Prague. In their work they describe numerical analysis for design and testing of bridge barriers. The authors use FEM with explicit time integration and prove that this method can be used for development and innovation of safety barrier systems [24].

In his other work, "Methodology of validation of FE Model for simulations of real crash tests", Drozba J. tries to determine a method that leads to creation of a validated finite element model before performing the full scale crash test [23]. He performs a non-linear dynamic impact simulation on this model in LS-DYNA. The author claims, that the methodology described in his paper, should help to improve accuracy of FE model used for a non-linear dynamic impact simulation, what in its turn would help to reduce necessary costs for developing new safety barriers [23]. For his simulation Mr. Drozba uses two types of vehicles - a passenger car and a lorry - and refers to a book by H. Ray, M. "Procedures for Verification and Validation of Computer Simulations Used for Roadside Safety Applications" [39].

From all these we can see that the area of investigation in this sphere is already well described, though the unique methods are not yet defined and commonly accepted. In our paper we will try to look at the application of numerical simulation from a slightly different point of view than those being described in above mentioned publications. All these works are devoted to simulation of a dynamic impact on the barrier and then to evaluation of the effectiveness of this simulation. However, our first objective is to compare two possible means of analyzing a crash barrier, that is simulation of static tests (loading with static force) using ANSYS Workbench and simulation of dynamic tests (a vehicle impact) using ANSYS LS-DYNA. Our next step is comparison of two types of crash barriers used on the roads of Czech Republic and, therefore, if possible, demonstration that a new type has certain benefits in comparison with the old one as the manufacturer claims it should have. Surely while evaluating the obtained results we will provide analysis to find out whether simulation results are in compliance with those obtained in the full-scale crash tests and specified by the manufacturer in technical documentation.

Therefore, we can possibly describe the subject of the present work as road restraint systems, being more precise - steel safety barriers. From a great range of different steel safety barriers two types have been taken for our analysis (both of the same manufacturer): JSNH4/H2 and JSAM-2/H2. The latter is a new type, which is claimed to have several benefits over JSNH4/H2.

It is worth to mention that the present master's thesis is closely connected with the bachelor thesis and is actually its continuation. If we could shortly describe our bachelor thesis, we would say that in it the numerical simulation of static tests (loading with static force) of a steel crash barrier using ANSYS Workbench has been made [32]. For these purposes we have selected a safety barrier JSNH4 with containment level H2. The numerical simulation has proved to be successful in terms of a final value of a shear force obtained during the test,

which was similar with the value obtained during real crash tests and, therefore, met the requirements for containment level H2. However, according to the criteria of consumed energy the value of internal energy was not sufficient for containment level H2. This was explained by the fact that classical FEM calculation neglects dynamic impact forces and does not simulate damage of the model with appearance of discontinuities (fissures, cracking, fatigue of the material, etc.). Therefore, as a possible solution the application of LS-DYNA program, which allows simulating the shock and fast processes, has been suggested [32]. Actually this has become the aim of the present work.

Resuming this, the main objectives of the master's thesis are as follows:

- to perform numerical simulation of an impact on a safety barrier JSNH4/H2 (a safety barrier analyzed in the bachelor thesis) using programme LS-DYNA,
- to perform numerical simulation of an impact to a new type of a safety barrier used on the roads nowadays, which has better properties and, therefore, a number of benefits in comparison with JSNH4/H2 - i.e. a safety barrier JSAM-2/H2.

Both crash barriers are produced by the same manufacturer, ArcelorMittal Ostrava a. s., and have the same containment level H2.

To fulfill the objectives we should perform separate tasks, which are the following:

- to study and analyze the corresponding standards and technical documentation,
- to change properly a model created for the purposes of the bachelor thesis (a safety barrier JSNH4/H2) in ANSYS Workbench,
- to create a model of a safety barrier JSAM-2/H2 in ANSYS Workbench,
- to set parameters of both models in LS-DYNA PrePost: defining deformation curves and impact conditions (velocity, vehicle density etc.), setting material characteristics to separate parts of the crash barriers, modifying contacts between corresponding parts and etc.
- to make calculations in ANSYS LS-DYNA,
- to evaluate and compare obtained results.

Evaluation and comparison of obtained results is divided into three subtasks:

- firstly, we need to compare results, obtained during numerical simulation of static tests fulfilled in the bachelor thesis using a steel barrier JSNH4/H2 in program ANSYS Workbench with the results obtained during numerical simulation of dynamic tests of the same crash barrier, but in program LS-DYNA.



- secondly, we need to prove that the numerical simulation results of both types of safety barriers are in compliance with the results obtained in the full-scale crash tests,
- thirdly, we need to compare and evaluate what benefits are brought by application of a new type of a crash barrier on the roads, i.e. we need to compare the results obtained for safety barriers JSNH4/H2 and JSAM-2/H2.

To fulfill the objectives of the master's thesis programmes ANSYS Workbench, LS-DYNA PrePost and ANSYS LS-DYNA are used.

ANSYS Workbench is an engineering system, which uses a finite element method and is multiphysical, i.e. it includes structural, thermodynamic, acoustic analysis, analysis of continuum, analysis of electrostatic and electromagnetic fields. It is widely used in engineering, automotive industry, energy and construction spheres and other areas [3].

LS-DYNA is a general-purpose finite element program. It is capable to simulate complex real world problems and is well known in automobile, aerospace, construction, military, manufacturing, and bioengineering industries. It supports highly non-linear, transient dynamic finite element analysis, which is a difference with ANSYS Workbench, which deals mainly with static analysis [33].

LS-DYNA PrePost is an advanced pre and post-processor that is delivered with LS-DYNA and which has very efficient and intuitive user interface [34].

In the present master's thesis we have used structural analysis methods and work both with linear and non-linear elements.

All three programmes are based on the finite element method that is a numerical method, which simulate loading, deformation and resonance development as well as other physical phenomena. The main principle of this method is in division of a finite volume of a construction into a certain number of elements and corresponding parameters are then defined in node points [60]. This method will be discussed in more details later on in corresponding chapters.

The theoretical part of this paper is mainly based on technical standards and corresponding technical documents such as ČSN EN 1317-1, ČSN EN 1317-2, harmonized ČSN EN 1317-5, TP 114, TP 203, TP 167, TP 101, TP 128, TP 129, TKP Chapters 11, 18 and 19 and other technical documentation. Some information concerning this issue was taken from reliable and trustworthy internet sources, including a webpage of safety barriers

manufacturer, ArcelorMittal Ostrava a. s. These sources are cited in the paper and their list is presented in a corresponding chapter.

The structure of the master's thesis is conditioned by the subject, objectives and separate tasks and consists of four chapters.

The first chapter represents introduction, where there is general information about the paper itself including the subject of our investigation, objectives and tasks defined, current state of the problem, used methods and theoretical basis described.

In the second chapter the theoretical part of the paper is presented, which includes a general information about road restraint systems, their definition, divisions, design, technical conditions and requirements for their application on the roads, tests performance and the process of defining technical parameters during design and construction of safety barriers. Moreover, this chapter describes the main standards and technical conditions, which were used during preparation of this work.

The practical part of the paper is described in the third chapter, where the selected types of safety barriers and their main parameters are outlined, the methods of numerical simulation of a safety barrier behavior are discussed and used programmes are mentioned. Besides, the steps of the numerical simulation of an impact on the barrier are described and obtained results are evaluated.

Finally, in the fourth chapter there is a conclusion made on the basis of described and tested models and the comparison of fulfilled calculations is made.

Moreover, the master's thesis includes list of sources, list of terms and abbreviations, list of tables and figures and list of symbols and their units of measurement.

## **2. Theoretical part**

### **2.1. General information**

One of the European Union's strategic objectives is to reduce the number of people killed or injured on the roads. Besides there is a well known multi-national road traffic safety project called Vision Zero, which aims to achieve a highway system with no fatalities or serious injuries in road traffic. Therefore, the requirements on road restraint systems are also becoming stricter and new standards have been implemented to define better the levels of safety required on road networks. The new EN 1317-5 standard for road safety barriers has been introduced in July 2013 and is entirely performance-based unlike older norms [6].

As it was mentioned in the previous chapter one of the means contributing to passive safety on the roads are road restraint systems. These systems help to increase safety of the road users and surroundings. Their primary purpose is to catch and redirect an uncontrolled vehicle, whilst ensuring adequate safety for passengers in the vehicle.

Therefore, the safety barrier is subject to very accurate, multiaspect development, testing, certification and approval processes before it is allowed to be installed on the roads.

The present chapter is devoted to a general review of road restraint systems in Czech Republic, history of their production, their types and classification principles. Besides it provides basic technical requirements for installing safety barriers on the roads, including description of testing procedures and parameters necessary for design and construction of safety barriers. Here the main standards and technical conditions, which discuss requirements for construction, design, maintenance, installation and testing of road restraint systems, are mentioned as well.

#### **2.1.1. Classification of road restraint systems**

The road restraint systems are proposed in areas, where there is an increased risk of vehicles and motorcyclists pulling off the road or pedestrians falling from the body of a road, resp. a vehicle collision with another road user (e.g. with another vehicle, pedestrian, etc.) or a solid obstacle [38].

Traffic barriers are categorized in two ways: according to a function they serve and according to how much they deflect when a vehicle crashes into them [38].

According to their functions the crash barriers are divided into [38]:

- roadside barriers used to protect traffic from roadside obstacles or hazards, such as slopes steep enough to cause rollover crashes, fixed objects like bridge piers, and bodies of water. Roadside barriers can also be used in central dividing strips, to prevent vehicles from colliding with hazards within the central dividing strips.
- median barriers used to prevent vehicles from crossing over a central dividing strip and striking an oncoming vehicle in a head-on crash. Unlike roadside barriers, they must be designed to be struck from either side.
- bridge barrier designed to restrain vehicles from crashing off the side of a bridge and falling onto the roadway, river or railroad below. It is usually higher than roadside barrier, to prevent trucks, buses, pedestrians and cyclists from vaulting or rolling over the barrier and falling over the side of the structure.
- work zone barriers used to protect traffic from hazards in work zones. Their distinguishing feature is that they can be relocated as conditions change in the road works. Two common types are used: temporary concrete barriers and water-filled barriers.

According to their stiffness crash barriers are divided into [38]:

- flexible barriers that include cable barriers and weak post corrugated guide rail systems. Impact energy in case of this type is dissipated through tension in the rail elements, deformation of the rail elements, posts, soil and vehicle bodywork, and friction between the rail and vehicle.
- semi-rigid barriers that include box beam guide rail, heavy post blocked out corrugated guide rail and three-beam guide rail. Impact energy is dissipated through deformation of the rail elements, posts, soil and vehicle bodywork, and friction between the rail and vehicle.
- rigid barriers usually constructed of reinforced concrete. The shape of a concrete barrier is designed to redirect a vehicle into a path parallel to the barrier. Impact energy is dissipated through redirection and deformation of the vehicle itself.

According to the list of EN 1317 compliant road restraint systems the road restraint products are divided into the following categories [20]:

- safety barriers,
- temporary safety barriers,
- parapets,
- terminals,
- vehicle attenuators,
- transitions,
- crash cushions,
- miscellaneous.

The crash barriers refer to the road restraint systems installed on the roadside or in the central dividing strip of the road (see ČSN EN 1317-1) and aimed at [20]:

- catching the vehicles,
- redirecting the uncontrolled vehicles back to the road after a crash but in such a way that there is no risk of a collision with other vehicles on the road,
- decelerating the vehicle gently to minimize the severity of an impact on people and vehicles.

All these should be made whilst ensuring adequate safety of vehicle occupants and other road users.

TPK Chapter 11 describes the following types of the crash barriers [47].

A crash barrier with a barrier strip, which is a crash barrier with one or more longitudinal elements (barrier strips, lower beams, bars etc.) connected by posts. It includes steel crash barriers except steel crash barriers of New Jersey shape, cable crash barriers and wooden steel crash barriers.

A steel crash barrier means a complete steel construction consisted of barrier strips, lower beams (depending on type), posts, spacers, connecting straps, bolts, washers, fasteners and etc. The examples of the steel crash barriers are Czech NH4 (JSNH4, OSNH4, ZSNH4 etc.), German NH3, Italian FRACASSO, Austrian VOEST-ALPINE.



**Figure 2.1: Example of a steel safety barrier [42]**

Depending on their functionality upon a vehicle impact the steel crash barriers are classified into deformable (easily deformed under an impact and having a greater dynamic deflection, usually road barriers) and non-deformable (with dynamic deflection of about 0,30 m - 0,50 m, usually bridge parapets) [22].

Depending on their location on the road the steel crash barriers can be single-sided and double-sided crash barriers.

There are several standards and technical conditions specifying properties, parameters, production, installation and other issues concerning the steel crash barriers. For example, Technical conditions TP 63 Steel crash barriers on roads (1999) include specifications for road and bridge crash barriers, their transitions to other types including transition to concrete barriers, description of supplementary components and construction parts [22].

Technical conditions TP 128 (1999) concern the particular type of steel crash barrier NH4 and describe its transitions to other types, additional parts and construction elements [51].

A cable crash barrier means a complete construction consisted of wire cables, steel posts and concrete anchorage blocks with anchor carcass (terminal and intermediate) [22].



**Figure 2.2: Example of a cable safety barrier [37]**

The main parts of the crash barrier are longitudinal cables, which are connected to posts, optionally supplemented with other elements [22].

The cable crash barriers of different structures were used abroad (Switzerland, Sweden, Denmark, England) and in Czech Republic. However, their construction was not always compliant with the road safety requirements. Only in 1988 in England a modern construction of the cable barriers has been developed, which has been successfully tested and has been claimed to catch gently even the heaviest trucks [22].

All cable crash barriers are of type of deformable barriers, which capture a vehicle when the collision occurs and evenly reduce its kinetic energy up to stopping the vehicle. Due to these reasons and because of the advantages in their installation, repair and maintenance English system of the cable crash barriers has been approved by the Ministry of Transport and Communications and technical conditions TP 106 (1998) have been issued. They provide specifications for their spatial arrangements on the roads and bridges, their transitions to other types, supplementary components and other construction parts [22].

The cable crash barriers are subjected to crash testing according to European standard EN 1317-2 for containment level N2.

The cable crash barriers have been often installed in the central dividing strip of speedways or on the verge of the mountain stretches of the road, where there is a risk of formation drifts. However, according to the recent researches the installation of the cable crash barriers in the central dividing strips is considered to be inappropriate, thus in Denmark, for example, this system is already forbidden and taken away [44].

A wooden steel crash barrier means a complete construction consisted of combined barrier strips, combined posts, connectors and fasteners, etc [22].



**Figure 2.3: Example of a wooden steel safety barrier [41]**

This system is used, for example, in France on the roads with a maximum permitted speed up to 90 km/h and traffic volume up to 5 000 veh/day, usually in naturally protected areas, in areas aimed for rest, etc [22].

In Czech Republic the wooden steel barriers were permitted to be used for a limited period in accordance with technical conditions TP 114 and TP 129 and on the basis of crash tests performed according to European standard EN 1317-2 for containment level N2 [22].

Technical conditions TP 149 Wooden steel crash barriers issued in 2000 describe construction, the principles of spatial arrangement of the barriers on the roads and bridges, their transitions to other types and different construction components. Application of these crash barriers is restricted to the roads with permitted speed up to 90 km/h (e.g. to separate cyclist and pedestrian traffic from other traffic, in protected areas, in areas for rest, in parking areas, etc.) [22].

A concrete barrier means a complete concrete construction composed from prefabricated segments and connecting parts (steel cables, connecting rods or loose locks) or a concrete monolithic construction. The examples of such barriers are New Jersey, City block, pedestrian islands [22].





**Figure 2.4: Example of a concrete safety barrier [45]**

Depending on their functionality during a vehicle impact they can be movable or unmovable, resp. single-sided or double-sided [22].

According to the method of construction they can be prefabricated (a predominant type in Czech Republic) and monolithic (often used abroad, e.g. in France). The connection of prefabricated movable crash barriers is usually made with loose locks or rods [22].

The main feature of the concrete crash barriers is their cross section, which influences the decrease of a vehicle kinetic energy during an impact. In Czech Republic a shape of "New Jersey" is commonly used, however, abroad (the USA, England) other types can be met as well. For example, F or Texas shapes are preferable for smaller passenger cars [22].

For this type of safety barriers technical conditions TP 139 A concrete crash barrier were issued in 2000, which contain specifications of shape and height of the barriers, load requirements, design, approval and delivery processes description, spatial arrangement and other issues [22].

The concrete barriers should be installed in areas, where their installation is technically necessary and economically beneficial, i.e. in case of a requirement for a higher containment level, when traffic volume is high, when there is a narrow central dividing strip, in combination with acoustic barriers and so on [22].

A parapet is a complete construction consisted of the same components as the crash barriers, but which is also equipped with a steel handrail, infill, eventually wires. The function

of this system is not only to capture a vehicle during collision, but also to protect pedestrians, cyclists against accidental fall from the free edge of the bridge [22].

Depending on their function the parapets can be bridge, protective, road or traffic safety parapets [22].



**Figure 2.5: Example of a parapet [42]**

The vehicle attenuators mean a complete construction composed of deformable elements (steel or plastic), which are assembled parallel or wedge. Then they include fasteners, guiding and anchor cables, supporting structures, connecting parts, etc. The function of this system is to reduce vehicle energy before an impact with a solid barrier [22].



**Figure 2.6: Example of a vehicle attenuator [2]**

According to their function they can be redirecting (used also for a side impact) and non-directing (the function is ensured only during frontal collision) [22].

According to their arrangement they can be parallel or V-shaped (wedge-shaped) with one or more elements side by side [22].

This system is described by ČSN EN 1317-3.

The use of vehicle attenuators is not common on road infrastructure in Czech Republic. However, they are used on branching junctions of speedways and before turning ramps.

Temporary barriers are frequently used during maintenance of the roads of category D, R, MR and roads of the 1<sup>st</sup> and 2<sup>nd</sup> classes [22].



**Figure 2.7: Example of a temporary safety barrier [35]**

They are used for permanent separation of opposite directional lanes at the intersections on the beams without free-of-way, however, only at a maximum permitted speed up to 60 km/h [22].

If they are used for a permanent separation of one-directional lanes at the intersection on beams with free-of-way, a maximum permitted speed here should be up to 50 km/h (an urban area) [22].

An opening barrier is a special type of a crash barrier, which is usually installed in the central dividing strip, where it is necessary to ensure the fast opening without using mechanical means. They are used, e.g., for giving a way for the emergency vehicle when an accident takes place or during road maintenance, etc. The requirements on containment level for the opening crash barriers are the same as for the barriers used in the central dividing strip [22].



**Figure 2.8: Example of an opening safety barrier [1]**

One more classification of the crash barriers is according to the Governmental Act. Thus, they are divided into the crash barriers being products, which are called "approved", and the crash barriers being a unit production, which are called "other" [20].

On the roads it is permitted to use only "approved" crash barriers.

On the bridges, near supporting walls, on galleries, on underbridges and portals it is permitted in accordance with TP 114 to use both "approved" and "other" crash barriers [49].

The "approved" crash barriers are products of road restraint systems, which are produced for repeat use on the roads. They are subject to standards ČSN EN 1317-1, ČSN EN 1317-2 and harmonized ČSN EN 1317-5. Besides they are subject to mandatory conformity assessment procedures and approval by the Ministry of Transport.

The "other" crash barriers refer to unit production. They are not products that could be offered to the market. It is an individual production according to the project documentation. The "other" crash barriers are permitted to be designed only on bridges and only in justified cases [20].

The reasons, when they can be used, may be the following [49]:

- they can be used near the monument objects, where the goldsmith and stone masons, i.e. crafts, is preferably applied instead of common "approved" barriers;
- they can be used on the bridge monolithic (but also prefabricated) concrete structures, where the concrete barrier is selected and concreted into the formwork directly on

the supporting bridge construction. Such barriers in this case are an integral part of the bridge.

- they can be used as well on architectural extremely exposed bridges assuming that this bridge will be located in an urban area with speed up to 80 km/h.

The "other" crash barriers are, therefore, designed individually. Most often they are statically analyzed in accordance with design standards as supporting structures [20].

The "other" crash barriers are also subject to conformity assessment in accordance with the Governmental Act, however, they are not subject to standards ČSN EN 1317-2 and ČSN EN 1317-5 and crash tests as well as to the approval of the Ministry of Transport [20].

## 2.1.2. Basic parameters

This chapter presents a description of the crash barrier basic parameters specified in corresponding standards, which are very significant when designing a crash barrier for installation on the road infrastructure.

Among these parameters we would discuss a crash barrier design load, a containment level, an acceleration severity index, a dynamic deflection and a working width.

When talking about the crash barrier design load we cannot, but notice, that it can be expressed in two ways: a load by a real impact or a load by a static force.

The design load of „approved“ crash barriers is specified by ČSN EN 1317-2. It is a load by a real impact, which the barriers are tested by.

**Table 2.1: Design load of „approved“ crash barriers [20]**

Impact ID (test number)	Impact speed [km/h]	Impact angle [degree]	Total vehicle weight [kg]	Kinetic energy $E_k$ [kJ]	Vehicle type
TB 11	100	20	900	40,6	passenger
TB 21	80	8	1300	6,2	passenger

**Table 2.1 - continuation [20]**

Impact ID (test number)	Impact speed [km/h]	Impact angle [degree]	Total vehicle weight [kg]	Kinetic energy $E_k$ [kJ]	Vehicle type
TB 22	80	15	1300	21,5	passenger
TB 31	80	20	1500	43,3	passenger
TB 32	110	20	1500	81,9	passenger
TB 41	70	8	10000	36,6	truck
TB 42	70	15	10000	126,6	truck
TB 51	70	20	13000	287,5	autobus
TB 61	80	20	16000	462,1	truck
TB 71	65	20	30000	572,0	truck
TB 81	65	20	38000	724,6	truck with a trailer

The design load of „other“ crash barriers is expressed with static force  $F_s$ .

**Table 2.2: Design load of „other“ crash barriers [20]**

Load class	Force $F_s$ [kN]	Height of force application above the adjacent roadway [m]
<b>A</b>	100	0,65
<b>B</b>	200	0,10 m below the upper edge of a crash barrier, however, max. 1,10 m
<b>C</b>	400	0,10 m below the upper edge of a crash barrier, however, max. 1,10 m
<b>D</b>	600	1,25

According to the standards only one force  $F_s$  is allowed to be applied on a crash barrier. However, it can be placed anywhere except the end parts. This force is considered with a bearing surface of 0,5x0,2 m (0,5 m in the horizontal direction). It acts horizontally in

direction perpendicular to the longitudinal axis of a crash barrier. The load distribution by element thickness is assumed to be at an angle of 45° [20].

According to ČSN EN 1991-2 the loads in table 2.2 have the same values as forces from a vehicle impact. However, this standard specifies only the loads on bridges, but not on crash barriers, therefore forces specified in this standard are not the loads on crash barriers. They are defined as the forces (reactions), which may arise from the test impact according to ČSN EN 1317-2 and which are transmitted with crash barriers to a supporting construction of the bridge. It should be noted also that the loads on the crash barriers are not specified by any European standard, because the crash barriers are tested only in the full-scale crash tests [20].

For “other” barriers used near protected monument objects and architectural extremely exposed bridges are recommended to use loads for load class A and B. For “other” barriers, which are an integral part of the bridge, load class C or D should be used depending on maximum permitted speed (for speed limit greater than 110 km/h load class D is required) [20].

Elaborating the issue TP 101 compares the intensity (efficiency) of selected crash tests and loads for crash barriers on bridges, where one can find the values of alternative force corresponding to relevant crash test categories (see table 2.3).

**Table 2.3: Comparison of crash test intensity (efficiency) and alternative loads on bridges [48]**

Relatively small deformable crash barrier (estimated dynamic deflection app. 0,1-0,5 m)	Alternative force [kN]	Relatively great deformable crash barrier (estimated dynamic deflection app. 1,5-2,5 m)
	0	TB21
TB21	5	TB22
	10	TB21   TB41 A1
TB22	15	TB11     TB31
A1	20	TB22       A2
	25	TB32     A1
TB21   TB41	30	TB41
TB11     TB31	35	TB11   TB31
	45	TB42
	50	B1
TB22	55	
TB32	60	TB32

Table 2.3 - continuation [48]

Relatively small deformable crash barrier (estimated dynamic deflection app. 0,1-0,5 m)	Alternative force [kN]	Relatively great deformable crash barrier (estimated dynamic deflection app. 1,5-2,5 m)
	65	
	70	
	75	
TB11	80	TB42
	85	
	90	TB51
TB42	100	
	110	
	120	
	130	
TB42	140	TB51
	150	
TB51	160	
	170	
	180	
TB51	200	TB81
	240	
	280	TB81
	300	
TB81	320	
	340	
TB81	380	
	400	
	460	

A crash barrier containment level is another significant parameter that is defined as a verified magnitude of a vehicle side impact, which a crash barrier is able to resist to without a vehicle overcoming it, whilst, on the other hand, ensuring a desired value of impact severity and vehicle behavior acceptability [20].

The containment level of “approved” crash barriers is specified in ČSN EN 1317-2.



**Table 2.4: Safety barrier containment level [20]**

Containment level			Required crash tests
Low angle containment	T1		TB 21
	T2		TB 22
		T3	TB 41 a TB 21
Common containment	N1		TB 31
	N2		TB 32 a TB 11
High containment		H1	TB 42 a TB 11
			L1 TB 42 a TB 32 a TB 11
		H2	TB 51 a TB 11
			L2 TB 51 a TB 32 a TB 11
		H3	TB 61 a TB 11
			L3 TB 61 a TB 32 a TB 11
Very high containment		H4a	TB 71 a TB 11
		H4b	TB 81 a TB 11
			L4a TB 71 a TB 32 a TB 11
			L4b TB 81 a TB 32 a TB 11

The low angle containment levels, i.e. T1, T2 and T3, are intended only for temporary crash barriers. However, the temporary barriers can be also tested for a high containment level [20].

If a crash barrier was successfully tested for some containment level, it means, that it meets the requirements for a lower containment level as well. However, there is an exception, which is the following [20]:

- containment levels N1 and N2 do not include T3,
- containment levels H do not include levels L and N2.

We need to outline that there is no hierarchy between containment levels H4a and H4b. These levels are defined by using different vehicle types. A vehicle for crash test TB 71 is of weight 30 t and of length 6,70 m, while a vehicle for crash test TB 81 has 38 t of weight and 11,25 m of length (it is so called a tandem vehicle) [20].

A containment level of “other” crash barriers is given by a load class.

There are several assumptions specified in standards that allow conversion between a load class and a containment level. They are as follows [20]:

- crash barriers of load class A have containment level H1,
- crash barriers of load class B have containment level H2,
- crash barriers of load class C have containment level H3,
- crash barriers of load class D have containment level H4.

We should remember that this conversion is only informative and it is not sufficient for making any conclusions.

Resuming this we should notice that the minimum containment levels, which the road restraint systems have to comply with, are also specified in the relevant standards (see table 2.5).

**Table 2.5: Minimum threshold levels for the road restraint systems [49]**

<b>Crash barriers</b>	EN 1317-2 (according to table 2)	N1
<b>Vehicle attenuators</b>	EN 1317-3 (according to table 3)	Level 50
<b>Crash barrier end parts</b>	EN 1317-4 (according to table 1)	P1
<b>Crash barrier transition parts</b>	EN 1317-4 (according to 6.1)	N1
<b>Parapets</b>	EN 1317-2 (according to table 2) and prEN 1317-6	N1

Discussing design parameters we cannot but mention Acceleration Severity Index (ASI), Theoretical Head Impact Velocity (THIV) and Vehicle Cockpit Deformation Index (VCDI). They are very important for determining the safety of vehicle occupants; therefore, they are always evaluated for passenger cars. These parameters should meet the requirements specified in table 2.6, where three levels of impact severity A, B, C are determined as functions of index values of ASI and THIV.

Notice that impact severity level A provides greater safety level for passengers in an uncontrolled vehicle than level B and logically level B provides greater safety level than level C [28].

**Table 2.6: Impact severity levels [20]**

<b>Impact severity level</b>	<b>Index values</b>		
<b>A</b>	ASI ≤ 1,0	a	THIV ≤ 33 km/h
<b>B</b>	ASI ≤ 1,4		
<b>C</b>	ASI ≤ 1,9		

Vehicle interior deformation is evaluated and recorded via VCDI index for all tests with passenger cars.

Talking about the crash barrier deformation we should remember that it is characterized by a dynamic deflection, a working width and a vehicle deflection. These three parameters are of a great use when installing the crash barriers and defining distances, which have to be provided before obstacles so that the system functions properly.

A dynamic deflection  $D_m$  is the maximum dynamic lateral displacement of any point of the front part of the restraint system. It is specified in ČSN EN 1317-2 [20].

A working width  $W_m$  is the maximum lateral distance between any part of a crash barrier on its front part before an impact and the maximum dynamic position of any part of a crash barrier during an impact. In other words it determines the distance between a crash barrier and a solid obstacle. It is defined in ČSN EN 1317-2 [20].

During the crash tests with heavy vehicles and buses we take into consideration one more parameter, i.e. a vehicle deflection.

A vehicle deflection  $Vl_m$  of a lorry (HGV) is its maximum dynamic lateral position from the front of not deformed barrier. It is evaluated from the recordings of high speed cameras or video recordings in such a way that a position and an angle of the vehicle platform is measured provided that theoretical load remains non-deformed and perpendicular to the vehicle platform or by using a test vehicle with theoretical load [20].

A vehicle deflection of an autobus is its maximum dynamic lateral position, which is evaluated as described above.

In the following tables levels of normalized working width and vehicle deflection are specified.

**Table 2.7: Levels of normalized working width [20]**

Classes of normalized levels of working width	Levels of normalized working width [m]
<b>W1</b>	$W_N \leq 0,6$
<b>W2</b>	$W_N \leq 0,8$
<b>W3</b>	$W_N \leq 1,0$
<b>W4</b>	$W_N \leq 1,3$
<b>W5</b>	$W_N \leq 1,7$
<b>W6</b>	$W_N \leq 2,1$
<b>W7</b>	$W_N \leq 2,5$
<b>W8</b>	$W_N \leq 3,5$

**Table 2.8: Levels of normalized vehicle deflection [20]**

Classes of normalized levels of vehicle deflection	Normalized levels of vehicle deflection [m]
<b>V11</b>	$Vl_N \leq 0,6$
<b>V12</b>	$Vl_N \leq 0,8$
<b>V13</b>	$Vl_N \leq 1,0$
<b>V14</b>	$Vl_N \leq 1,3$
<b>V15</b>	$Vl_N \leq 1,7$
<b>V16</b>	$Vl_N \leq 2,1$
<b>V17</b>	$Vl_N \leq 2,5$
<b>V18</b>	$Vl_N \leq 3,5$
<b>V19</b>	$Vl_N \leq 3,5$

Normalized values are calculated from measured values of corresponding parameters according to the following equations [20]:

a) normalized dynamic deflection:  $D_N = D_m \cdot \sqrt{\frac{M_t(V_t \sin \alpha_t)^2}{M_m(V_m \sin \alpha_m)^2}}$  [m]

b) normalized working width:  $W_N = W_U + \left[ (W_m - W_U) \sqrt{\frac{M_t(V_t \sin \alpha_t)^2}{M_m(V_m \sin \alpha_m)^2}} \right]$  [m]

c) normalized vehicle deflection: 
$$VL_N = VL_m \cdot \sqrt{\frac{M_t(V_t \sin \alpha_t)^2}{M_m(V_m \sin \alpha_m)^2}} \text{ [m]}$$

where

$D_m$  [m] is a measured maximum dynamic deflection,

$W_m$  [m] is a measured working width,

$W_u$  [m] is a non-deformed width of the system,

$VL_m$  [m] is a measured vehicle deflection,

$M_t$  [kg] is a specified (defined by standards) total weight,

$V_t$  [m/s] is a specified (defined by standards) speed,

$\alpha_t$  [°] is a specified (defined by standards) angle,

$M_m$  [kg] is a measured total weight,

$V_m$  [m/s] is a measured speed,

$\alpha_m$  [°] is a measured angle.

On the basis of above mentioned test parameters (crash barrier behavior, impact severity index ASI-THIV, vehicle deformation VCDI and crash barrier deformation) the acceptability criteria are defined. These criteria are specified in standards and some of them are as follows [49]:

- a safety barrier must catch or redirect a vehicle without total destruction of safety barrier's principal longitudinal elements (e.g. a rupture of a barrier strip must not take place);
- no larger part of a crash barrier is allowed to be entirely separated or present a great danger for other traffic, pedestrians or people in specified area;
- a vehicle must remain during an impact and after it in upright position, though slightly transverse or longitudinal rolling and rotating around a vertical axis is permitted;
- a vehicle must leave a crash barrier after an impact for the area set in standards;
- during an impact and after it more than one vehicle wheel must not get behind a crash barrier (top or bottom);
- during an impact and after it a rollover (including rolling over on its side) must not take place;
- during crash tests with heavy goods vehicles (HGVs) and buses no more than 5% of weight of the load is allowed to separate or spill until the wheels of the vehicle leave the exit area.

More detailed information about the acceptability criteria can be found in corresponding standards.

## 2.1.3. Steel safety barriers

In previous chapters we have discussed the road restraint systems in general. However, the subject of our interest is a particular type of these systems that is a steel crash barrier. The present chapter aims at giving basic information on steel safety barriers, including history of their production in Czech Republic, the process of design and development and the requirements for their installation on road infrastructure.

### 2.1.3.1. History

Production of road crash barriers in Czech Republic began in 1969 in Ostrava and its vast development was closely connected with the name of Ostrava steelworks "Nová huť Klementa Gottwalda", nowadays ArcelorMittal [40].

At that time crash barriers were not tested in real crash tests. Their design and production were conducted on the basis of calculations and experience of experts. These have been mainly single-sided and double-sided crash barriers of type NHKG that are installed on the vast network of the roads in Czech Republic till now and have been the ancestor of the steel crash barriers of ArcelorMittal. These barriers were the only one type, which were used till 1993 on the roads in Czech Republic. For these barriers special document Steel road barrier (1972), Proceedings of the technical design of constructions and their parts – Part S 6.2 Safety systems (1989) and Standardization guidelines for installing barriers (1990) were issued [40].

The main components of the barrier are rolled barrier strips of thickness 4 mm, deformation tube junctions and posts from rolled U-shaped profiles. The crash barrier was designed on the basis of calculation of an impact of a vehicle having weight of 13 765 kg, moving with speed 85 km/h and colliding at angle of 10° [22].

The system of crash barriers "NHKG" includes road crash barriers as well as bridge crash barriers, but according to new regulations this system cannot be certified (road crash barriers) or allowed to be used (bridge crash barriers) for new roads, but it is permitted to be used for repair and maintenance [40].

Later a new system of steel crash barriers NH3 has been introduced. It is a German type of crash barriers that has been tested in the full scale crash tests according to ČSN EN 1317-1

and 1317-2 and has been approved on the basis of technical conditions TP 59 (1993) and TP 60 (1994). After that for this system technical conditions TP 63 (1994) have been issued.

The basic structural components of barriers NH3 are rolled barrier strips of thickness 3 mm (A and B profiles), spacers and posts made of rolled I or Sigma profiles. It includes various types of road and bridge barriers, both single-sided and double-sided [22].

The system of steel crash barriers NH4 is actually a continuation of barriers NHKG that unlike barriers NHKG complies with the requirements of current regulations (ČSN EN 1317-2, TP 114 and TP 129). This in its turn means that NH4 crash barriers can have advantages in terms of installation, repair and maintenance [40].

The system of barriers NH4 can be of two types: single-sided and double-sided. The single-sided crash barriers NH4 have nearly the same main components as crash barriers NHKG have. The difference is mainly in reducing a working width by means of anchoring the ends of the barriers. As far as the double-sided barriers are concerned, in type NH4 the construction of the spacer has been changed and anchoring of the ends has been added. The single-sided barriers have been successfully tested according to ČSN EN 1317-1 and 1317-2 for containment level N2, the double-sided barriers have undergone tests for containment level H1 (in Testing Institute in Lyon, France, 1997). Based on these tests, the crash barriers have been approved and allowed to use repeatedly and for them technical conditions TP 128 have been issued [40].

Besides, at this time a new crash barrier for bridges ZSNH4/H2 with containment level H2 has been designed. This crash barrier has been successfully verified with barrier tests in Czech Republic. These tests were conducted by the Technical and Test Institute for Construction in Prague (TZÚS) in 2003 [40].

Nowadays on roads in Czech Republic the steel crash barrier produced by either ArcelorMittal or Voest-Alpine from Austria are used [43].

ArcelorMittal Distribution Solutions Czech Republic s. r. o. (AMDS CR) is the only producer of steel crash barriers in Czech Republic and is a member of European Union Road Federation (ERF). It produces more than 80 % of crash barriers used on Czech roads. From 2003 ArcelorMittal closely works with the Technical and Test Institute for Construction in Prague (TZÚS) [43].

Production of AMDS CR, where production of crash barriers from ArcelorMittal Ostrava a. s. was transferred, includes nine types of steel crash barriers with various parameters for road

routes and bridges approved for use in Czech and Slovak Republic and three types of steel barriers approved for use in the Baltic States. Since the beginning of crash barrier production ArcelorMittal have produced nearly 45 000 km of crash barriers [6].

In ArcelorMittal Ostrava a. s. so far hot rolled profiles were used for the production of posts. These profiles were made of steel S235JR. Due to the growing requirements for road safety and therefore on increasing containment level on the one side, and seemingly opposite market demands for weight reduction of crash barriers on the other, AMDS CR continues a process of developing new crash barriers. Technologists and designers are working on the application of steel of higher qualities in their constructions. The goal of the development is to reduce weight and increase containment level. For these purposes micro-alloyed steels, which yield strength is greater than 275 MPa, are used. The first application of micro-alloyed steel was the posts of road barrier JSNH4/H2. This barrier has been successfully tested in 2008 and currently is delivered for new roads and motorways in Czech and Slovak Republic. In 2010 a new type of a barrier strip AM has been designed and successfully tested. This barrier strip is actually continuation of type NH4, but the difference is that it is made of micro-alloyed steel S355MC, which is characterized by greater strength than steel S235JR used for production of NH4. This fact enables to reduce the thickness of a material from 4 mm to 2,8 mm, which is more than to a quarter. A barrier strip AM has been used for a single-sided crash barrier with containment level N2 and with containment level H1 and for a double-sided crash barrier with containment level H1. In 2012 a crash barrier with AM barrier strip tested for containment level H2 has appeared on the market [7].

The tendency of weight reduction and improvement of mechanical properties of the crash barriers continues. Currently ArcelorMittal is working with manufacturers to develop new, more competitive barriers using High Strength Low Alloy (HSLA) steels such as S420MC. For steel, the new EN 1317-5 standard typically sets minimum yield stress for barriers at 235 MPa – the same level as in the previous standard. However, manufacturers are now free to replace structural steels such as S235JR with High Strength Low Alloy steels that are lighter per meter, better able to absorb energy in the event of a crash, and more cost-competitive [8].

Besides for increasing road safety and fulfillment of Vision Zero since 2008 ArcelorMittal have worked on the development of special motorcycle crash barrier JSAM-M/H1 and at the end of 2013 it has been placed for 142 m test section Šebrov in district Blansko. This crash barrier should help to reduce or even eliminate the consequences of accidents with motorcyclists. After the development and production of motorcycle crash barriers it has been



successfully tested, certified and accepted by the Ministry of Transport of Czech Republic for use on Czech roads [46].

As far as the corrosion protection is concerned earlier the corrosion protection coatings were used. Nowadays ArcelorMittal offers a full range of coating solutions. These include heavy gauge hot dip galvanizing (technology used since 1971) as well as new high performance metallic coatings such as Magnelis. The manufacturer claims that due to a distinctive metallic chemical composition of zinc with 3,5% aluminum and 3% magnesium Magnelis lasts much longer than traditional coatings such as hot dip galvanization. Tests have proven that this new technology has superior corrosion resistance in soils compared to zinc-heavy coatings and perhaps sooner on the manufacturer's opinion it will be widely used for corrosion protection of steel crash barriers [8].

### **2.1.3.2. Steel safety barrier installation on road infrastructure**

The decision, whether to place a crash barrier on the road, how to place it and what type of a crash barrier is applicable for this or that situation, should be based on the requirements of relevant standards, on a designer's own considerations (not all dangerous places are listed in standards), on the requirements from governmental organizations or on any other justified requirements.

Generally a crash barrier is installed for the following purposes [49]:

- to protect road users against an impact on solid obstacles or against driving in to a dangerous place;
- to protect infrastructure and environment near it (e.g. protection of people and buildings near roadways).

A crash barrier is allowed to be used if it has been approved and/or authorized for installation by a central authority of state administration in matters of transport.

Common sites for installation of a traffic barrier are:

- bridge ends,
- near steep slopes from roadway edges,
- at drainage crossings or culverts where steep or vertical drops are present,

- near large signs/illumination poles or other roadside elements which may pose hazards.

When it is decided that installation of a crash barrier is needed, careful calculations taking into account the speed and traffic volume, the distance from the edge of a roadside to the hazard, and the distance or offset from the edge of a roadside to the barrier, are completed [49].

To know what type of a crash barrier to place on the road we need to define containment level, which is determined on the basis of a risk degree of a certain road section and an environment protection degree. For these purposes two tables are specified in TP 114.

Thus, according to TP 114 a road, resp. a road section, where a crash barrier is purposed to be placed, is divided into sections, which environment and risk degree are specified in table 2.9, and into other sections, for which a containment level is determined according to a road type in table 2.10 [49].

**Table 2.9: Determining a containment level for road sections according to a risk degree and protection of their environment [49]**

№	Annual average of daily intensities of heavy vehicle traffic T in both directions [number of vehicles/24 h]	<1000		1000 to 5000		>5000	
		N	V	N	V	N	V
1	The source of drinking water near the road.	H2	H3	H2	H3	H3	H4
2	Railway lines or tramway lines parallel to the road situated near the road. When determining risk degree the permitted speed, intensity and composition of traffic for railway lines as well as railway location are considered.	H1	H2	H2	H3	H2	H3
3	Public area with high frequency of pedestrians.	H1	H2	H2	H3	H2	H3
4	Ground based constructions.	H1	H2	H1	H2	H2	H3
5	Central dividing strip of directionally divided roads.	H1	H2	H1	H2	H2	H3
6	Between parallel roads, if at least one of them is of category D, R and MR.	H1	H2	H1	H2	H2	H3

**Table 2.9 - continuation [49]**

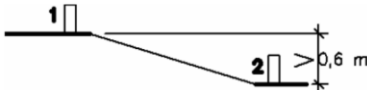
№	Annual average of daily intensities of heavy vehicle traffic T in both directions [number of vehicles/24 h]	<1000		1000 to 5000		>5000	
		N	V	N	V	N	V
7	For dividing traffic led on different levels when a height difference is more than 0,60 m (e.g. in central dividing strip or between parallel roads). 	H2	H3	H2	H3	H3	H4
8	Water stream or water reservoir with depth of normal water more than 2 m.	N2	H1	H1	H2	H2	H3
9	A cragged cliff or embankment of height more than 3 m with a slope more than 1:1,5.	N2	H1	H1	H2	H1	H2
10	Other dangerous places (except bridge portal supports), e.g. trees, outside sides of curves with radius less than 300 m in longer descent more than 4 % for roads of category I (not valid for branches of intersections).	N2	H1	H1	H2	H1	H2
11	Noise protection walls not designed as restraint systems.	N2	N2	N2	N2	N2	N2

Table 2.9 shows containment levels depending on daily intensity of heavy vehicle traffic, i.e. on the number of heavy vehicles per 24 hours, defined as an annual average. This table is divided into three intensity groups and for each group a containment level is defined.

The sections of a road with several risk factors are considered to have a high risk degree.

**Table 2.10: Determining containment levels for road sections on the basis of road types [49]**

№	Road type (category)	Containment level
1	Outside sideways of speed and directionally divided roads (category D, R, MR)	min. N2
2	Other	N1 to N2

After defining a containment level a suitable crash barrier can be selected. It is recommended to prefer "approved" crash barriers to "other" crash barriers, if possible. A selected crash barrier should have design parameters compliant with space requirements specified in relevant standards (ČSN 73 6101, ČSN 73 6110, ČSN 73 6201). Mainly the compliance should be [49]:

- between the distance of a crash barrier front part from the edge of the road (e.g. for new constructions projected according to ČSN 73 6101 it should be 1,00 m) and dynamic deflection of a crash barrier for corresponding containment level;
- between the width of a central dividing strip and working width of a crash barrier;
- between the distance from a crash barrier front part to a solid obstacle and working width of a crash barrier.

It is also good to remember that there is always a possibility (in normal operation), that an impact may be of such intensity that exceeds any impacts (even several times), which a crash barrier has been designed and tested for.

As we have mentioned previously, a safety barrier is mounted in places, where relevant standards and regulations demand its installation. However, there exist other cases, where the designer and the customer should decide in the frames of the project documentation, because not all dangerous places are covered by standards [49].

Thus, a crash barrier must be installed in places, where due to the nature of a road there is a high risk of vehicle driving outside the road and where in this case there is a great danger for vehicle's passengers or for people moving in the vicinity of a road.

The main reasons of vehicle leaving the road are sleeping or micro-sleep during monotonous driving, poor conditions of a road surface (water, snow, and ice), speeding or dangerous way of driving. From this it follows that in this respect the most dangerous roads are roads with high speed driving. In contrast, sweeps, rams, entrances and exits to buildings are considerably safer, because the problem of micro-sleep is not topical here and road surface conditions would cause a small danger at small speeds [49].

We should bear in mind that though the main purpose of crash barriers is to provide safety for road users, however, they also present a risk during the impact. To minimize the consequences of accidents due to the vehicle collision with a safety barrier it is recommended to install it as far as possible from the lane.

It is recommended to place a crash barrier or at least guiding elements on the roads near the rock notches, because they are sometimes of a very rough surface and fail to put aside a vehicle as a smooth surface does [49].

Sometimes the inner side of a curve is more dangerous than the outer one. After an impact takes place a steel crash barrier tends to "break through" to the side and form a bag, which is very dangerous. It does not concern ramps and sweeps of a small radius with driving speed up to 60 km/h [49].

Quite common situation is when the green areas between exit and entrance branches are bordered from all their sides with crash barriers, even if there is no obstacle there. In these very cases it is not recommended to install crash barriers. If there is an obstacle (a post, a sign), the collision with it can be prevented by appropriate ground adjustment [49].

It is also not recommended to install crash barriers along the rural roads, which run parallel to roads. Rural roads are tertiary roads with negligible traffic of agricultural vehicles, which the barriers have not been either designed or tested for [49].

The other example, when a crash barrier has no function, is the internal sides of ramps (often of a small radius), when there is no obstacle and the driving speed does not exceed 60 km/h and when a ramp is not in a high embankment [49].

Crash barrier installation near the exits of petrol stations has also no reasons.

A crash barrier can be omitted as well in case when there is a long continuous obstacle, which is not needed to be protected and which is able to redirect a vehicle itself (e.g. a smooth concrete wall) [49].

As for the directional course and height of a crash barrier the standards say that they should be continuous. The length is defined on the basis of a crash barrier type and size of an obstacle or a hazardous place and is not permitted to be shortened without justified reasons to less than the minimum length specified in technical conditions [49].

In a central dividing strip it is allowed to install both double-sided and two parallel single-sided crash barriers, however, the distance between these parallel crash barriers should enable deformation of a crash barrier.

The double-sided crash barriers are preferably installed in the axis of a central dividing strip, but it is prohibited to install them when greater slopes present.

Before a continuous obstacle, which itself is able to prevent a vehicle from getting to opposite direction, the double-sided crash barrier can be replaced by two single-sided crash barriers.

We have already said that not correctly installed barriers are a hazard to road users and this is particularly the case at the ends of barriers. When the ends are not treated correctly, then during an impact a vehicle could roll over or the elements of the barrier may penetrate the passenger compartment with serious consequences for occupants [49].

"End Treatment" (or terminal) is the term applied to devices specially designed to ensure that the ends of barriers provide safe conditions for occupants of vehicles that may impact this area of a barrier. The type of end treatment used depends on the barrier. Some treatments function only to provide a safe terminal for the barrier, while others also function as an anchor for the system [49].

A crashworthy end treatment must be provided on both approach and departure ends of barriers that [49]:

- terminate within a clear zone,
- are located in an area where they are likely to be hit head-on by an errant vehicle.

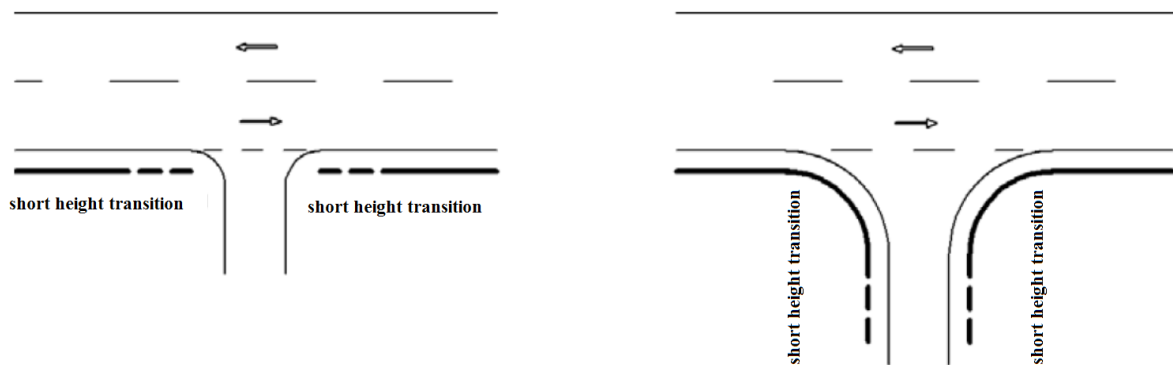
A clear zone, also known as clear recovery area or horizontal clearance, is defined as a lateral distance in which a motorist on a recoverable slope may travel outside of the roadway and return their vehicle safely to the roadway. In order to provide for adequate safety in roadside conditions, hazardous elements such as fixed obstacles or steep slopes can be placed outside of the clear zone to reduce or eliminate the need for roadside protection [49].

A barrier end treatment may fulfill its function by:

- permitting controlled vehicle penetration into an area behind the device,
- decelerating a vehicle to a safe stop within a relatively short distance,
- catching and redirecting the vehicle,
- a combination of the above.

There are two types of end treatment: a long and short height transitions. A long height transition is usually of a length app. 8-12 m and a short height transition has a length of about 4 m. A long vertical height transition is usually preferred, whereas a short height transition is allowed only in justified cases (e.g. on connections, exits and junctions) or on the ends of a crash barrier in a driving direction on directionally divided roads and on

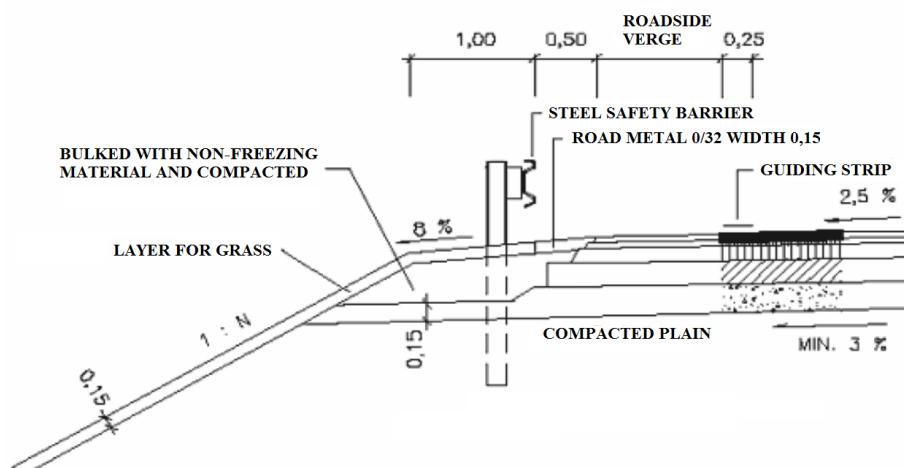
the beginning of a crash barrier in a driving direction, if this vertical height transition is covered by a crash barrier [49].



**Figure 2.9: A crash barrier on connections, exits and junctions [54]**

For more detailed information about crash barrier placement and installation parameters such as the height of a crash barrier above the road and its minimum length we would recommend to refer to corresponding standards, because the scope of this work does not comprise all information covered in standards and give only a short description of main issues concerning safety barrier installation requirements.

Concluding this part of the chapter we would like to present several examples of a safety barrier installation, which are taken from TP 203 and from lit. [38] and shown below.



**Figure 2.10: Example of a steel barrier placement on the road [38]**

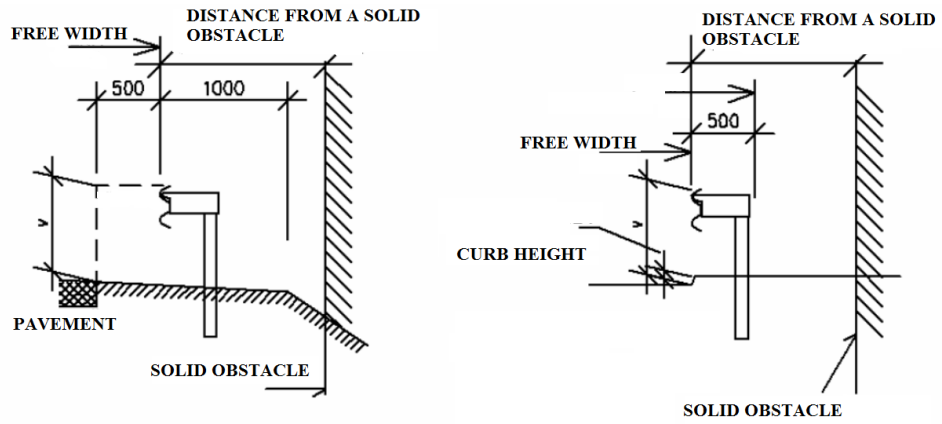


Figure 2.11: Single-sided crash barrier placement on a roadside [54]

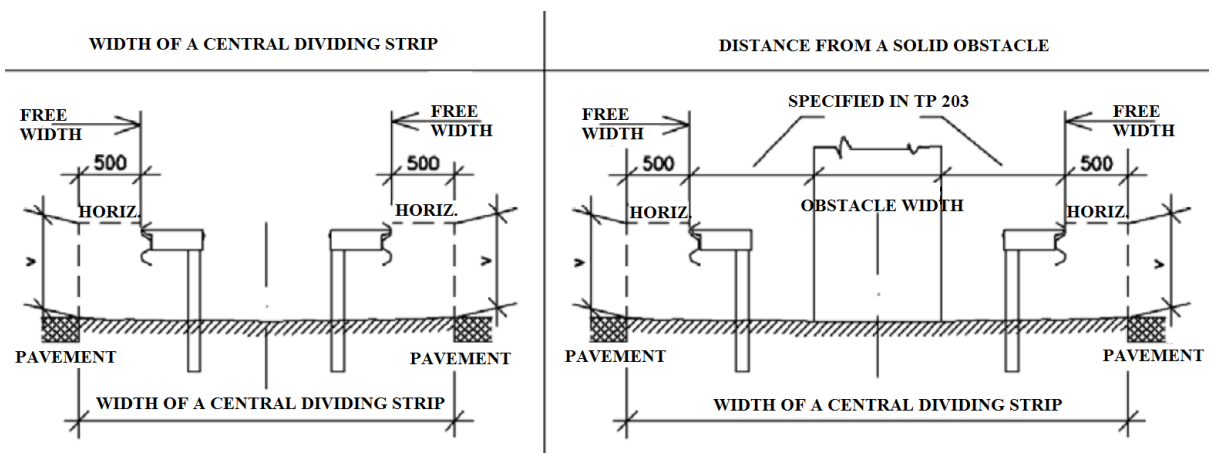


Figure 2.12: Single-sided crash barrier installation in a central dividing strip [54]

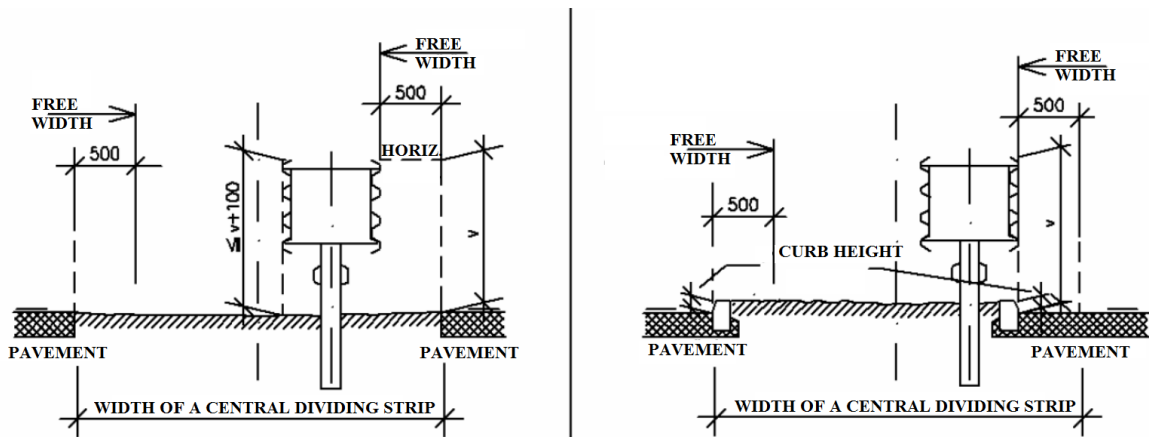


Figure 2.13: Double-sided crash barrier installation in a central dividing strip [54]



## **2.2. Numerical simulation and selected types of road safety barriers**

The present chapter comprises general information about numerical simulation and describes two types of crash barriers chosen for the analysis held on in the present work. It provides several drawings of each crash barrier and its parts as well as material characteristics and installation requirements. It also gives some basic information about the programmes used for the purposes of the thesis.

### **2.2.1. Numerical simulation**

Considering benefits and drawbacks of crash tests on the one hand and those of calculations/numerical simulation on the other hand there is an attempt to combine strong sides of both methods and use them for the sake of the final result. The main core of this subchapter is a description of the above mentioned issue as well as a description of computer programmes used for the further numerical simulation and results evaluation.

#### **2.2.1.1. Crash tests, calculations and numerical simulation**

As we have mentioned several times before, the crash barriers can be used on roads only when they comply with requirements specified in TP 114/2010. Compliance with these requirements is verified by crash tests according to ČSN EN 1317-2. On the basis of these crash tests the final containment level is determined. For majority of containment levels there should be two or more types of crash tests. It is valid for “approved” crash barriers.

For “other” crash barriers calculation is used. However, it is not common because of several reasons. The strongest of these reasons is that these calculations are not currently able to provide a sufficient basis for assessing the complex suitability of application of a certain crash barrier as a road restraint system from the point of view of forecast of “acceptability of an impact from all aspects”. Other reason, why calculations are not often used, is the lack of methodological guidelines, recommendations and documents dealing with this issue. However, for bridge crash barriers the calculations are allowed and moreover sometimes recommended in accordance with corresponding standards [48].

Further on we would like to underline some advantages and disadvantages of both methods and continue with numerical simulation as a promising method for forecasting behavior of the crash barrier during collision.

The implementation and evaluation of crash tests, although for some cases and situation is strictly prescribed, is not only expensive and complex for equipping the laboratory, but also the application of the results of the crash tests in predicting how the barrier will behave in practice, i.e. on roads and during certain impacts, is problematic, because [48]:

- impacts on sections of crash barriers with different length or of crash barriers otherwise modified or anchored end (i.e. otherwise deformable; impacts at different distances from the ends of the section than it was during crash test; impacts on not completely straight or deliberately concave or convex crash barriers (especially at greater curvature); or in the case of other, though seemingly very similar vehicle (differing, for example, only in some construction details), etc.) are sometimes substantially different than impacts during crash tests;
- dispersion of the results of the same crash tests, i.e. crash tests conducted with the same parameters of the vehicle and crash barrier and with the same movement of the vehicle, is considerable;
- the course of the impact can be greatly influenced with even a relatively small change of the height of the center of gravity of the vehicle or its load, which, however, during the tests is rather estimated than measured and its regulation is not strictly followed (mainly it concerns stability problems, i.e. the rollover of the vehicle over the crash barrier or rollover of the crash barrier itself). Moreover, the height of the impact forces can significantly affect, e.g., a mechanism of crash barrier breaking during overload and its load can influence the character of movement of both the crash barrier and the vehicle during the impact, etc [48].

Therefore, crash barrier classification as being satisfactory or unsatisfactory made only on the basis of evaluation of prescribed crash tests is rather a convention and compliance with the requirements of the regulations than technically based guarantee that the consequences of all (or at least the majority) impacts of a particular class will be acceptable in all aspects in practice.

As far as the calculations are concerned the problem is not only to establish the coherence (i.e. the properties of designing computational model, which moreover cannot be usually verified), but also to list the properties and circumstances, which have a decisive influence on what happens during an impact. It is highly likely that when creating a computational model

something significant could not be taken into account because of some reasons and, therefore, final results could not predict anything fundamentally. E.g. it cannot be expected, that the calculation will show the possibility of ejection of some part of a crash barrier, which can endanger the occupants of the vehicle or random pedestrian; that it will show the possibility of breakthroughs of fuel tank and subsequent fire; that it will show the possibility of creating a “bag” or the possibility of repelling the vehicle to distant lanes of the road or the possibility of rollover of the vehicle or that it will predict the influence on impact process by existence of reflecting curb in front of or under the crash barrier, etc., unless it is theoretically managed and unless the computational model contain the relevant criteria [48]. Moreover, many important input data defining the computational model of the crash barriers are difficult to obtain, even though it is clearly defined, what they have to define.

Thus, summing all mentioned above, we can say that the crash tests can provide us with information of what has taken place once or twice in real conditions, however, on the basis of these results we cannot give a reliable prediction, what will happen during other, though a very similar, impact. On the other hand with the help of calculations we can create graphs and tables, which will describe average global mechanical behavior of the crash barrier during all possible and impossible impacts, which are though helpful, e.g., for comparison different crash barriers of approximately the same type or for comparison of the effects of different impacts, however, without sufficient guarantees, that impacts will be in such a way as it is described by these diagrams [48].

Therefore, the possible solution is to combine these two methods. Several crash tests would show whether the crash barrier is able to function acceptably (in all aspects) at least in some collisions, and computational model, for which precision the results of the crash tests would be used, would enable to obtain a series of predictions in respect of what effects would be very likely caused by the impact with other parameters (e.g. the impact with other intensity and/or the impact of other vehicle and/or the impact to the crash barrier of different length and different arrangement) than those corresponding to the parameters during the tests [48].

Then calculations could be used as “means making the preparation of crash tests”, bringing in comparison with the “trial and error” substantial savings. It concerns, e.g., the fact, that with the help of calculations it is often possible to predict the influence of the change in construction of the crash barriers (e.g. construction changes of connecting parts, changes of the element length etc.) on their strength and stiffness, and then to select the appropriate parameters of the crash tests. Moreover, the calculation results can be used to design and

test new and completely innovative types of crash barriers. And this is where numerical simulation can play significant role saving time and decreasing expenses [48].

With the rapid development of computer science and increasing powers of computers it has become possible to use it for different purposes in mechanical engineering. Numerical simulation, especially FEM, is widely and effectively used in automobile industry during simulation of crash test of new vehicles. Therefore, there is a question if it is possible to replace a part of crash tests for crash barriers by their simulation using FEM methods with explicit time integration and use it during design and innovation of a crash barrier system in a way, that on the basis of calculation results the acceptability criteria would be defined in compliance with the requirements of ČSN EN 1317-2. These criteria would be defined on the basis of the same parameters, which are currently obtained from the measurements during real crash tests [48].

A real crash test is surely a worthy source of information about vehicle and crash barrier behavior during collision and is a basis for numerical simulation. For these purposes one crash test would be performed, which could validate the FEM simulation. Then after validation in this simulation other types of vehicles could be used. It would result in cost savings for performance of expensive and time consuming crash tests. Besides, there is a definite limit of measurement during one crash test. This limit can result in fact, that not all parameters of the crash barrier affecting its deformation properties are revealed. This can cause a situation when the design would not be optimal. Numerical simulation with explicit integration enabling to model strongly non-linear dynamic processes can help to solve this problem as well.

However, there are several problems. One of them is that it is time consuming and the second is that there are no unified and verified methods prescribed in any regulations how to do these simulations.

In present work we would try to simulate the vehicle impact on two crash barriers and prove that numerical simulation in this area has great perspectives.

### **2.2.1.2. ANSYS Workbench and LS-DYNA**

Before we start describing the steps of our simulation, we should say a few words about the programmes themselves and their basic characteristics.

As it was already touched in introduction ANSYS is a program, which works on the basis of the finite element method.

FEM allows solving different types of problems in the sphere of mechanics such as, for example, performing stress-strain analysis with static, cyclic and dynamic loading, various linear and non-linear problems, self-oscillation and forced vibrations of the system with damping and without damping, contact problems of elasticity etc [60].

The base is a Lagrange principle, which says that the body is in balance if the total potential energy of deformation of the system is minimal. Therefore, the variational methods and finding functionals are used. FEM encompasses methods for connecting many simple element equations over many small subdomains, named finite elements, to approximate a more complex equation over a larger domain. The basic steps in the finite element method are creating CAD model, discretization of the model, constructing equations for each discrete point, replacement of displacement function with polynomial expression and defining function of displacement, introducing the boundary conditions, calculation of the system of linear algebraic equations, calculation of deformation and stresses for each node points, graphic view on the model and extracting important values. Thus, in the result we have the development of displacement, stress and deformation and calculated internal forces, which act on this or that construction [60].

Thus, the first task of an engineer, who works with ANSYS, is to create a geometric model, which is as much as possible compliant with the real object (for a pre-determined targets), on which will be generated finite element mesh. ANSYS provides a user-friendly working environment Workbench, which enables relatively easy way to create a geometric model.

As it is written on website supporting ANSYS users, ANSYS Workbench is a flexible framework that supports the industry's broadest suite of engineering technology. An innovative project schematic view ties together the entire simulation process, guiding the user through even complex multiphysics analysis in a simple way. With bidirectional CAD connectivity, powerful highly-automated meshing, a project-level update mechanism, pervasive parameter management and integrated optimization tools, the ANSYS Workbench platform delivers productivity, enabling Simulation Driven Product Development [3].

Work environment of ANSYS Workbench works on the principle of preprocessor and postprocessor, as in ANSYS Mechanical. Preprocessor provides tools for creating geometric model itself, defining its material properties, defining boundary conditions and setting loads, generating finite element mesh. Postprocessor is used for evaluation of solved problem.

The results are available to the user in a graphical and textual form, whereby the user can choose the type of graphical output. The calculation is performed outside the working environment Workbench. For these purposes the classic environment of ANSYS, APDL system, is used. It works with data sent by the preprocessor.

It is very important to create such a model that we can ensure the accuracy of the calculation, but at the same time to find a compromise between the complexity of the model (hence its accuracy) and time and data demands.

The second program used in this thesis is ANSYS LS-DYNA.

It is a useful tool for those, who need to analyze problems involving contact, large deformation, nonlinear materials, high frequency response phenomena and/or problems requiring explicit solution. That is our case.

Thus, ANSYS Workbench environment can be used for creating models and defining different parameters as well as boundary conditions and then using explicit dynamic file export we can create an input file (.k) that is run by the LS-DYNA solver. LS-DYNA PrePost program provides a user-friendly yet powerful way to specify parameters (e.g. deformation curves, test properties and etc.) of the model and view the results of simulation.

## **2.2.2. Types of safety barriers under analysis**

This chapter describes construction, parameters and installation of selected types of safety barriers, i.e. JSNH4/H2 and JSAM-2/H2. Both types are designed and produced by the same manufacturer, ArcelorMittal s.r.o., and are equivalent in respect to containment level, that is in terms of crash test types performed for their validation and certification. However, they differ in materials used, so that JSAM-2/H2 is made of new micro-alloyed steel, which allows, as the manufacturer claims, the reduction of overall weight while preserving the same and even better functionality.

### **2.2.2.1. Safety barrier JSNH4/H2**

A safety barrier of type JSNH4/H2 is a road single-sided barrier with containment level H2, working width of 1,85 m (W6), dynamic deflection of 1,75 m, ASI of 1,186 and system weight

of 42,68 kg/m. It is tested by crash tests TB 11 (a passenger car of weight 900 kg, speed 100 km/h and impact angle 20°) [52]. Its construction is shown in Figure 2.14.

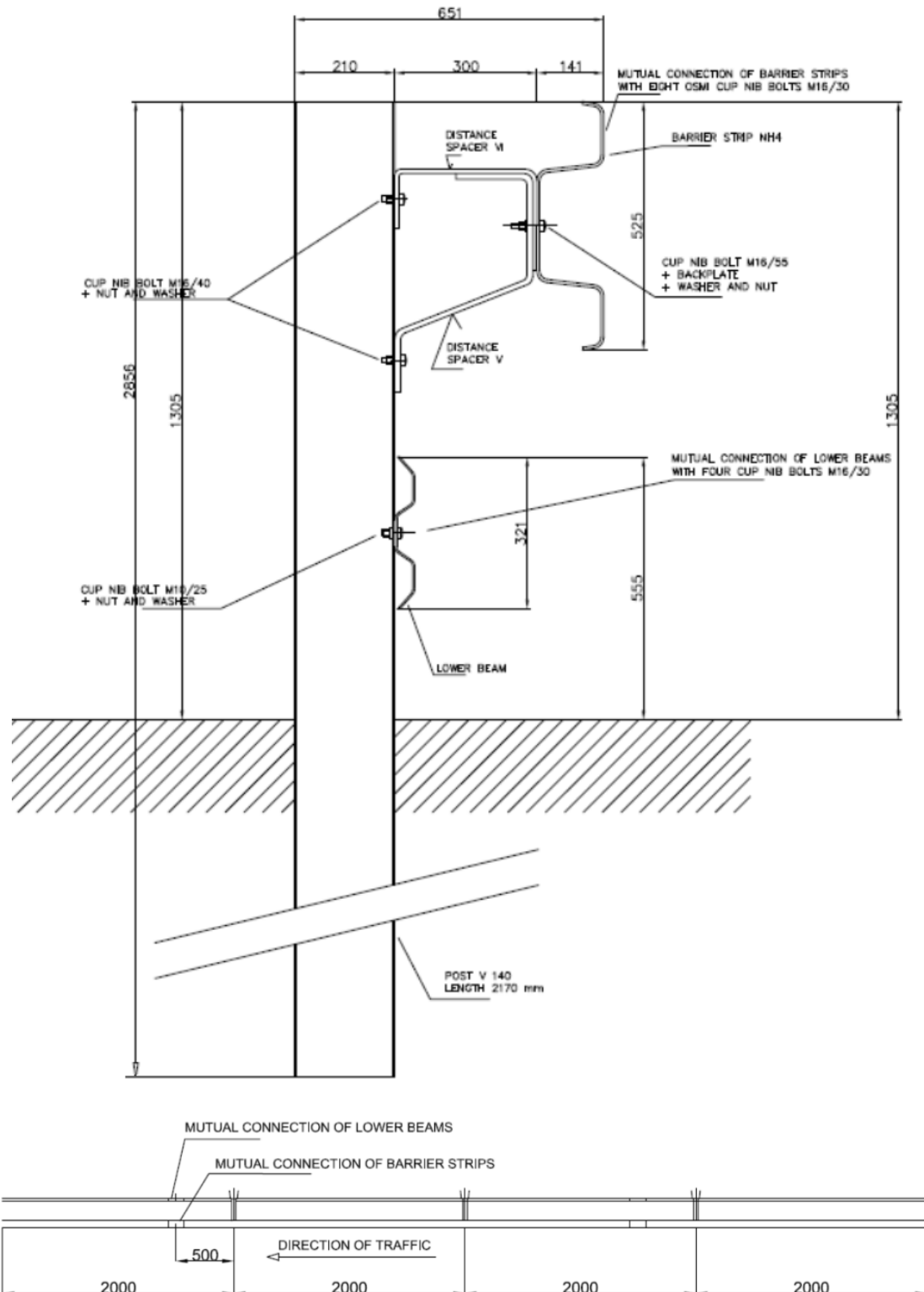


Figure 2.14: Safety barrier JSNH4/H2 [52]

This type of a safety barrier can be used for containment level H2 and other containment levels smaller than it has been tested for as follows from the table:

**Table 2.11: Containment levels JSNH4/H2 can be used for [52]**

Containment level	Where it can be used
N2	on sideways with width behind the front part of a crash barrier at least 0,70 m and in central dividing strips around the obstacles dimensioned for vehicle impacts
H1	on sideways with width behind the front part of a crash barrier at least 1 m and in central dividing strips with width at least 2,40 m as two parallel crash barriers
H2	in places where behind the front part of a crash barrier there is a plane surface (slope up to 10%) with width at least 1,50 m and in central dividing strips with width at least 2,85 m as two parallel crash barriers

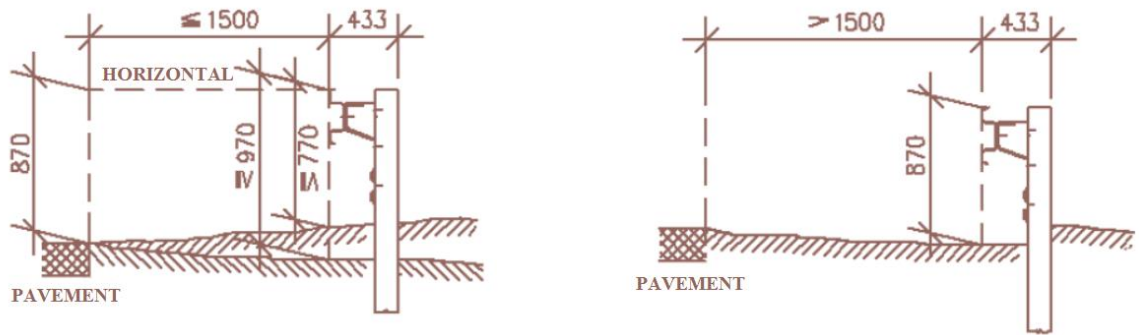
The distance of JSNH4/H2 from a solid obstacle depends on the containment level the barrier is used for and it is shown in table 2.12.

**Table 2.12: Distance of the front part of a crash barrier from a solid obstacle [52]**

Crash barrier type	Containment level	Distance [m]
JSNH4/H2	N2	0,80
	H1	1,15
	H2	1,85

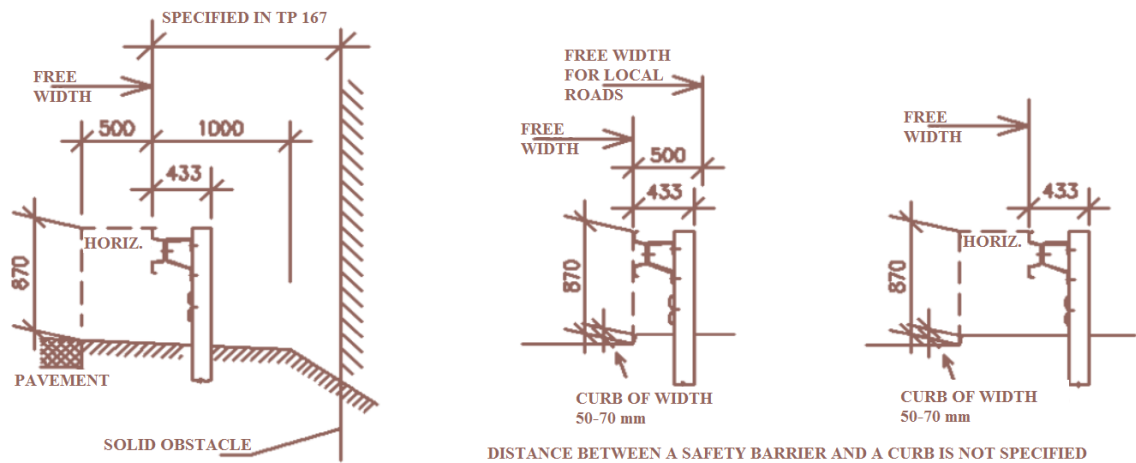
The height of JSNH4/H2 is measured from the upper edge of a barrier strip and is shown in Figure 2.15.





**Figure 2.15: Height of JSNH4/H2 [52]**

The next figure illustrates JSNH4/H2 placement on the roadside verge.

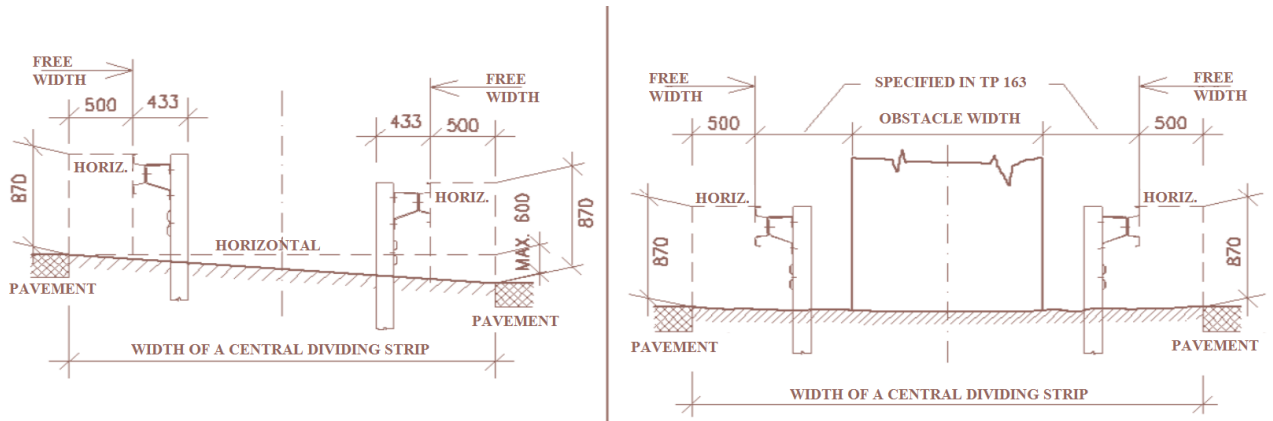


**Figure 2.16: JSNH4/H2 installation on the roadside verge [52]**

The standards specify minimum length of JSNH4/H2, which is 28 m for speed  $\leq 80$  km/h and 44 m for speed  $> 80$  km/h. Nevertheless it is worth to remind that the length of a crash barrier before an obstacle is defined not only with its minimum length, but also with a type of an obstacle (a height of an obstacle up to 0,4 m and more than 0,4 m) and with a distance between the front part of a crash barrier and an obstacle [52].

The most dangerous case is when an obstacle is above the terrain more than 0,4 m and is distanced from a crash barrier up to 3 m. In this case the length of a crash barrier is determined also by permitted speed. Thus, for speed  $< 60$  km/h the length of JSNH4/H2 before an obstacle will be 28 m, for speed 60-90 km/h it is 52 m and for speed  $> 90$  km/h it is 72 m [52].

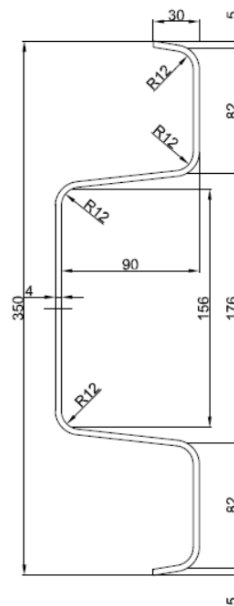
If an obstacle is far from the front part of a crash barrier for more than 3 m, then the length is defined as the minimum length in a way it is mentioned above.



**Figure 2.17: Example of JSNH4/H2 installation in a central dividing strip [52]**

If talking about the main constructional parts of JSNH4/H2 it consists of barrier strips, two parts of a spacer, lower beams and posts.

For JSNH4/H2 a barrier strip NH4 is used. Its height above the road is 0,870 m.



**Figure 2.18: Barrier strip of JSNH4/H2 [52]**

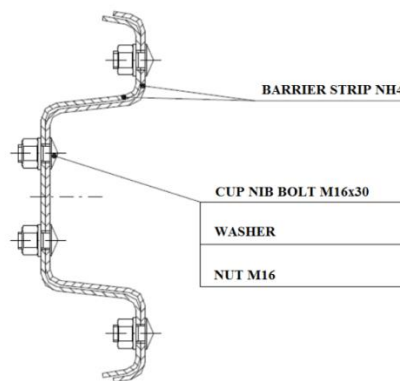
NH4 is made of a sheet of thickness 4 mm. The cross section of NH4 has height of 350 mm (in non-calibrated part) and width of 94 mm. The length of one barrier strip is 4250 mm [52].

There are two types of a barrier strip: direct (used when the radius is greater than 100 m) and arched (used for internal and external curves with the radius of 6 m up to 100 m) [52].

One end of a barrier strip is calibrated and the other one is not calibrated. The calibrated end with a cross section 341 mm has such a shape modification, which makes it possible to put it closely to a non-calibrated end of other barrier strip and fasten these two ends [52].

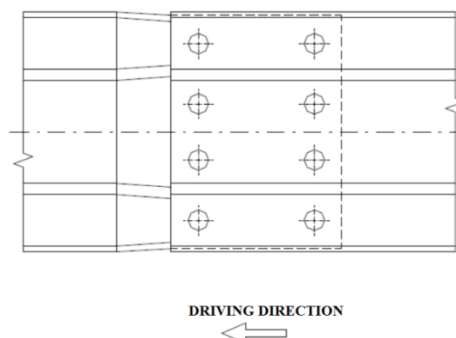
The holes for interconnection of barrier strips can have two types of shape: on the non-calibrated end they are drop shaped with diameter 18 mm and on the calibrated end they are round with the same diameter. The holes for connecting a barrier strip with a spacer or to a post are oval with diameter 18 mm and with length 60 mm [52].

It is worth saying that barrier strips are connected in such a way that the end of one barrier strip is overlapped with the beginning of the other. Two barrier strips are interconnected with eight cup nib bolts M16x30 and nut M16 with washer 17,5 [10].



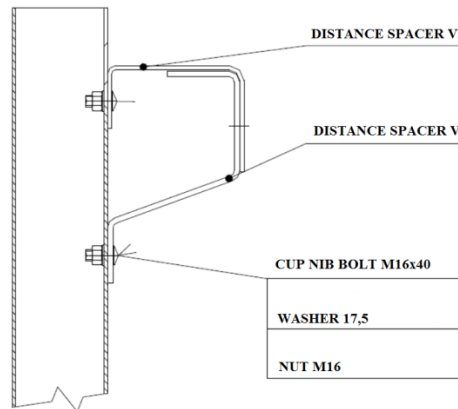
**Figure 2.19: Barrier strip interconnection [10]**

The orientation of a barrier strip should be such that it begins with a calibrated part in the driving direction and over it the non-calibrated end of a previous barrier strip is laid.



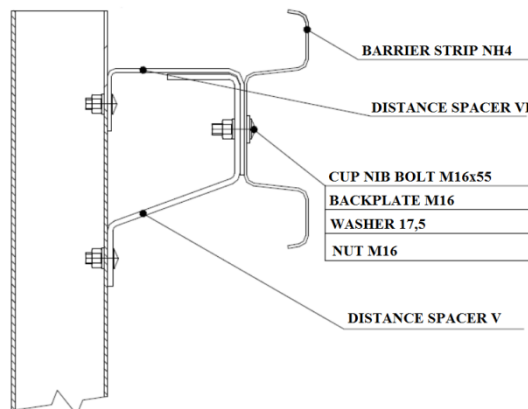
**Figure 2.20: Orientation of NH4 [10]**

Spacer V is the lower part of a spacer made of a steel profile 50/8 mm, while spacer VI is the upper part of a spacer made of a steel profile 50/6 mm. Both parts are connected to a post using cup nib bolts M16x40 with nuts M16 and washers 17,5 [10].



**Figure 2.21: Spacer and post interconnection [10]**

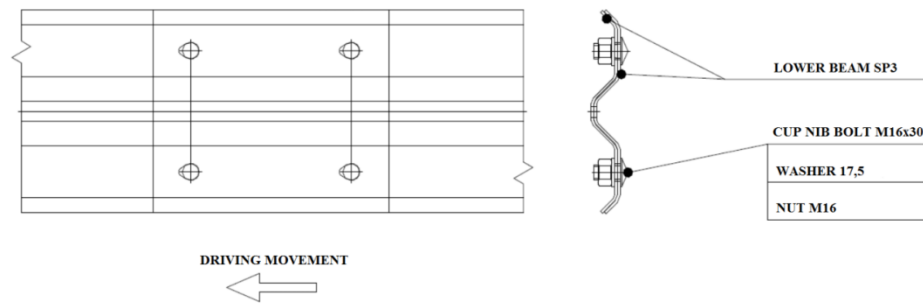
A barrier strip is connected with a spacer with one cup nib bolt M16/55. There is a backplate M16 behind the bolt head and a washer 17,5 behind the nut M16 [10].



**Figure 2.22: Barrier strip connection with a spacer [10]**

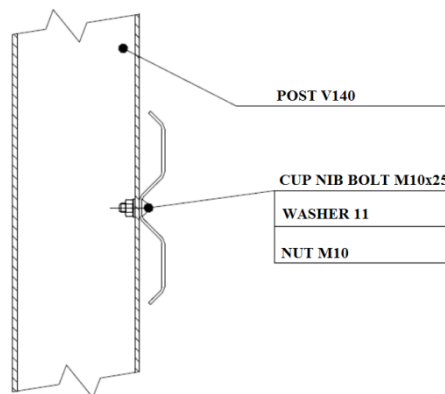
A lower beam is rolled from a sheet of thickness of 3 mm. It has a cross section with height 214 mm and with width 28 mm. The length of a lower beam is similar as the length of a barrier strip, i.e. 4250 mm [10].

Two lower beams are interconnected with four cup nib bolt M16x30 with nuts M16 and washers 17,5 in such a way that the end of one lower beam is overlapped with the beginning of the second lower beam [10].



**Figure 2.23: Lower beam interconnection [10]**

A lower beam is connected to a post with a cup nib bolt M10x25, a nut M10 and a washer 11 [10].



**Figure 2.24: Lower beam and post interconnection [10]**

A post has a V-shaped cross section with a wall thickness of 5 mm and with width of 140 mm, therefore it is denoted as a post V140. It has the length of 2170 mm and is installed every 2 m of a crash barrier [52].

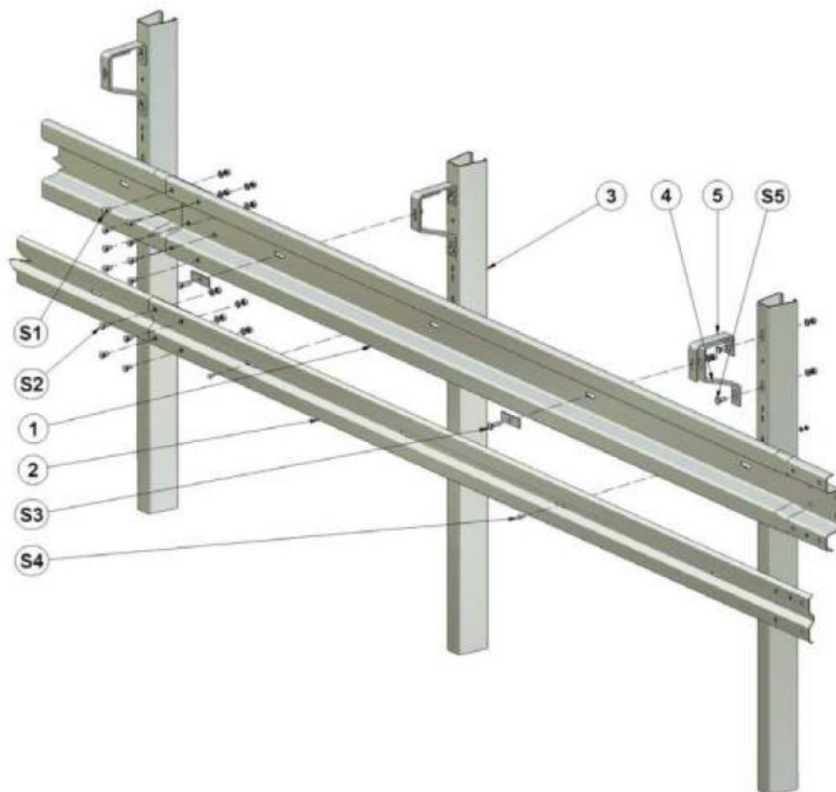
Usually the posts of length 1500 mm, 1900 mm and 2170 mm are spiled, if a ground surface is paved at least with depth of 100 mm. In exceptional cases (i.e. when it is not possible to spile or when the depth is limited) the posts are concreted into the foundation base with width of at least 0,40 m and with depth of 0,80 m. In this case the posts can be shortened so that they could be concreted to the depth of at least 0,50 m [52].

There are two height transitions used: long (the length of two barrier strips) and short (the length of one barrier strip). For both transitions a camming reducer is needed. For a long height transition a camming reducer is NH4 8,5%, for a short one it is NH4 17,3% [52].

When a long height transition is applied the first two posts are common posts with length of 2170 mm, remaining four posts are of length 1900 mm [52].

In case of a short height transition the posts bearing the barrier strips are of length 1900 mm, the posts bearing the lower beams have length of 1500 mm [52].

Concluding a description of JSNH4/H2 construction and interconnection of its separate parts we would like to present a sketch of the safety barrier and a table of its basic elements taken from technical conditions of the manufacturer.



**Figure 2.25: JSNH4/H2 safety barrier model [4]**

**Table 2.13: Basic components of JSNH4/H2 [4]**

Name	Position in Fig. 2.25	Material	Pcs/4m
Barrier strip NH4	1	S235JR	1
Lower beam SP3	2	S235JR	1
Outer post V140 2170	3	S355MC	2
Spacer NH4 V	4	S235JR	2
Spacer NH4 VI	5	S235JR	2

**Table 2.13 - continuation [4]**

Name	Position in Fig. 2.25	Material	Pcs/4m
Cup nib bolt M16x30-4.6-tZn	S1		8
Washer 17.5-tZn	S1		8
Nut M16-6-tZn	S1		8
Cup nib bolt M16x30-4.6-tZn	S2		4
Washer 17.5-tZn	S2		4
Nut M16-6-tZn	S2		4
Cup nib bolt M16x55-4.6-tZn	S3		2
Backplate M16	S3		2
Washer 17.5-tZn	S3		2
Nut M16-6-tZn	S3		2
Cup nib bolt M10x25-4.6-tZn	S4		2
Washer 11-tZn	S4		2
Nut M10-6-tZn	S4		2
Cup nib bolt M16x40-4.6-tZn	S5		4
Washer 17.5-tZn	S5		4
Nut M16-6-tZn	S5		4

From the table we can see that two types of steel are used for JSNH4/H2 safety barrier: S235JR for the majority of the parts and S355MC for posts.

S235JR is unalloyed, carbon, hot-rolled structural steel generally suitable for welding [16]. Its chemical composition is shown in table 2.14.

**Table 2.14: Chemical composition of S235JR [16]**

Nominal thickness $\leq$ 40 mm. C max = 0.17						
Nominal thickness $\leq$ 40 mm. CEV max = 0.35						
C	Mn	P	S	N	Cu	CEV
max 20	max 1,4	max 0,04	max 0,04	max 0,012	max 0,55	max 0,38

**Table 2.15: Mechanical properties of S235JR [16]**

Nominal thickness [mm]	≤ 16
Minimum yield strength ReH [MPa]	235
Nominal thickness [mm]	> 3 ≤ 100
Tensile strength Rm [MPa]	360-510
Nominal thickness [mm]	> 3 ≤ 40
Minimum elongation $L_0 = 5,65\sqrt{S_0}$ [%]	26
<b>Notch impact test</b>	
Temperature [°]	20
Min. absorbed energy [J]	27

S355MC is a thermo-mechanically rolled fine grained hot rolled weldable material suitable for cold forming [26]. Its chemical composition and mechanical properties are described by the following tables.

**Table 2.16: Chemical composition of S355MC [26]**

The sum of Nb, V and Ti shall be max 0,22 %								
C	Si	Mn	P	S	V	Nb	Ti	Al
max 0,12	max 0,5	max 1,5	max 0,025	max 0,02	max 0,2	max 0,09	max 0,15	min 0,015

**Table 2.17: Mechanical properties of S355MC [26]**

Nominal thickness [mm]	-
Minimum yield strength ReH [MPa]	355
Nominal thickness [mm]	-
Tensile strength Rm [MPa]	430-550
Nominal thickness [mm]	to 3
Minimum elongation $L_0=80$ mm (%)	19
Nominal thickness [mm]	from 3
$L_0 = 5,65\sqrt{S_0}$ [%]	23
<b>Notch impact test</b>	
Temperature [°]	- 20
Min. absorbed energy [J]	40 (the average from 3 samples)



### 2.2.2.2. Safety barrier JSAM-2/H2

A safety barrier of type JSAM-2/H2 is a single-sided crash barrier with containment level H2, working distance of 1,6 m (W5), dynamic deflection of 1,5 m, ASI of 1,1 and system weight of 29 kg/m. It has been tested with the same crash tests as JSNH4/H2: TB 11 and TB 51 [53]. Its construction is shown in Figure 2.26.

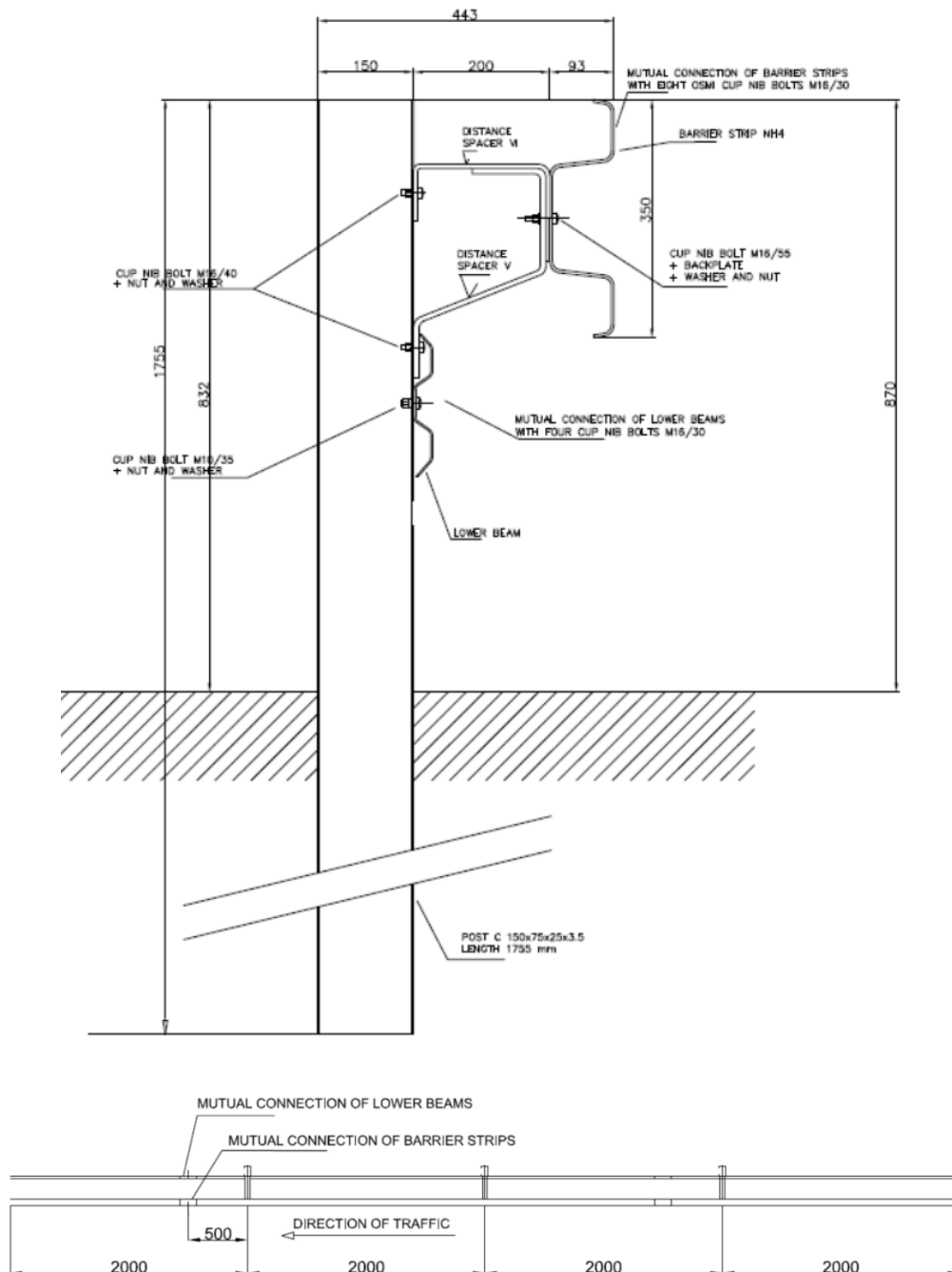


Figure 2.26: Safety barrier JSAM-2/H2 [53]

JSAM-2/H2 has been designed for containment level H2 and can be used for the following containment levels:

**Table 2.18: Containment levels of JSAM-2/H2 [53]**

Containment level	Where it can be used
Up to H1	on normalized sideways roads with width behind the front part of a crash barrier at least 1 m and in central dividing strips with width at least 2,40 m as two parallel crash barriers (if TP 114 permit to use H1)
H2	in places, where behind the front part of a crash barrier there is a flat surface (slope up to 10 %) of width at least 1,50 m and in central dividing strips with width of at least 2,60 m as two parallel crash barriers (if TP 114 permit to use H2)

The distance of JSAM-2/H2 from a solid obstacle depends on the containment level the barrier is used for and it is shown in table 2.19.

**Table 2.19: Distance of the front part of a crash barrier JSAM-2/H2 from a solid obstacle [53]**

Crash barrier type	Containment level	Distance [m]
JSAM-2/H2	N2	0,80
	H1	1,10
	H2	1,60

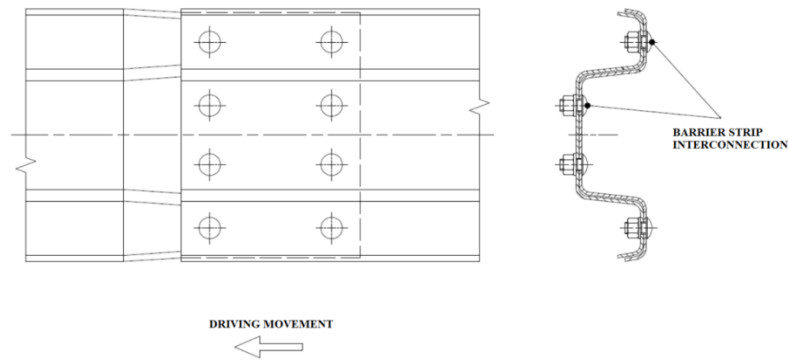
As far for the height measuring and installation are concerned the process is the same as in case of a safety barrier JSNH4/H2 described in the previous chapter and shown on corresponding figures.

The minimum length of JSAM-2/H2 is defined for speed  $\leq 80$  km/h as 52 m and for  $> 80$  km/h as 80 m [53].

A safety barrier JSAM-2/H2 consists of barrier strips, two parts of a spacer, a lower beams and posts [53].

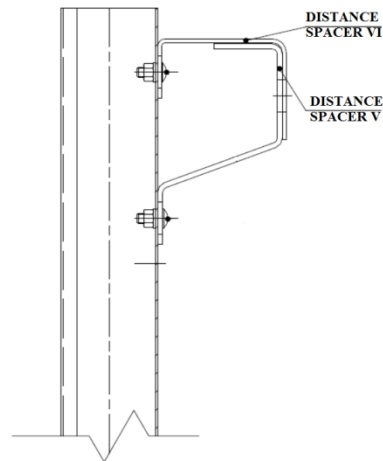
A barrier strip is of type AM having thickness of 2,8 mm. The cross section of AM has the same height as NH4, i.e. 350 mm, and width of 92,8 mm. The length of one barrier strip is the same as NH4 has, i.e. 4250 mm. Its upper edge is 0,870 mm above the roadside [9].

Two barrier strips are interconnected with eight cup nib bolts M16x30, nuts M16 and washers 17,5.



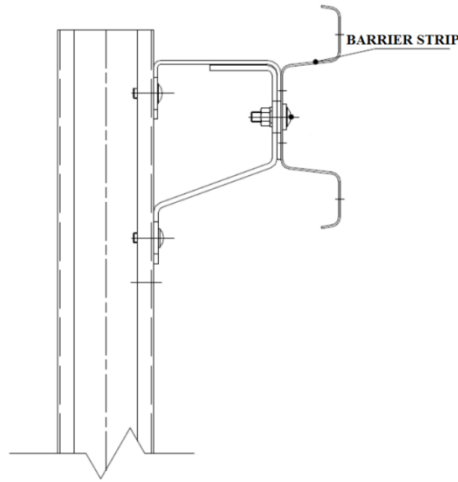
**Figure 2.27: Barrier strip interconnection [9]**

Spacer V is the lower part of a spacer made of a steel profile 50/8 mm, whereas spacer VI is the upper part of the spacer made of a steel profile 50/6 mm. Both parts are connected to the posts with cup nib bolts M16/40, nuts M16 and washers [9].



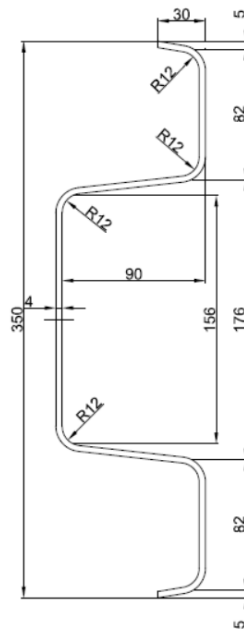
**Figure 2.28: Spacer parts interconnection [9]**

A barrier strip is fastened to a spacer with one cup nib bolt M16x55 and a nut M16. There is a backplate under the head of a bolt and a washer 17,5 under the nut [9].



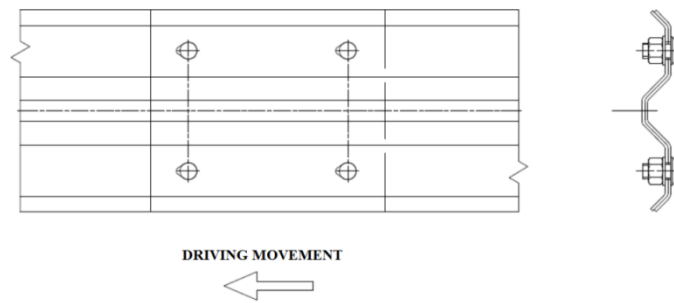
**Figure 2.29: Barrier strip and distance spacer interconnection [9]**

A lower beam AM is rolled from a sheet of thickness of 2,8 mm. The cross section has the height of 214 mm and the width of 28 mm. The length of a lower beam is the same as the length of a barrier strip, i.e. 4250 mm [9].



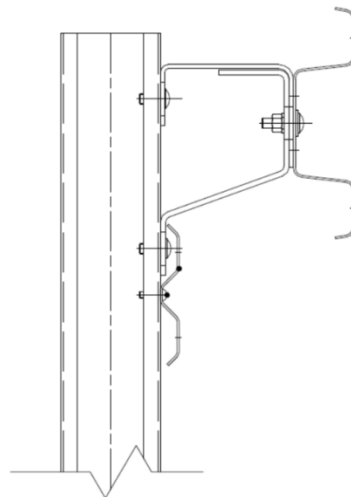
**Figure 2.30: Lower beam of JSAM-2/H2 [52]**

Lower beams are interconnected with four cup nib bolts M16x30, nuts M16 and washers 17,5 in such a way that the end of one lower beam is overlapped over the beginning of the other [9].



**Figure 2.31: Lower beam interconnection [9]**

A lower beam is connected to a post with one cup nib bolt M10x25, a nut M10 and a washer 11 [9].



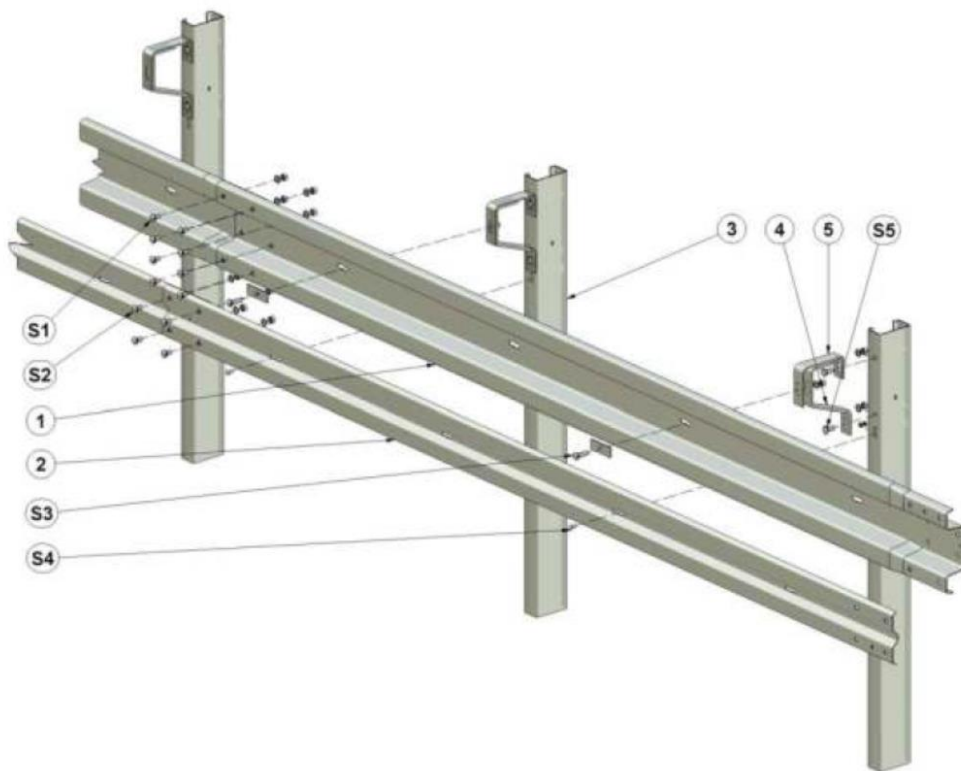
**Figure 2.32: Lower beam and post interconnection [9]**

A post is made of a bent sheet metal of thickness of 3,5 mm. It has C-shaped cross section of 150x75x25 mm. The length of a post is 1755 mm and it is placed every 2 m. The posts are commonly spiled [9].

As in the case of JSNH4/H2 there are two vertical height transitions used:

- a long one (the length of two barrier strips). For a barrier strip AM a camming reducer NH4 8,5% is used, whereas for a lower beam a camming reducer SP3 8,5% is applied.
- a short one (the length of one barrier strip). For a barrier strip AM a camming reducer NH4 17,3% is used, whereas for a lower beam a camming reducer SP3 17,3% is applied.

Below we can see the construction of JSAM-2/H2 and a list of its main elements (both a figure and a table taken from technical conditions of the manufacturer).



**Figure 2.33: JSAM-2/H2 safety barrier model [5]**

**Table 2.20: Basic components of JSAM-2/H2 [5]**

Name	Position in Fig. 2.33	Material	Pcs/4m
Barrier strip AM	1	S355MC	1
Lower beam AM	2	S355MC	1
Post C150x75x25 - 1755	3	S420MC	2
Spacer NH4 V	4	S235JR	2
Spacer NH4 VI	5	S235JR	2
Cup nib bolt M16x30-4.6-tZn	S1		8
Washer 17.5-tZn	S1		8
Nut M16-6-tZn	S1		8
Cup nib bolt M16x30-4.6-tZn	S2		4
Washer 17.5-tZn	S2		4
Nut M16-6-tZn	S2		4

**Table 2.20 - continuation [5]**

Name	Position in Fig. 2.33	Material	Pcs/4m
Cup nib bolt M16x55-4.6-tZn	S3		2
Backplate M16	S3		2
Washer 17.5-tZn	S3		2
Nut M16-6-tZn	S3		2
Cup nib bolt M10x25-4.6-tZn	S4		2
Washer 11-tZn	S4		2
Nut M10-6-tZn	S4		2
Cup nib bolt M16x40-4.6-tZn	S5		4
Washer 17.5-tZn	S5		4
Nut M16-6-tZn	S5		4

Notice that in case of JSAM-2/H2 there are three types of steel used: S235JR, S355MC and S420MC. The two formers have been described in the previous chapter in connection with a safety barrier JSNH4/H2. The latter one is a new type, which has more controlled mechanical properties, much lighter and therefore contributes in the overall weight reduction.

S420MC is defined as a hot-rolled, high-strength, low-alloy steel, which chemical composition and mechanical properties are listed in the following tables [27].

**Table 2.21: Chemical composition of S420MC [27]**

The sum of Nb, V and Ti shall be max 0,22 %								
C	Si	Mn	P	S	V	Nb	Ti	Al
max 0,12	max 0,5	max 1,6	max 0,025	max 0,015	max 0,2	max 0,09	max 0,15	min 0,015

**Table 2.22: Mechanical properties of S420MC [27]**

Nominal thickness [mm]	-
Minimum yield strength ReH [MPa]	420
Nominal thickness [mm]	-
Tensile strength Rm [MPa]	480-620
Nominal thickness [mm]	to 3
Minimum elongation L <sub>0</sub> =80 mm (%)	16
Nominal thickness [mm]	from 3

Table 2.22 - continuation [27]

$L_0 = 5,65\sqrt{S_0}$ [%]	19
<b>Notch impact test</b>	
Temperature [°]	- 20
Min. absorbed energy [J]	40 (the average from 3 samples)

Concluding this chapter the following table presents general characteristics of both selected types of safety barriers showing their similarities and differences. Differences are marked in bold and dashed.

Table 2.23: Comparison of JSNH4/H2 and JSAM-2/H2

	JSNH4/H2	JSAM-2/H2
<b>Manufacturer</b>	ArcelorMittal Distribution Solutions Czech Republic, s.r.o.	ArcelorMittal Distribution Solutions Czech Republic, s.r.o.
<b>Type</b>	Single-sided safety barrier	Single-sided safety barrier
<b>Containment level</b>	H2	H2
<b>Dynamic deflection</b>	<b><u>1,75 m</u></b>	<b><u>1,5 m</u></b>
<b>Working width</b>	<b><u>1,85 m</u></b>	<b><u>1,6 m</u></b>
<b>Acceleration severity index</b>	<b><u>1,186</u></b>	<b><u>1,1</u></b>
<b>Material</b>	S235JR, S355MC	S235JR, S355MC, <b><u>S420MC</u></b>
<b>Type of a barrier strip</b>	NH4: <b><u>thickness 4 mm</u></b> , length 4250 mm	AM: <b><u>thickness 2,8 mm</u></b> , length 4250 mm
<b>Lower beam</b>	SP3: <b><u>thickness 3 mm</u></b> , height 214 mm, width 28 mm, length 4250 mm	AM: <b><u>thickness 2,8 mm</u></b> , height 214 mm, width 28 mm, length 4250 mm
<b>Post</b>	<b><u>V140: thickness of a wall 5 mm, width 140 mm, length 2170 mm</u></b>	<b><u>C 150x75x25: thickness of a wall 3,5 mm, width 150 mm, length 1755 mm</u></b>
<b>Weight</b>	<b><u>42,67 kg/m</u></b>	<b><u>29 kg/m</u></b>

As we can see from the table application of a new steel type, i.e. S355MC for barrier strips and lower beams and S420MC for a post, has allowed producing these parts of safety barrier

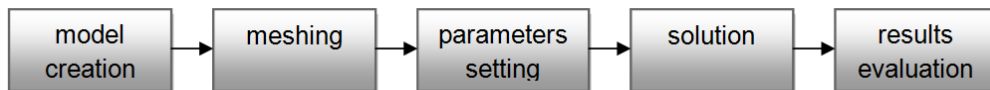


JSAM-2/H2 with smaller thickness. Besides, the post has been changed both in terms of cross section and its dimensions. All these have had an effect on such important parameters as dynamic deflection, working width and acceleration severity index, which values have decreased; herein containment level has remained the same. This basically improves characteristics of a safety barrier. But the main achievement concerns the weight, which the manufacturer has managed to decrease to app. 32% that is from 42, 67 kg/m to 29 kg/m. This fact is not only beneficial in terms of costs, but also in respect to influence on environment as well as in terms of maintenance and installation.

On the basis of mentioned characteristics, parameters and sketches of both selected types of safety barriers JSNH4/H2 and JSAM-2/H2 we have created corresponding models in ANSYS Workbench, specified all necessary parameters and made numerical simulation. A detailed procedure as well as evaluation of obtained results is discussed in the next chapters.

### 3. Practical part

The present part is devoted to the very numerical simulation of a vehicle impact on two selected types of safety barriers. The whole process of simulation resp. steps performed during it can be described as follows:



**Figure 3.1: Simulation process**

As shown in Figure 3.1 the first step is a model creation, during which we create separate parts of safety barriers in accordance with corresponding sketches and technical documentation of the manufacturer. 3D models of safety barriers have been created in programme DesignModel, which is a part of ANSYS Workbench.

Then again using ANSYS Workbench the discretization of geometrical models has been fulfilled. After meshing we need to transfer our models into format that can be used in LS-DYNA PrePost, which serves for analysis preparation in LS-DYNA. ANSYS Workbench allows direct data export using k-file format. Material, cross sectional and partially contact properties as well as the minimum time step and termination conditions have been defined in LS-DYNA PrePost, though some contact definitions have been made automatically in ANSYS Workbench.

Having defined all necessary parameters and properties we can move to solution, which is performed in LS-DYNA using FEM methods.

Our last step is results comparison and evaluation in compliance with the objectives of the present paper mentioned in the first chapter.

All these steps are described in the next subchapters in more details.

### 3.1. Geometrical model creation

The models of safety barriers JSNH4/H2 and JSAM-2/H2 have been created in ANSYS Workbench. We have used Cartesian coordinate system and the following units: m, N, s, kg, rad/s, °C.

The process of creation of geometrical models of both barriers is pretty much the same; therefore we would speak about it in general specifying some details for a concrete type where necessary.

Actually the process of simulation will look as follows:



Figure 3.2: System's inputs and outputs

From this figure we see that there are some inputs to the system. These inputs are provided by a vehicle with corresponding characteristics, which we shall model as well. The outputs are supposed to be values of internal energy, displacement, velocities and so on. On the basis of outputs we would be able to make some conclusion about our system.

Basically the whole system we need to create for numerical simulation can be presented as shown in Figure 3.3.

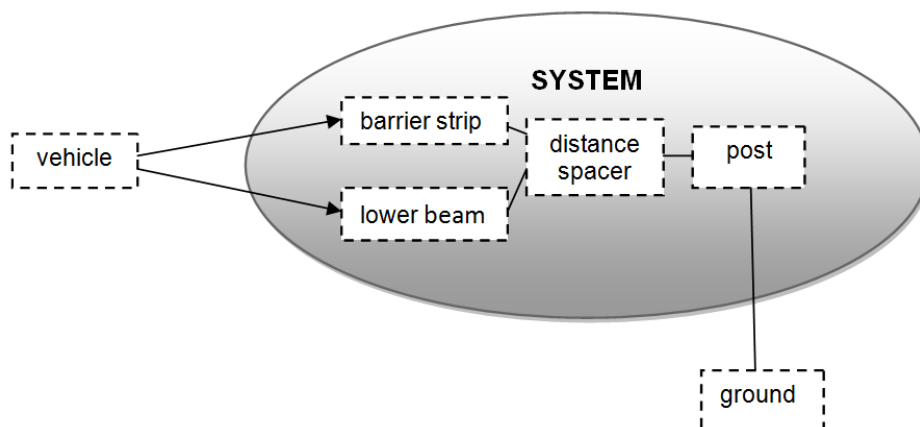


Figure 3.3: Structure of the system

where we have the model of a safety barrier and an environment, which is the ground fixing the post and preventing barrier's movement, and a vehicle colliding with a safety barrier.

A model of a safety barrier itself consists of a post, two parts of a spacer, barrier strips and lower beams. These elements are actually interconnected using bolts, nuts and washers specified in technical documentation of the manufacturer. Besides the geometrical model has mutual connection of two barrier strips as well as two lower beams. This interconnection in a real system is provided with eight bolts for barrier strips resp. six bolts for lower beams, using nuts and washers as well. However, we have replaced these connecting elements with bonded face contacts, which allow the nodes of an unstructured part to be bonded to a face of another unstructured part and do not take into account friction between elements. Bonded contact alleviates the requirement that for joining purposes two nodes need to reside at the same physical location. The nodes that are to be bonded to a face may have an offset with respect to the face and the offset is a user-defined maximum physical normal distance of a node from a face which can be bonded together [3]. During the analysis the nodes are kept at the same relative position on the face to which they are bonded. This simplification reduces time consumption and complexity of calculation on the one hand and gives sufficient results in respect to our objectives on the other hand.

All parts of each geometrical model have exactly the same sizes as specified in technical documentation of the manufacturer and shown on sketches in previous chapters.

For purposes of numerical simulation we need to create a model of the ground and a vehicle, which will impact the safety barrier under consideration.

The ground in both cases is represented by rectangular blocks of dimensions 1300x1500x1945 mm for JSNH4/H2 and 1300x1500x1600 mm for JSAM-2/H2. Notice that the height of rectangular blocks differs. It is explained by different height of the posts of JSNH4/H2 and JSAM-2/H2: JSNH4/H2 has a post of height 2170 mm and JSAM-2/H2 post is of 1755 mm, whereas the height of the post under the ground is the same, i.e. 832 mm.

In the ground we have created a cylinder of radius 250 mm and height of 1345 mm for JSNH4/H2 resp. of radius 250 mm and height 1000 mm for JSAM-2/H2. The difference in height again is due to the dimensions of the posts of two types of safety barriers. This cylinder will represent the fact that the post is concreted to the base and fixed in such a way to the ground.

To be able to perform proper simulation and obtain reasonable results we need to make a hole in a cylinder to place there the post as well as a hole in the ground to place there the cylinder. ANSYS Workbench allows making it easily using Boolean operations. Generally Boolean algebra used in ANSYS Workbench provides a means for combining sets of data, using such logical operators as intersect, union, subtract, etc. We can apply Boolean operations to almost any solid model construction. The only exceptions are that Boolean operations are not valid for entities created by concatenation and that some Boolean operations cannot always be performed on entities that contain degeneracies [3].

In our case we need to use Subtract operation, where we should specify the target body, from which we want to subtract some part, and a tool body, using which we will subtract this part [3]. In case of subtraction from the ground the target body is the ground itself and the tool body is a cylinder. Similarly in case of subtraction from the cylinder the target body is the cylinder and the tool body is the post. It is the way how we have created the ground.

As far as a vehicle is concerned it is represented by a semi-cylinder of radius 124,97 mm and height 700 mm. It is located in such a way that its upper edge is on the level of upper edge of the post and its height is sufficient enough to impact both a barrier strip and a lower beam (see Figure 3.3). On this stage the vehicle does not touch the crash barrier and is only app. 20 mm distanced from it.

Because we would solve our problem as a symmetrical one, we suppose the symmetry in a place of loading of our model. This fact explains why we have used a semi-cylinder instead of a whole cylinder for a model of a vehicle. The impact area in case of symmetry is app. 0,25x0,25 m that is in compliance with standards as mentioned in previous chapters.

During calculation process the programme takes the whole area of each two resp. more parts, which touch each other and calculates it. However, the real contact area could be much smaller. For example, a contact area of two barrier strips is only 320 mm, whereas the length of one barrier strip is 4250 mm. But if we do not make some modifications, then the programme would take the whole length of a barrier strip. It is very unpractical and time consuming. Thus, to decrease the complexity of calculations, to save time and to increase the efficiency we have separate contact areas from the whole area using Slice operation, which slice a body in a certain place and thus allows working separately with "sliced" parts. The Slice feature has five options: Slice by Plane, Slice Off Faces, Slice by Surface, Slice Off Edges and Slice by Edge Loop [3]. For our purposes we have used Slice by Plane option, where we have defined a plane, by which we want to slice a certain body.

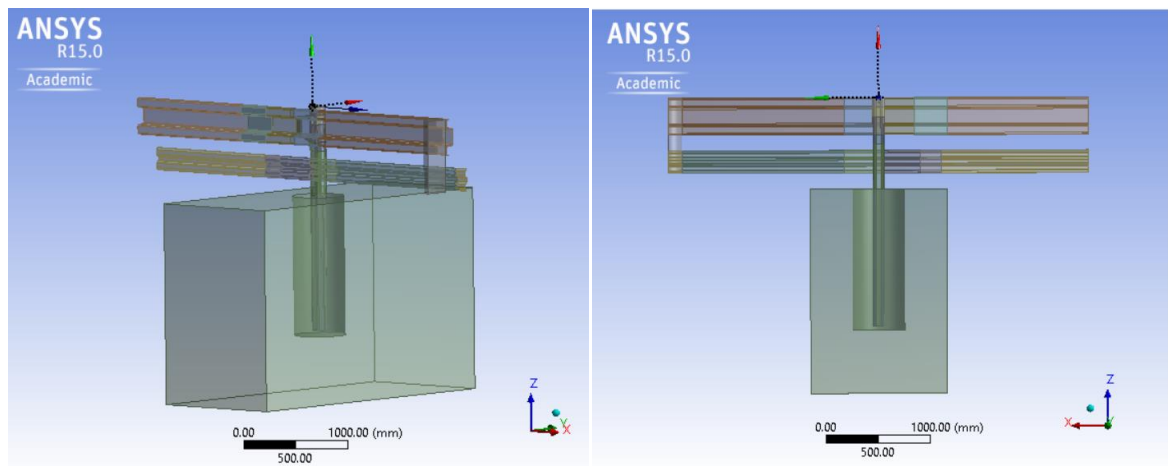
In such a way we have separated the following contact areas of a barrier strip:

- contact areas of two barrier strips,
- a contact area of a barrier strip with a distance spacer,
- a contact area of a barrier strip and a vehicle.

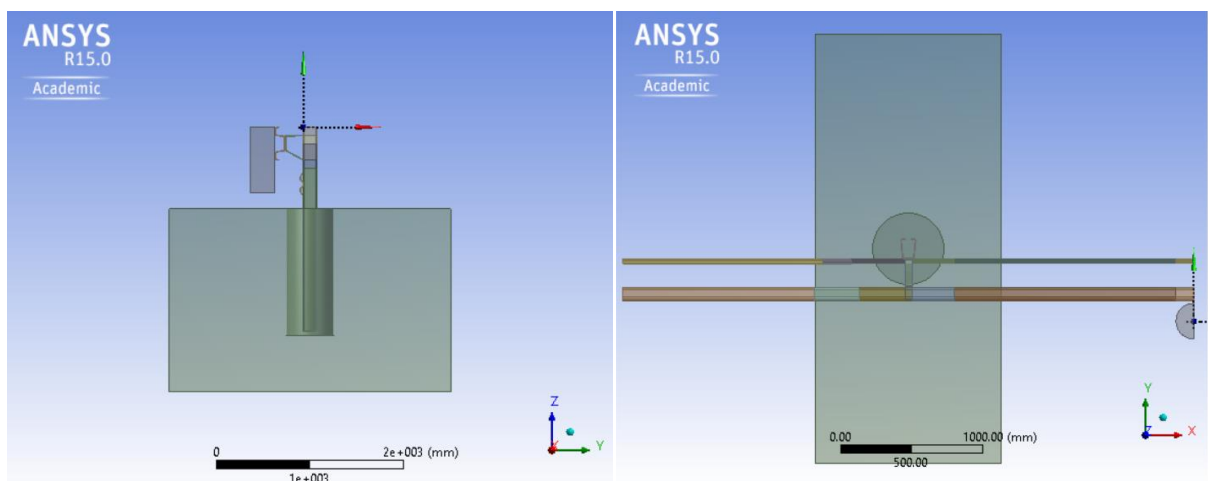
A lower beam has been sliced in place of two lower beams overlapping, in place of contact with the post and in place of an impact with a vehicle.

The post has been sliced as well in places of contact with a distance spacer, a lower beam and the ground.

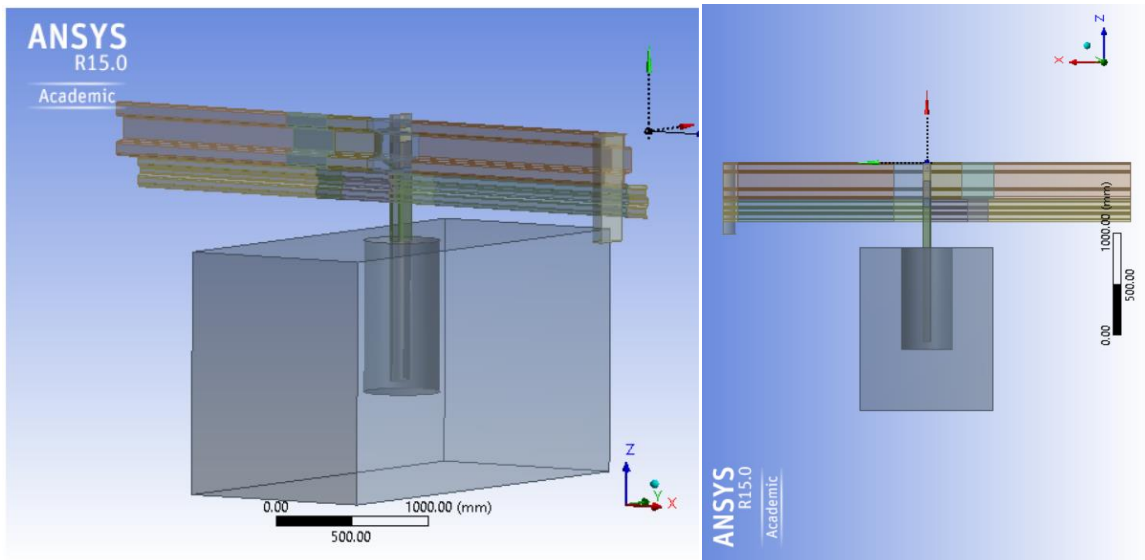
In the result of all fulfilled operations our model consists of 24 parts/bodies. Remaining 3 bodies represent a vehicle, the ground and a concrete base.



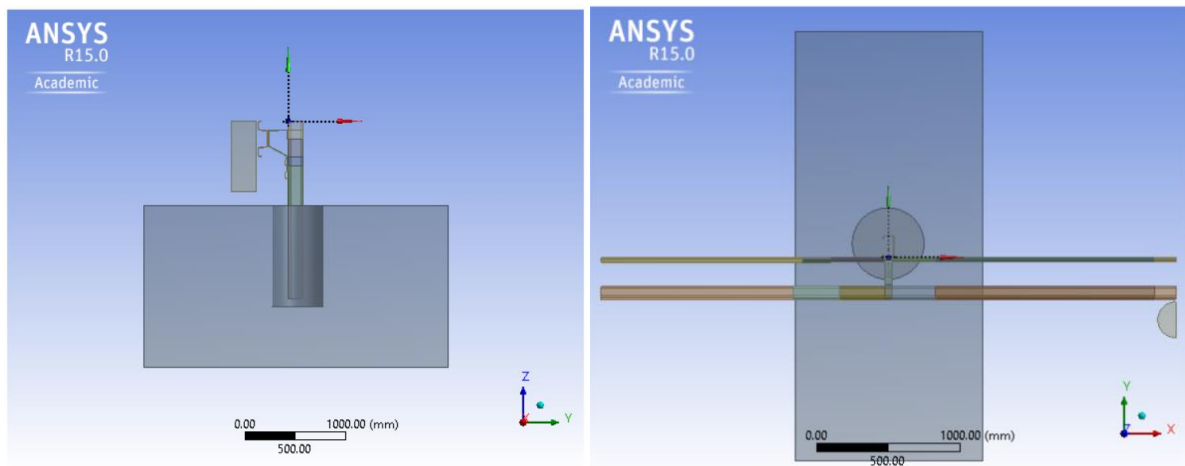
**Figure 3.4: Geometrical model of JSNH4/H2**



**Figure 3.5: Geometrical model of JSNH4/H2 - side and top view**



**Figure 3.6: Geometrical model of JSAM-2/H2**



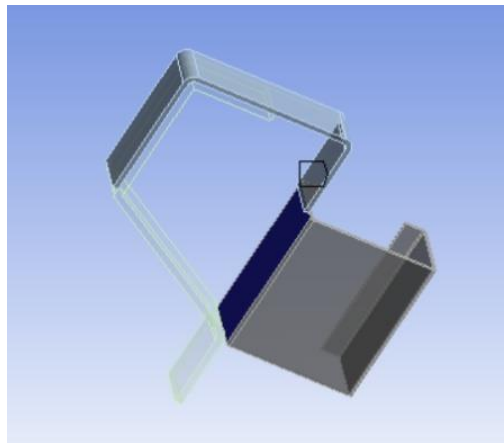
**Figure 3.7: Geometrical model of JSAM-2/H2 - side and top view**

The notion of rigid body is widely used for numerical simulation and represents one object in a model. It consists of a set of target nodes called rigid body nodes and a single pilot node. The motion of the rigid body is governed by the degrees of freedom (DOFs) at the pilot node, allowing accurate representation of the geometry, mass, and rotary inertia of the rigid body [3]. In our model, for instance, rigid bodies are a barrier strip, a lower beam, the post (precisely their sliced elements) etc.

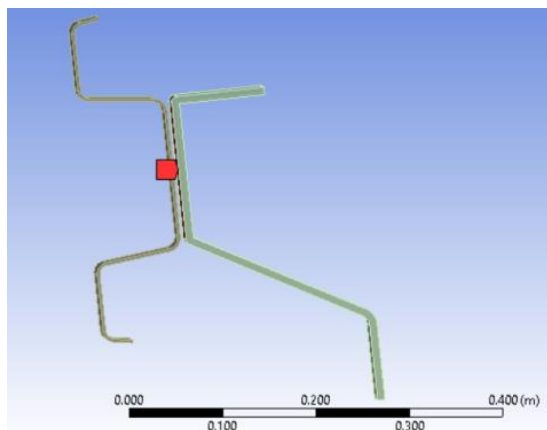
A part is defined as a group of elements having a unique combination of material, type or other properties [3]. In our case we have 27 parts, each of which is for one body. But we can group several bodies together, so that a part can consist of a number of bodies.

Simulation of a vehicle impact on a safety barrier using FEM is highly non-linear dynamic process, therefore correct contact setting is very important. Contacts ensure that during calculation there will be correct interaction of separate parts of a model (between a safety barrier and a vehicle as well as between elements of a safety barrier itself). One contact region is always created with two areas or a group of areas. One of the areas or a group of areas is so called "contact bodies" and the other one is so called "target bodies" [3]. As it was mentioned previously all contacts are of type "Bonded".

Originally the model has had 35 contacts, but after examining them we have concluded that several of them are needless and would cause mistakes during calculation process. Therefore we have suppressed them, so that the programme would not take these contacts into account. The examples of these contacts can be seen from the following figures:

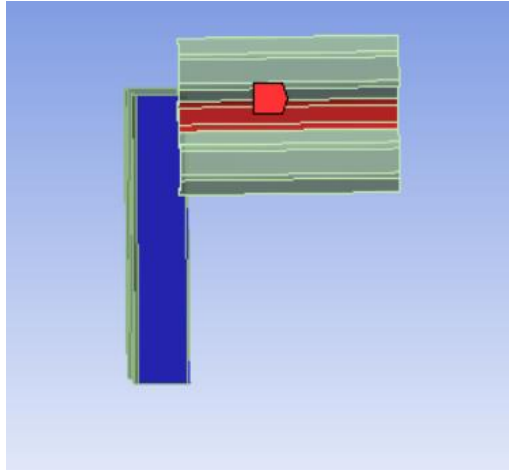


**Figure 3.8: "Imaginary" contact between the upper part of a distance spacer and sliced part of a post**



**Figure 3.9: "Imaginary" between a barrier strip and the lower part of a distance spacer**





**Figure 3.10: "Imaginary" contact between a barrier strip and a post**

From these examples we see that actually there is no contact between two parts, but the programme automatically assigned the contact. We have found 9 needless contact regions and after suppressing these regions we have only 26 contact areas for each of the models.

Other information about the contacts is presented in table 3.1:

**Table 3.1: Contact regions**

<b>Type:</b>	Bonded
<b>Scope Mode:</b>	Automatic
<b>Behavior:</b>	Program Controlled
<b>Trim Contact:</b>	Program Controlled
<b>Trim Tolerance:</b>	$1,3904 \cdot 10^{-2}$ m
<b>Maximum Offset</b>	$1 \cdot 10^{-7}$ m

After creation of geometrical model we shall make discretization using programme tools. Meshing means dividing the model into finite number of elements. The mesh tools in ANSYS Workbench provide a convenient path to many of the most common mesh controls, as well as to the most frequently performed meshing operations. Mesh controls allow establishing such factors as the element shape, midside node placement, and element size to be used in meshing the solid model [3]. We have used default meshing and for our purposes this meshing is sufficient. The resulted structure has the following parameters: smoothing is medium, element size is 20 mm, minimum edge length is in the range from 2,36 mm to 3 mm. Other properties of meshing are presented in the following tables:

**Table 3.2: Meshing properties for JSNH4/H2 model**

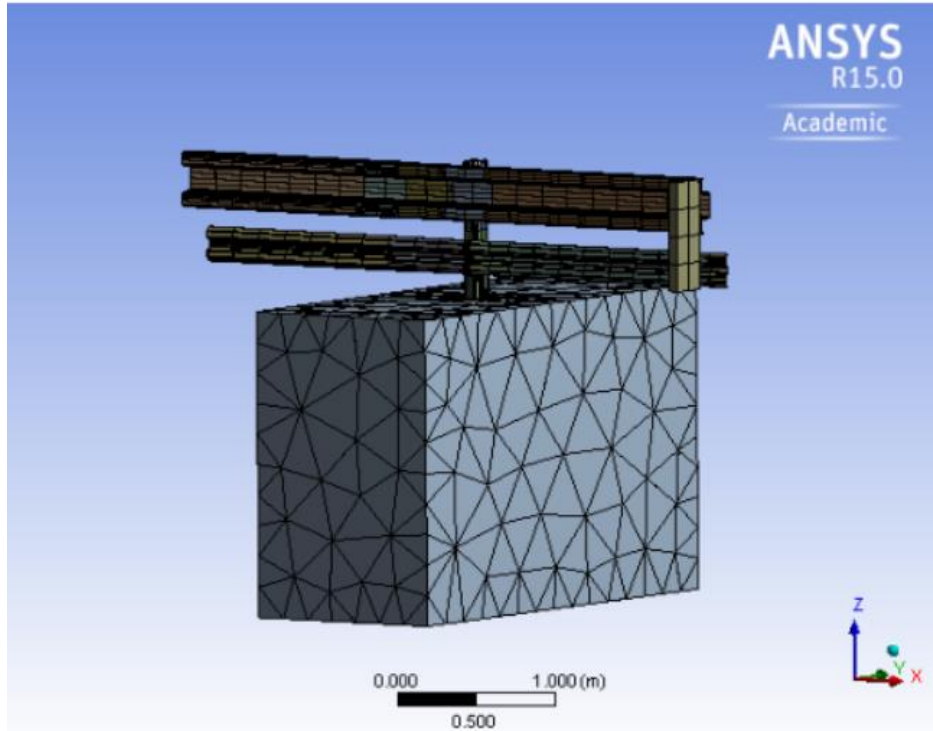
<b>Dimensions:</b>	
Relevance Center	Medium
Element Size	0,20 m
Smoothing	Medium
Span Angle Center	Medium
Minimum Edge Length	$3 \cdot 10^{-3}$ m
<b>Inflation:</b>	
Inflation Option	Smooth Transition
Transition Ratio	0,272
Maximum Layers	5
Growth Rate	1,2
<b>Statistics:</b>	
Nodes	8044
Elements	12801

**Table 3.3: Meshing properties for JSAM-2/H2 model**

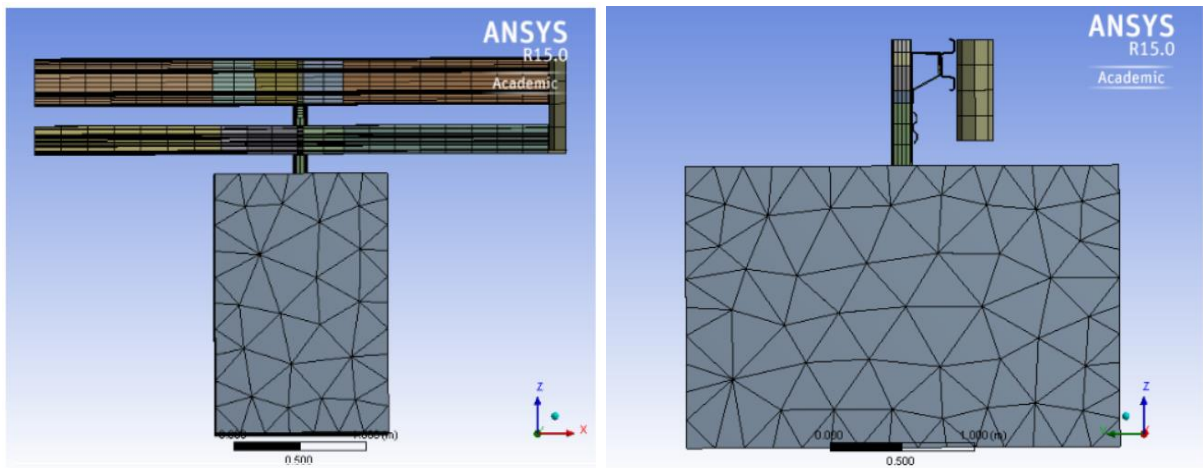
<b>Dimensions:</b>	
Relevance Center	Medium
Element Size	0,20 m
Smoothing	Medium
Span Angle Center	Medium
Minimum Edge Length	$2,3562 \cdot 10^{-3}$ m
<b>Inflation:</b>	
Inflation Option	Smooth Transition
Transition Ratio	0,272
Maximum Layers	5
Growth Rate	1,2
<b>Statistics:</b>	
Nodes	7266
Elements	11022

In the result we have a model of JSNH4/H2 consisting of 8044 nodes and 12801 elements and a model of JSAM-2/H2 consisting of 7266 nodes and 11022 elements.

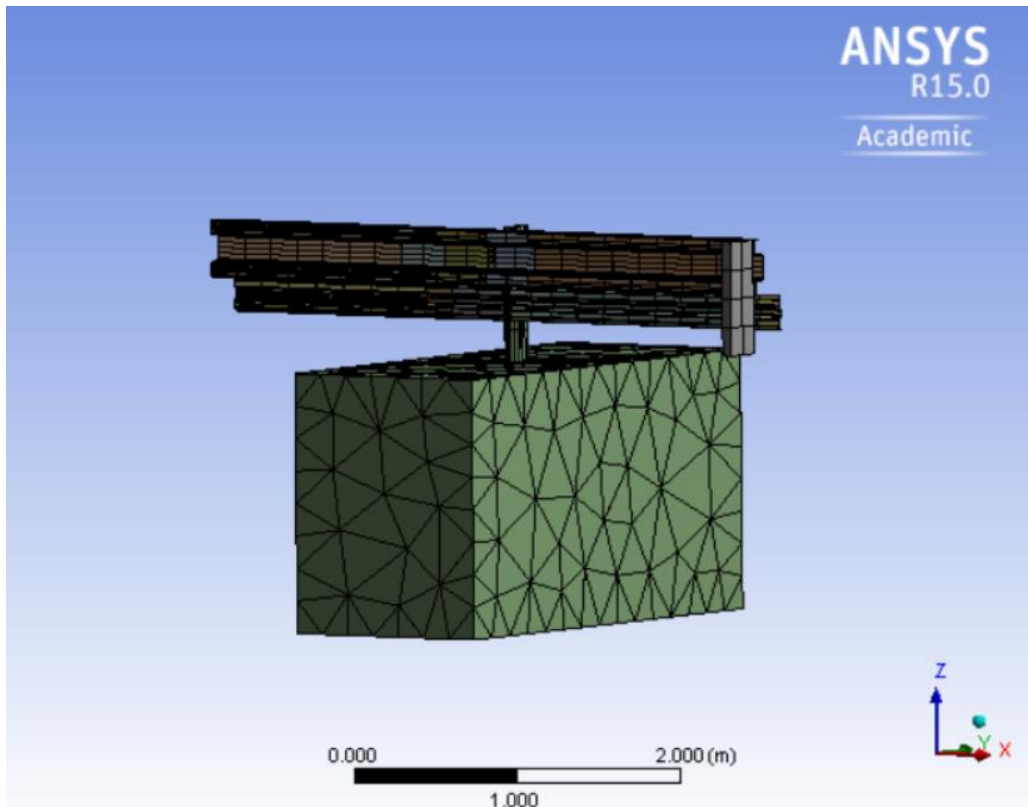
The following figures illustrate the meshed models:



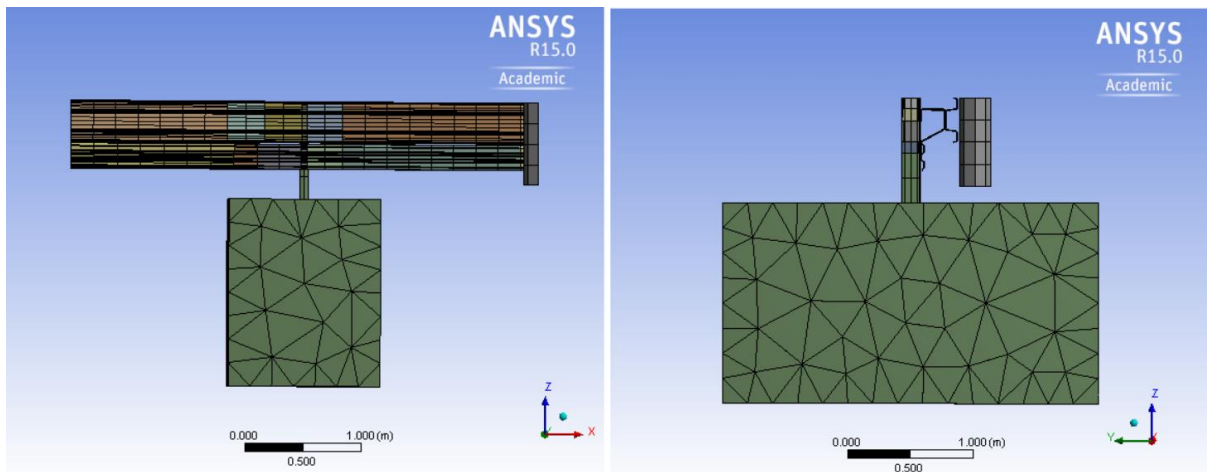
**Figure 3.11: Meshing of JSNH4/H2**



**Figure 3.12: Meshing of JSNH4/H2 - front and side view**



**Figure 3.13: Meshing of JSAM-2/H2**



**Figure 3.14: Meshing of JSAM-2/H2 - front and side view**

Below there are several tables showing general information about the whole model and its separate parts.

**Table 3.4: Parameters of the whole construction - JSNH4/H2**

<b>Dimensions of axes:</b>	
Length, X-axis	4000 mm
Length, Y-axis	3000 mm
Length, Z-axis	2819,9 mm
<b>Properties:</b>	
Volume	$7,6171 \cdot 10^3 \text{ m}^3$
Weight	59794 kg
<b>Statistics:</b>	
Bodies	27
Nodes	8044
Elements	12801

**Table 3.5: Parameters of the whole construction - JSAM-2/H2**

<b>Dimensions of axes:</b>	
Length, X-axis	4000 mm
Length, Y-axis	3000 mm
Length, Z-axis	2435,8 mm
<b>Properties:</b>	
Volume	$6,2679 \cdot 10^3 \text{ m}^3$
Weight	16665 kg
<b>Statistics:</b>	
Bodies	27
Nodes	7266
Elements	11022

In the following table separate parts of the construction and their parameters are listed:

**Table 3.6: Properties of separate parts of JSNH4/H2**

Name	Properties		Statistics	
	Volume [m <sup>3</sup> ]	Mass [kg]	Nodes	Elements
Sloup	1,6564*10 <sup>-4</sup>	1,3003	104	25
Sloup	1,8513*10 <sup>-4</sup>	1,4533	104	25
Sloup	3,3128*10 <sup>-4</sup>	2,6006	96	23
Sloup	1,7149*10 <sup>-4</sup>	1,3462	104	25
Sloup	8,4185*10 <sup>-4</sup>	6,6085	184	66
Sloupek_spodni_cast	2,5333*10 <sup>-3</sup>	19,887	368	154
Distancni dil VI	1,2878*10 <sup>-4</sup>	1,0109	68	16
Distancni dil V	2,1796*10 <sup>-4</sup>	1,711	88	28
Svodnice	2,7745*10 <sup>-4</sup>	2,1779	164	40
Svodnice	3,2973*10 <sup>-3</sup>	25,884	666	288
Svodnice	6,7227*10 <sup>-4</sup>	5,2773	222	72
Svodnice	1,0671*10 <sup>-4</sup>	0,83767	156	38
Svodnice	6,4026*10 <sup>-4</sup>	5,026	186	60
Svodnice	6,8294*10 <sup>-4</sup>	5,3611	264	86
Svodnice_2	6,9734*10 <sup>-4</sup>	5,4741	222	72
Svodnice_2	2,9201*10 <sup>-3</sup>	22,923	752	322
Pasnice	9,6135*10 <sup>-5</sup>	0,75466	100	24
Pasnice	1,1425*10 <sup>-3</sup>	8,9689	396	168
Pasnice	2,7731*10 <sup>-4</sup>	2,1769	132	42
Pasnice	3,6975*10 <sup>-5</sup>	0,29025	124	30
Pasnice	2,2185*10 <sup>-4</sup>	1,7415	108	34
Pasnice	1,479*10 <sup>-4</sup>	1,161	128	31
Pasnice_2	1,5022*10 <sup>-4</sup>	1,1792	88	21
Pasnice_2	1,0515*10 <sup>-3</sup>	8,2544	464	196
Auto	1,7172*10 <sup>-2</sup>	134,8	30	12
Valec	0,26156	2053,2	2317	9622
Obdelnik	7,3214	57473	409	1281

**Table 3.7: Properties of separate parts of JSAM-2/H2**

Name	Properties		Statistics	
	Volume [m <sup>3</sup> ]	Mass [kg]	Nodes	Elements
Sloup1	9,8802*10 <sup>-5</sup>	0,77559	98	32
Sloup2	1,0729*10 <sup>-3</sup>	8,422	228	120
Slouph2	1,1043*10 <sup>-4</sup>	0,86684	84	26
Slouph3	1,976*10 <sup>-4</sup>	1,5512	80	26
Slouph4	1,0229*10 <sup>-4</sup>	0,80297	84	26
Slouph5	4,5797*10 <sup>-4</sup>	3,5951	114	48
Vzpera1	1,2878*10 <sup>-4</sup>	1,0109	68	16
Vzpera2	2,1822*10 <sup>-4</sup>	1,7131	86	26
Svodh1	2,248*10 <sup>-4</sup>	1,7647	156	38
Svodh2	4,8662*10 <sup>-4</sup>	3,82	222	72
Svodd1	1,0358*10 <sup>-4</sup>	0,81314	88	21
Svodnice12	2,2855*10 <sup>-3</sup>	17,941	666	288
Svodnice13	4,496*10 <sup>-4</sup>	3,5293	186	60
Svodnice14	7,4933*10 <sup>-5</sup>	0,58822	148	36
Svodnice15	4,7208*10 <sup>-4</sup>	3,7058	222	72
Svodnice16	4,7957*10 <sup>-4</sup>	3,7646	300	98
Svodnice22	2,0377*10 <sup>-3</sup>	15,996	800	343
Pasnice12	1,0531*10 <sup>-3</sup>	8,2669	396	168
Pasnice13	2,0717*10 <sup>-4</sup>	1,6263	108	34
Pasnice14	3,4528*10 <sup>-5</sup>	0,27105	116	28
Pasnice15	2,5896*10 <sup>-4</sup>	2,0328	132	42
Pasnice16	1,3811*10 <sup>-4</sup>	1,0842	132	32
Pasnice21	1,4013*10 <sup>-4</sup>	1,1	88	21
Pasnice22	9,8091*10 <sup>-4</sup>	7,7002	480	203
Valec	1,7172*10 <sup>-2</sup>	134,8	30	8
Beton	0,19528	476,48	1796	8027
Zemina	6,0437	15961	358	1111

The last thing we defined in ANSYS Workbench was the boundary conditions.

For both models we have defined displacement (A and D in Figures 3.15 and 3.16) of barrier strips and lower beams from right and left sides so that these elements cannot move in direction of x-axis, whereas in direction of y-axis and z- axis there is a free movement. Then we have specified displacement of a vehicle, so that the movement in direction of x-axis (B in Figures 3.15 and 3.16) and z-axis (C in Figures 3.15 and 3.16) is restricted. The movement of the ground (E, F, G in Figures 3.15 and 3.16) is not allowed in either direction.

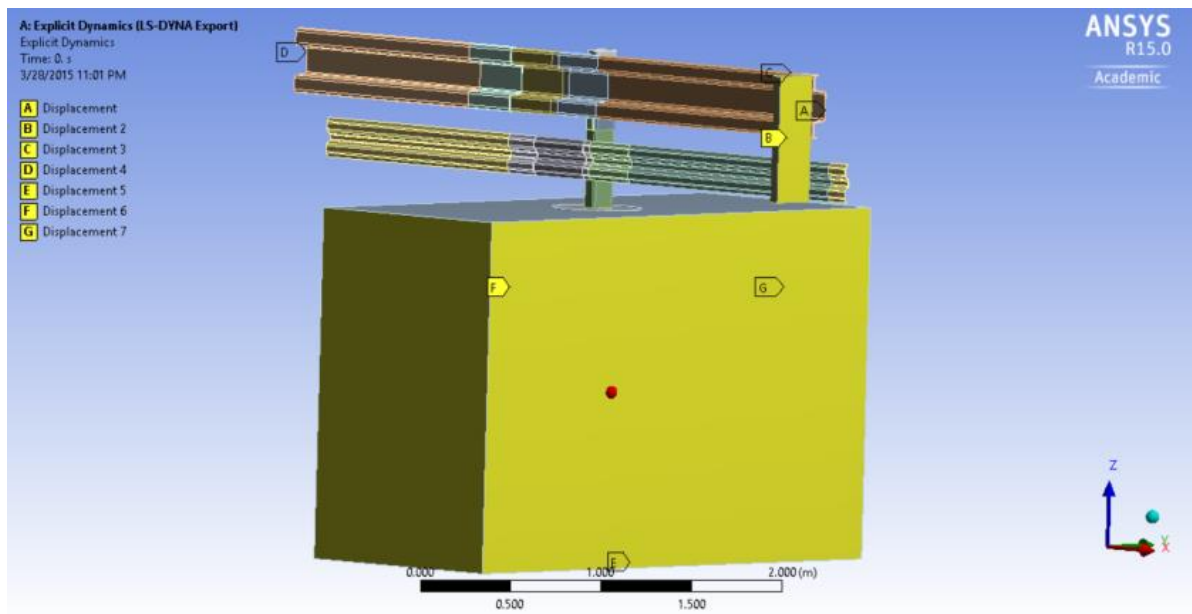


Figure 3.15: Boundary conditions for JSNH4/H2

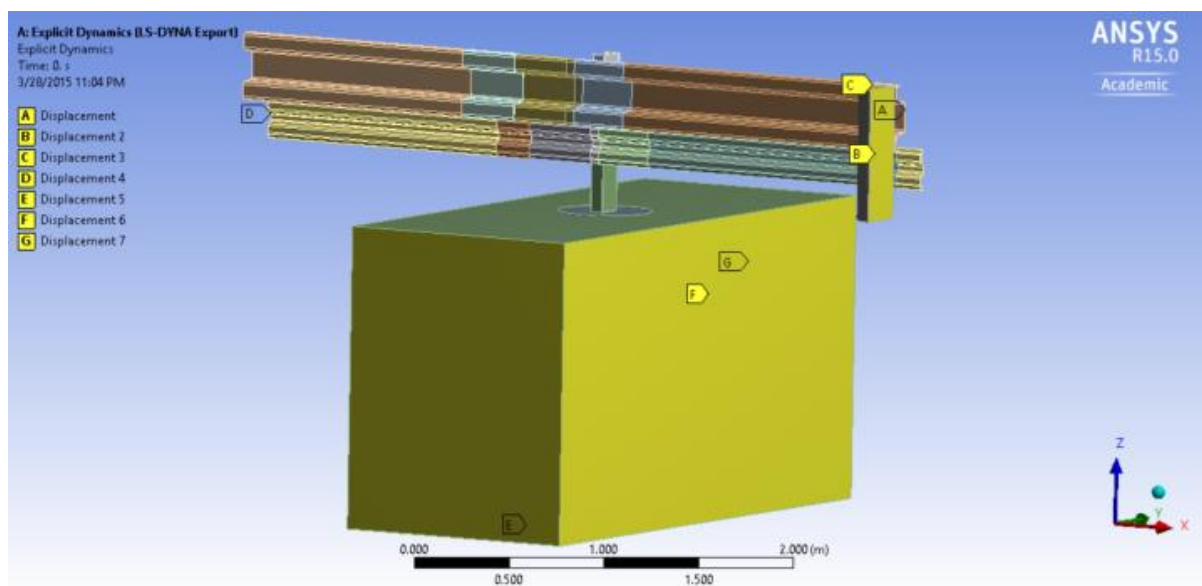


Figure 3.16: Boundary conditions for JSAM-2/H2



After creating geometrical models of both types of safety barriers, generating meshing and defining displacement we have created k-file. It allows using our models in LS-DYNA PrePost, where we will specify all other necessary parameters such as material properties of each part of the safety barriers, crash test characteristics and numerical simulation parameters. Actually this issue is discussed in the next chapter of the present paper.

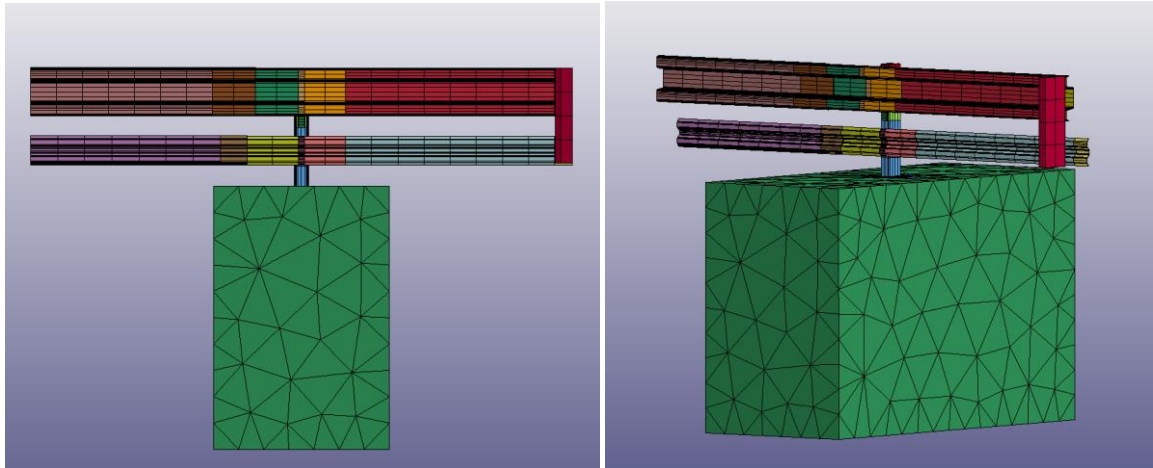
## **3.2. Definition of geometrical model properties and numerical simulation parameters in LS-DYNA PrePost**

From previous chapters we know that LS-DYNA is a general purpose transient dynamic finite element program capable of simulating complex real world problems. LS-DYNA PrePost in its turn is an advance pre/post-processor for LS-DYNA, which provides full support for LS-DYNA keywords, LS-DYNA model visualization, model creation and editing and post-processing. Its main post-processing capabilities include states result animation, fringe component plotting, and XY history plotting. The user interface here is designed to be both efficient and intuitive [33].

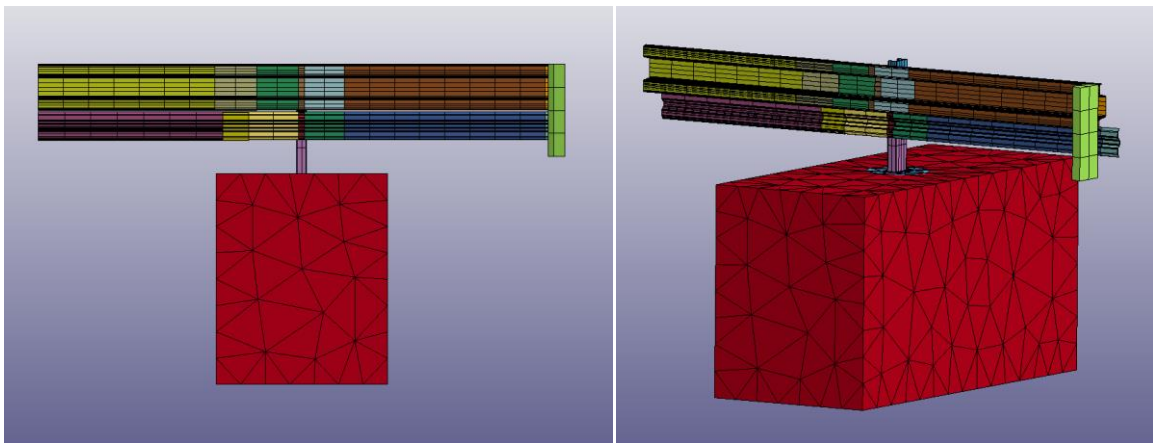
LS-DYNA PrePost works with k-files. The keyword input provides a flexible and logically organized database that is simple to understand. Similar functions are grouped together under the same keyword. For example, under the keyword \*ELEMENT there are included solid, beam, shell elements, spring elements, discrete dampers, seat belts, and lumped masses. Besides there can be defined different sections. For example, there is a control section for resetting LS-DYNA defaults, a material section for defining material properties, an element section where element part identifiers and nodal connectivities are defined, a section for defining parts, and so on [34].

Several sections that are essential for our models would be discussed in details in this chapter.

After creating k-file in ANSYS Workbench and uploading it to LS-DYNA PrePost we have obtained the following models:



**Figure 3.17: JSNH4/H2 in LS-DYNA PrePost**



**Figure 3.18: JSAM-2/H2 in LS-DYNA PrePost**

As we remember we have two models corresponding to two safety barriers types - JSNH4/H2 and JSAM-2/H2 - created in ANSYS Workbench and exported to LS-DYNA PrePost. For each of the models we need to perform several simulations of crash tests to be able to evaluate whether the respective model fulfills the requirements for containment level H2 or not. Crash tests we want to perform numerical simulation for are TB11, TB42 and TB51.

According to TP 114 TB11 is defined to be a crash test with a passenger car of weight 900 kg and with the following crash conditions: crash speed 100 km/h, crash angle 20°, kinetic energy 40,6 kNm [49].

Analogically TB42 is a crash test, when a safety barrier suffers from an impact of a lorry of weight 10 000 kg, at crash speed 70 km/h and crash angle 15°, with kinetic energy 126,6 kNm [49].

TB51 presents a crash test with the following parameters: an impact of a bus of weight 13 000 kg, crash speed 70 km/h, crash angle 20°, kinetic energy 287,5 kNm [49].

Thus, we see that besides some common parameters for each crash test such as material properties of safety barriers and contact adjustment we need to set crash test parameters such as crash speed and angle as well as vehicle density, which can be calculated from vehicle mass defined in TP 114.

All these adjustments can be made in Keyword Manager, from where we have access to all important for us keyword sections. The most important in our case are such sections as BOUNDARY, CONTACT, CONTROL, DEFINE, INITIAL and MAT. Other sections as, for instance, TITLE is just for our information and does not influence numerical simulation results.

Let start from the less important sections and continue with more important ones where we have to set parameters correctly to be able to perform numerical simulation and obtain reliable results.

In keyword section DAMPING we can define damping either globally or by part identifier [34]. For all our models we have define GLOBAL option, which defines mass weighted nodal damping that applies globally to the nodes of deformable bodies and to the mass center of the rigid bodies.

DATABASE keyword control section is primarily used to control the output of ASCII databases and binary files output by LS-DYNA [34]. We have here binary d3plot for complete output states and binary restart file to be able to make a restart from certain point of numerical simulation if needed.

In NODE keyword section we can see different nodes of our models and their coordinates in the global coordinate system [34]. Also, the boundary conditions in global directions can be specified. We do not make any changes in this section after exporting our models from ANSYS Workbench to LS-DYNA PrePost.

In keyword SECTION the element formulation, integration rule, nodal thickness, and cross sectional properties are defined [34]. We do not change anything there as well and just control if everything is correct.

Very interesting section is a SET section, where we can find the list of nodes, parts and segments. It provides us with a convenient way of defining groups of nodes, parts, elements, and segments, thus, helping to work with the model and make appropriate adjustments [34].

In ELEMENT section we can find identifiers and connectivities for all elements, in our case for solids. Option SOLID defines three-dimensional solid elements including 4-noded tetrahedrons and 8-noded hexahedrons [34]. Also, here a local coordinate system for orthotropic and anisotropic materials and further parameters can be defined.

For us it is very important to control whether the boundary conditions specified in ANSYS Workbench have been transferred to LS-DYNA PrePost correctly. This can be made in section BOUNDARY, where we have PRESCRIBED\_MOTION\_SET card. This card defines an imposed nodal motion (velocity, acceleration, or displacement) on a node or a set of nodes [34]. After looking at defined boundary conditions there we have been ensured that everything is correct, i.e. we have seven displacements defined for corresponding component of a safety barrier or for a vehicle, or for the ground. These displacements have been described in previous chapter and there is no need to describe them again.

Because crash impact simulation using FEM is a non-linear dynamic process, it is very important to set contacts between different parts of the model correctly. Therefore, one of the most important sections is a CONTACT section, which actually allows defining many different contact types. The surface definition for contact is made up of segments on solid element surfaces [34]. Here we need to make several changes, because not all contacts were defined correctly after exporting, thus, causing the errors during numerical simulation. Besides several significant contacts such as contact between a vehicle and barrier strip/lower beam or contact between barrier strip/lower beam, distance spacer and the post need more accurate definition, because they greatly influence numerical simulation itself as well as the obtained results.

One contact is presented by two regions or a group of regions, where one of them is so-called "master" and other is a "slave". There are a lot of different methods how to define contacts and solve the calculation of contact forces. Among these methods are Penalty Method, Kinematic Constrain Method and Distributed Parameter Method [34].

For all contact regions except those between a vehicle and barrier strip/lower beam and between barrier strip/lower beam, distance spacer and the post we have used TIED\_NODES\_TO\_SURFACE\_OFFSET, which is based on Penalty Method, where during simulation the penetration between nodes of "slave" and "master" regions is controlled and if

there is penetration through the "master" region the force and moment (if applicable) resultants are transferred discrete spring elements between the slave nodes and master segments. Besides in this option we need to specify different parameters such as whether slave and master side forces included, birth and death time when contact surface becomes active/deactivated, different coefficients of friction and scale factors and so on [34]. After specifying the contact type nodes-to-surface we leave almost all other parameters as default. Some of these parameters with their corresponding values are listed below in the following table:

**Table 3.8: Parameters for tied nodes to surface offset contacts**

Name	Value	Description
<b>SSTYP</b>	4	slave segment set or node set type "4" means node set ID for node to surface contact
<b>MSTYP</b>	0	master segment type "0" means segment set ID
<b>SBOXID</b>	0	includes only slave segments within specified box
<b>MBOXID</b>	0	includes only master segments within specified box
<b>SPR</b>	1	includes the slave side in the DATABASE_NCFORC and the DATABASE_BINARY_INTFOR interface force files "1" means that slave side forces are included.
<b>MPR</b>	1	includes the master side in the DATABASE_NCFORC and the DATABASE_BINARY_INTFOR interface force files "1" means that master side forces are included.
<b>FS</b>	0	static coefficient of friction
<b>FD</b>	0	dynamic coefficient of friction "0" is default value
<b>DC</b>	0	exponential decay coefficient "0" is default value
<b>VC</b>	0	coefficient for viscous friction, which is necessary to limit the friction force to a maximum
<b>VDC</b>	0	viscous damping coefficient in percent of critical
<b>PENCHK</b>	0	small penetration in contact search option "0" is default value meaning that check is turned off
<b>BT</b>	0	birth time when contact surface becomes active "0" is default value
<b>DT</b>	$1.000 \times 10^{20}$	death time when contact surface is deactivated default value

**Table 3.8 - continuation**

<b>Name</b>	<b>Value</b>	<b>Description</b>
<b>SFS</b>	0	scale factor on default slave penalty stiffness
<b>SFM</b>	0	scale factor on default master penalty stiffness
<b>SST</b>	-1.666*10 <sup>-7</sup>	optional thickness for slave surface (overrides true thickness) Negative value determines whether or not a node is tied to depend only on the separation distance relative to the absolute value of these thicknesses.
<b>MST</b>	-1.666*10 <sup>-7</sup>	optional thickness for master surface (overrides true thickness)
<b>SFST</b>	1	scale factor for slave surface thickness (scales true thickness) "1" is default value
<b>SFMT</b>	1	scale factor for master surface thickness (scales true thickness) "1" is default value
<b>FSF</b>	1	Coulomb friction scale factor "1" is default value
<b>VSF</b>	1	viscous friction scale factor "1" is default value
<b>SOFT</b>	2	soft constraint option "2" means pinball segment based contact
<b>SOFSCL</b>	0	scale factor for constraint forces of soft constraint option
<b>LCIDAB</b>	0	load curve ID defining airbag thickness as a function of time
<b>MAXPAR</b>	1.025	maximum parametric coordinate in segment search default value
<b>SBOPT</b>	3	it is a segment-based contact option "3" is for warped segment checking.
<b>DEPTH</b>	5	it is a search depth in automatic contact. It defines the accuracy of calculation for crash applications. "5" is quite a great value, so that the accuracy is very high, but on the other hand is quite expensive in terms of calculations
<b>BSORT</b>	0	it is the number of cycles between bucket sorts
<b>FRCFRQ</b>	1	it specifies the number of cycles between contact force updates for penalty contact formulation. This option can provide a significant speed-up of the contact treatment.

For contact between a vehicle and barrier strip/lower beam and for contact between barrier strip/lower beam, distance spacer and the post we have specified

AUTOMATIC\_SINGLE\_SURFACE contact, which allows avoiding duplicate contact treatment [34]. We have to do this, because duplicate contact treatment can lead to numerical instabilities.

But before making this we have to create two new entities SET\_PART using Entity Creation option. The first entity comprises such parts as a vehicle, contact part of a barrier strip and a lower beam. The second entity consists of contact parts of a barrier strip, a lower beam, a distance spacer and the post.

After this for both new entities we have specified automatic single surface contact, which parameters are listed in the following table:

**Table 3.9: Parameters for automatic single surface contact**

Name	Value	Description
<b>SSTYP</b>	2	slave segment set or node set type "2" means part set ID
<b>MSTYP</b>	2	master segment type "2" means part set ID
<b>SBOXID</b>	0	includes only slave segments within specified box
<b>MBOXID</b>	0	includes only master segments within specified box
<b>SPR</b>	1	includes the slave side in the DATABASE_NCFORC and the DATABASE_BINARY_INTFOR interface force files "1" means that slave side forces are included
<b>MPR</b>	1	includes the master side in the DATABASE_NCFORC and the DATABASE_BINARY_INTFOR interface force files "1" means that master side forces are included
<b>FS</b>	0.7	static coefficient of friction
<b>FD</b>	0.5	dynamic coefficient of friction
<b>DC</b>	0.1	exponential decay coefficient
<b>VC</b>	0	coefficient for viscous friction, which is necessary to limit the friction force to a maximum
<b>VDC</b>	10	viscous damping coefficient in percent of critical
<b>PENCHK</b>	0	small penetration in contact search option "0" is default value meaning that check is turned off
<b>BT</b>	0	birth time when contact surface becomes active "0" is default value

**Table 3.9 - continuation**

<b>Name</b>	<b>Value</b>	<b>Description</b>
<b>DT</b>	1.000*10 <sup>20</sup>	death time when contact surface is deactivated default value
<b>SFS</b>	1	scale factor on default slave penalty stiffness
<b>SFM</b>	1	scale factor on default master penalty stiffness
<b>SST</b>	0	optional thickness for slave surface (overrides true thickness)
<b>MST</b>	0	optional thickness for master surface (overrides true thickness)
<b>SFST</b>	1	scale factor for slave surface thickness (scales true thickness) "1" is default value
<b>SFMT</b>	1	scale factor for master surface thickness (scales true thickness) "1" is default value
<b>FSF</b>	1	Coulomb friction scale factor "1" is default value
<b>VSF</b>	1	viscous friction scale factor "1" is default value
<b>SOFT</b>	2	soft constraint option "2" means pinball segment based contact
<b>SOFSCL</b>	0	scale factor for constraint forces of soft constraint option
<b>LCIDAB</b>	0	load curve ID defining airbag thickness as a function of time
<b>MAXPAR</b>	1.025	maximum parametric coordinate in segment search default value
<b>SBOPT</b>	3	it is a segment-based contact option "3" is for warped segment checking
<b>DEPTH</b>	5	it is a search depth in automatic contact. It defines the accuracy of calculation for crash applications. "5" is quite a great value, so that the accuracy is very high, but on the other hand is quite expensive in terms of calculations
<b>BSORT</b>	0	it is the number of cycles between bucket sorts
<b>FRCFRQ</b>	1	it specifies the number of cycles between contact force updates for penalty contact formulation. This option can provide a significant speed-up of the contact treatment.

From two tables we see that there is difference in settings of the following parameters: SSTYP, MSTYP, FS, FD, DC, VDC, SFS, SFM, SST and MST. For us four main parameters are important: static coefficient of friction (FS), dynamic coefficient of friction (FD), exponential decay coefficient (DC) and viscous damping coefficient (VDC). If friction and



viscous damping coefficients can be neglected between such parts of models as between, e.g., overlapping parts of barrier strip, then above mentioned coefficients are of a great significance when we speak about contact surfaces between a vehicle and barrier strip/lower beam or between lower beam and the post or between barrier strip, distance spacer and the post, i.e. contact surfaces, for which we have created separate entities and specified automatic single surface contact. In case of these contact surfaces friction coefficients as well as exponential decay coefficient and viscous damping coefficient cannot be equal to zero as in case of contact surfaces specified in tied-node-to-surface contact card. It is due to the fact that mainly in these contact regions the interaction between separate parts during an impact takes place and therefore their correct definition is very important for performing numerical simulation and obtaining trustworthy results [34].

One of the crucial steps in preparing models for numerical simulation is material definition. From technical documentation of the manufacturer we know that we need to define the following steel types:

1. JSNH4/H2:

- a) steel type S235JR for a barrier strip, a lower beam and a distance spacer,
- b) steel type S355MC for a post.

2. JSAM-2/H2:

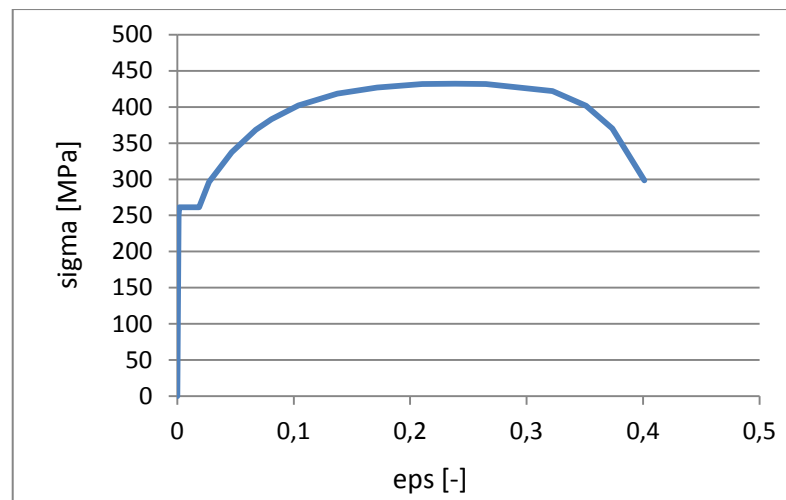
- a) steel type S235JR for a distance spacer,
- b) S355MC for a barrier strip and a lower beam,
- c) S420MC for a post.

Besides we need to define material properties for a vehicle, the ground and a concrete base.

There are a lot of material types presented in MAT keyword section. To define material properties of safety barrier models we have used material type 123 MODIFIED\_PIECEWISE\_LINEAR\_PLASTICITY, which allows defining an elasto-plastic material with an arbitrary stress versus strain curve and arbitrary strain rate dependency [34]. Here besides mass density, Young's modulus, Poisson's ratio, Yield stress and other coefficients we have to specify load curve for a certain steel type. The load curve can be defined in keyword section DEFINE, where we should input corresponding values of stress and deformation. Then curves are discretized internally with equal intervals along the abscissa for fast evaluation in constitutive models [34].

We can easily define a load curve for steel S235JR, because we possess information about values of stress and corresponding deformation. But there is a problem with steel types S355MC and S420MC, because the manufacturer is not eager to share information about load curves and it is necessary to make experimental tests of steel types, which could differ according to manufacturing rank. However, we have a load curve for steel type S355J0, which is from the same grade as S355MC and differs from it mainly in yield strength. Thus, we have afforded to use a load curve of S355J0 for our purposes. As far as S420MC is concerned, unfortunately we have not succeeded to find a load curve for this steel and we have been forced to use S355J0 for the post of JSAM-2/H2 model. We are aware that this fact can influence the obtained results. However, even with this incompliance we would obtain approximate behavior of a safety barrier and could fulfill our aims and decide on appropriateness of using numerical simulation.

As it was mentioned above steel S235JR ensures plastic deformation of the constructions. On the following figure S235JR load curve is shown and then table 3.10 lists values of stress and corresponding displacement.



**Figure 3.19: S235JR stress-strain curve**

On the horizontal axis a relative elongation is presented, whereas the vertical axis represents normal stress in MPa. The point that underlines stress value of 250 MPa is called the elastic limit, which is the lowest stress, at which permanent deformation can be measured. Beyond the elastic limit, permanent deformation will occur. Approximately in the point corresponding to stress of 261,357 MPa the yield limit is located. This is a point in the stress-strain curve, at which the curve levels off and plastic deformation begins to occur. According to our stress-strain curve stress of 432,264 MPa can be defined as a tensile strength, i.e. the maximum stress that a material can withstand while being stretched or pulled before failing or breaking.

The following table gives corresponding values of stress and strain of S235JR steel.

**Table 3.10: Plastic deformation of S235JR steel**

<b>Stress <math>\sigma</math> [MPa]</b>	<b>Plastic strain <math>\epsilon</math> [-]</b>
0	0
250	0
261,357	0,000394
261,374	0,017438
296,166	0,025916
337,484	0,045536
368,188	0,066076
383,139	0,079596
401,873	0,102776
418,229	0,136256
427,002	0,170476
431,52	0,208996
432,264	0,237316
431,495	0,263716
421,987	0,321016
401,378	0,349976
370,112	0,372516
298,677	0,399776

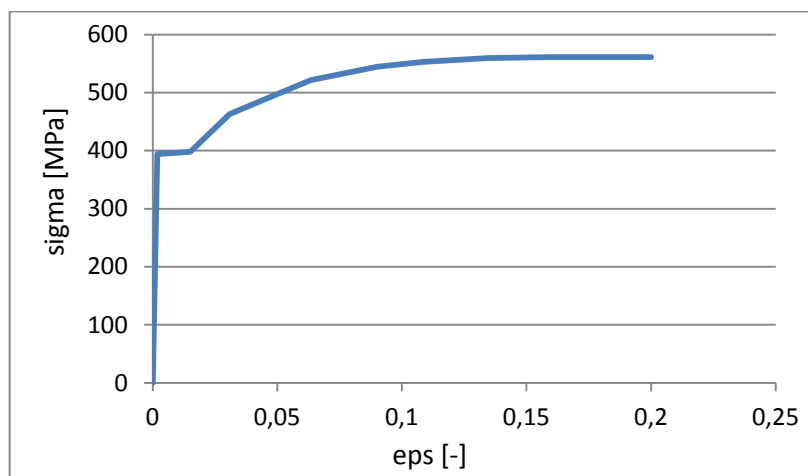
The following table presents properties of steel S235JR, some of which should be also specified in DEFINE keyword section.

**Table 3.11: Properties of steel S235JR**

<b>Mass density [kg/m<sup>3</sup>]</b>	7850
<b>Young's Modulus [Pa]</b>	$2,1 \cdot 10^{11}$
<b>Poisson's Ratio [-]</b>	0,3
<b>Bulk Modulus [Pa]</b>	$1,75 \cdot 10^{11}$
<b>Shear Modulus [Pa]</b>	$8,0769 \cdot 10^{10}$
<b>Compressive Yield Strength [Pa]</b>	$2,5 \cdot 10^8$
<b>Tensile Yield Strength [Pa]</b>	$2,5 \cdot 10^8$
<b>Tensile Ultimate Strength [Pa]</b>	$4,6 \cdot 10^8$

After defining a load curve in DEFINE keyword section by putting stress and strain values we can modify material type in MAT section (in our case it is MODIFIED\_PIECEWISE\_LINEAR\_PLASTICITY) by specifying in corresponding card created previously a load curve and putting values of mass density, Young's Modulus, Poisson's Ratio and Yield stress for this particular steel.

In such a way we have created material corresponding to steel S235JR. The same we would make for steel type S355J0. Its stress-strain curve is shown in Figure 3.20 and corresponding stress and strain values as well as steel properties are listed in tables 3.12 and 3.13.



**Figure 3.20: Stress-strain curve of steel S355J0**

**Table 3.12: Plastic deformation of steel S355J0**

Stress $\sigma$ [MPa]	Plastic strain $\epsilon$ [-]
0	0
394,282	0
398,173	0,01317
463,306	0,02896
521,525	0,06144
544,678	0,08838
553,195	0,10660
559,473	0,13264
561,373	0,15788
561,500	0,18584

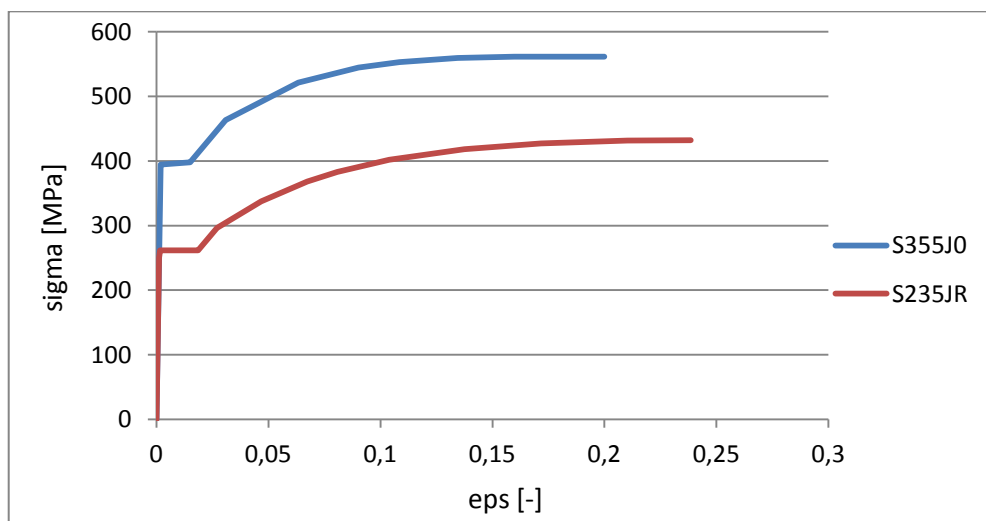
From the figure as well as from the table we can see that elastic limit is at a point of 394,282 MPa, yield limit is at a point of 398,173 MPa and tensile strength is at a point of 561,500 MPa.

Properties of steel S355J0 is presented in the following table:

**Table 3.13: Properties of steel S355J0 [17]**

<b>Mass density [kg/m<sup>3</sup>]</b>	7850
<b>Young's Modulus [Pa]</b>	$2,1 \cdot 10^{11}$
<b>Poisson's Ratio [-]</b>	0,3
<b>Bulk Modulus [Pa]</b>	$1,75 \cdot 10^{11}$
<b>Shear Modulus [Pa]</b>	$8,0769 \cdot 10^{10}$
<b>Yield Strength [Pa]</b>	$2,5 \cdot 10^8$

Figure 3.21 compares stress-strain curves of S235JR and S355J0. Thus, we can see that S355J0 can resist higher values of stress.



**Figure 3.21: Comparison of S235JR and S355J0**

Having completed these steps we have defined materials for safety barrier models JSNH4/H2 and JSAM-2/H2. But besides the safety barrier itself our system consists of a vehicle, the ground and a concrete base. It logically flows, that we need to define corresponding materials for these elements as well.

Let's begin with a vehicle. The process of definition of material is quite similar to that we have described above. But in this case we have no need to define any load curve. In MAT section we have material type 001-ELASTIC, which is suitable for definition of our vehicle. This type of material is isotropic elastic and available for beam, shell and solid elements in LS-DYNA. The axial and bending damping factors here can be used to damp down numerical noise [34]. Thus, we just need to choose this material type and specify the values of mass density, Young's Modulus, Poisson's ratio, axial and bending damping factor (if necessary) and defining these properties the process of material definition for our vehicle would end. Thus, we have the following values for specification of vehicle material type:

**Table 3.14: Parameters for specification of vehicle material type**

<b>Mass density [kg/m<sup>3</sup>]</b>	2,621*10 <sup>4</sup> (passenger car)/ 2,912*10 <sup>5</sup> (lorry)/ 3,785*10 <sup>5</sup> (bus)
<b>Young's Modulus [Pa]</b>	2,000*10 <sup>11</sup>
<b>Poisson's ratio [-]</b>	0,3
<b>Axial damping factor [-]</b>	0
<b>Bending damping factor [-]</b>	0

Notice that the value of mass density differs depending on what type of crash test we want to simulate. We have calculated mass density from the weight of a car and dimensions of a car model according to the following formula:

$$\rho = \frac{m}{2V} \left[ \frac{kg}{m^3} \right]$$

where  $\rho$  is a mass density [kg/m<sup>3</sup>],  $m$  is a car mass [kg],  $V$  is a volume [m<sup>3</sup>].

We have “2” in the denominator of the formula, because we are solving symmetrical task; thus, we need to divide mass density of a corresponding vehicle onto “2”.

For our car model we have used semi-cylinder with radius of 124,97 mm and height of 700 mm. The volume can be calculated from the formula for semi-cylinder:

$$V = \frac{\pi r^2 h}{2} [m^3]$$

where  $V$  is a volume [m<sup>3</sup>],  $r$  is a radius [m],  $h$  is a height [m].

We have the same volume for all crash tests:  $V=0,01717 \text{ m}^3$ , but the value of mass is different. According to TP 114 a passenger car is of mass 900 kg, a lorry is of mass 10 000 kg and a bus is of mass 13 000 kg. Using this information we can calculate mass density for each crash test. So we obtain a mass density of  $2,621 \cdot 10^4 \text{ kg/m}^3$  for a passenger car, a mass density of  $2,912 \cdot 10^5 \text{ kg/m}^3$  for a lorry and a mass density of  $3,785 \cdot 10^5 \text{ kg/m}^3$  for a bus.

For the ground we have used material type 025-GEOLOGIC\_CAP\_MODEL, where we have specified a number of parameters listed in the following table:

**Table 3.15: Parameters for ground material specification**

Name	Description	Value
<b>RO [kg/m<sup>3</sup>]</b>	Mass density	2100
<b>BULK [Pa]</b>	Initial bulk modulus	$4,102 \cdot 10^7$
<b>G [Pa]</b>	Initial shear modulus	$3,076 \cdot 10^7$
<b>ALPHA</b>	Failure envelope parameter	2
<b>THETA</b>	Failure envelope linear coefficient	0,292
<b>GAMMA</b>	Failure envelope exponential coefficient	0
<b>BETA</b>	Failure envelope exponent	0
<b>R</b>	Cap, surface axis ratio	3
<b>D [Pa]</b>	Hardening law exponent	$7,524 \cdot 10^{-7}$
<b>W [Pa]</b>	Hardening law coefficient	0,0313940
<b>X0 [Pa]</b>	Hardening law exponent	0
<b>C</b>	Kinematic hardening coefficient	1
<b>N</b>	Kinematic hardening parameter	1
<b>FTYPE</b>	Formulation flag	1 - default - means soil or concrete (cap surface may contract)
<b>VEC</b>	Vectorization flag	0 - default - means vectorized (fixed number of iterations)

At last it remains to define material properties for a concrete base, in which the post is concreted. For these purposes we have used material type 159-CSCM\_CONCRETE, which is a smooth or continuous surface cap model available for solid elements in LS-DYNA [34].

There is an option of inputting our own material properties or requesting default material properties for normal strength concrete. We have specified the following parameters:

**Table 3.16: Material properties for a concrete base**

<b>Name</b>	<b>Description</b>	<b>Value</b>
<b>RO [kg/m<sup>3</sup>]</b>	Mass density	2500
<b>INCRE</b>	Maximum strain increment for subincrementation	A default value is set during initialization based upon the shear strength and stiffness.
<b>ERODE</b>	Elements erode when damage exceeds 0,99 and the maximum principal strain exceeds some erosion value	1,05
<b>RECOV</b>	The modulus is recovered in compression	0 - default
<b>ITRETRC</b>	Cap retraction	0 - default - cap does not retract
<b>PRED</b>	Pre-existing damage	0 - default - no pre-existing damage
<b>FPC [Pa]</b>	Unconfined compression strength	$3 \cdot 10^7$ - default
<b>DAGG [m]</b>	Maximum aggregate size	0,019 - default

Defining all these material properties for safety barriers, a vehicle, the ground and a concrete base we need to assign corresponding materials to each part of the model. This is made in PART keyword section, which defines parts, i.e. combines material information, section properties, hourglass type and other parameters.

Material for the ground, a vehicle and a concrete cap is common for both models: JSNH4/H2 and JSAM-2/H2.

In model of JSNH4/H2 we have defined S235JR for a barrier strip, a lower beam and a distance spacer and S355J0 has been determined for a post.

Model JSAM-2/H2 has a barrier strip, a lower beam and a post from S355J0 and a distance spacer from S235JR.

This is basically all what we need for full definition of our models. Our next step is to define parameters for each crash test we want to perform.

Let us remind that we would like to make numerical simulation for crash tests of type TB11, TB42 and TB51, which is performed for containment level H2. In material properties for



a vehicle we have already defined mass density for each type of a car used in this or that crash test. Now we need to define crash speed and crash angle, which can be made in INITIAL keyword section, where we specify initial velocity in global y-direction.

As it was mentioned several times TP 114 besides other parameters specify crash speed and crash angles for each crash test. But we cannot merely take defined speed value for a certain crash test and thus generate initial velocity. It is due to the fact that a vehicle we have created would crash safety barrier at a right angle, whereas in standards specified crash angles are in range from 8 to 20 degrees. Logically the initial velocity of a vehicle that would crash at a right angle should be less than this specified in standards and we have to calculate it according to the following formula:

$$v_{ct} = v_{st} \cdot \sin(\alpha_t) \text{ [m/s]}$$

where  $v_{ct}$  is an initial speed for simulation [m/s],  $v_{st}$  is a speed specified in standards [m/s],  $\alpha_t$  is an angle specified in standards.

Thus, we have the following values:

**Table 3.17: Calculated velocity for different crash test types**

Crash test	Vehicle type	Velocity $v_{st}$ [m/s]	Angle $\alpha_t$ [°]	Calculated velocity $v_{ct}$ [m/s]
TB11	Passenger car	27,78	20	9,50
TB42	Lorry	19,44	15	5,03
TB51	Bus	19,44	20	6,65

Our last step before launching numerical simulation is to determine time step information and termination conditions. For these purposes we can use CONTROL keyword section, which has several cards [34]. Among them are:

- ACCURACY, which defines control parameters that can improve the accuracy of the calculation.
- BULK\_VISCOSITY, where quadratic viscosity coefficient (default is "1,5") and linear viscosity coefficient (default is "0,06") are specified.
- CONTACT changes defaults for computation with contact surfaces.
- ENERGY provides controls for energy dissipation options. Energy and its related parameters, i.e. hourglass energy, stonewall energy dissipation, sliding interface

energy dissipation, Rayleigh energy dissipation, are computed and included in the energy balance.

- HOURGLASS defines hourglass and bulk viscosity properties.
- SOLID provides controls for solid element response.
- and at last TERMINATION, which provides an alternative way of stopping the calculation before the termination time is reached, and TIMESTEP, which sets structural time step size control.

In TERMINATION we have specified termination time (0,5), termination cycle (100000000) and reduction (or scale) factor for initial time step size to determine minimum time step (0,1).

In the result we have three models for each safety barrier, i.e. for JSNH4/H2 and JSAM-2/H2, which correspond to different types of crash tests (TB11, TB42, TB51).

Thus, from this point everything is ready and we can launch numerical simulation separately for each model in simulation environment ANSYS LS-DYNA Solver using our k-files.

### **3.3. Calculation in LS-DYNA and evaluation of obtained results**

As it was mentioned above LS-DYNA is a general purpose finite element code for analyzing the large deformation dynamic response of structures including structures coupled to fluids. The main solution methodology is based on explicit time integration. An implicit solver is also currently available including structural analysis and heat transfer. LS-DYNA contains approximately one-hundred constitutive models and ten equations-of-state to cover a wide range of material behavior [33].

Calculation for each type of our models generally lasted from 22 to 24 hours. In the result we have obtained solution of specified problem with animation available, which shows quite well what happens to a safety barrier while a vehicle impact occurs. Besides animation we can see and use for our analysis different graphs for the whole construction or for its separate part depending on our purposes. These graphs depict, for example, kinetic energy, internal energy and total energy, then x-, y-, z- or resultant body displacement, x-, y-, z- or resultant body velocity, x-, y-, z- or resultant body acceleration.

Some graphs are just informative (e.g. x- or z- body displacement, x- or z- body velocity), while the others supply us with significant information that is worth for further results

evaluation (e.g. internal energy as well as body displacement, velocity and acceleration in y-axis direction).

Firstly we would concentrate our attention on the results obtained for safety barrier JSNH4/H2.

For this model three different crash test simulations have been performed: TB11, TB42 and TB51.

Making recapitulation, TB11 is a crash test with a passenger car of weight 900 kg, at crash speed 100 km/h, at crash angle 20° and kinetic energy 40,600 kNm [49].

The first graph of our interest is the one showing a vehicle kinetic energy development.

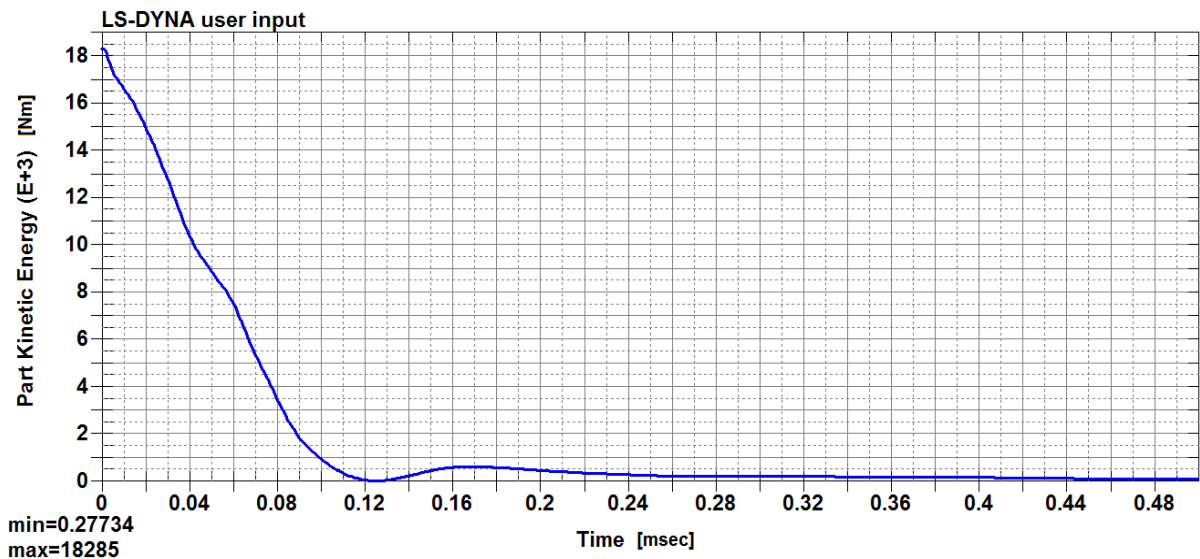
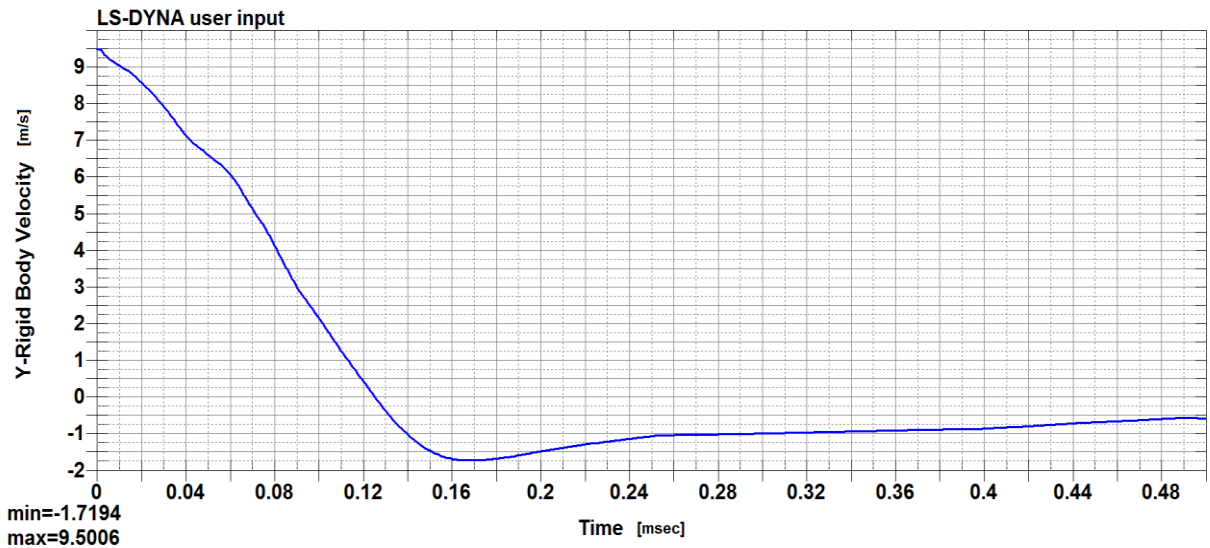


Figure 3.22: Kinetic energy of a vehicle - JSNH4/H2, TB11

We see that maximum value of a vehicle kinetic energy while colliding with a safety barrier is 18,282 kNm. If we take into account the symmetry of our task, then the total kinetic energy will be  $E_t = E_s * 2 = 18,282 * 2 = 36,569$  kNm, where  $E_t$  is the total kinetic energy of a car and  $E_s$  is a kinetic energy obtained while solving symmetrical task.

We see that the value of 36,569 kNm is less than the one the vehicle crashes with in real crash tests and which is specified in standards (see table 2.1). The difference is approximately 4 kNm. We have to take this fact into account while considering the criteria of consumed energy.

Further on we have obtained graphs of vehicle velocities in different directions (x-, y-, z-). Nevertheless, taking into account boundary conditions specified for a vehicle movement and discussed in previous chapters the only graph, which is important for us, is the one depicting a vehicle velocity in y-axis direction, i.e. in the direction of a vehicle movement.

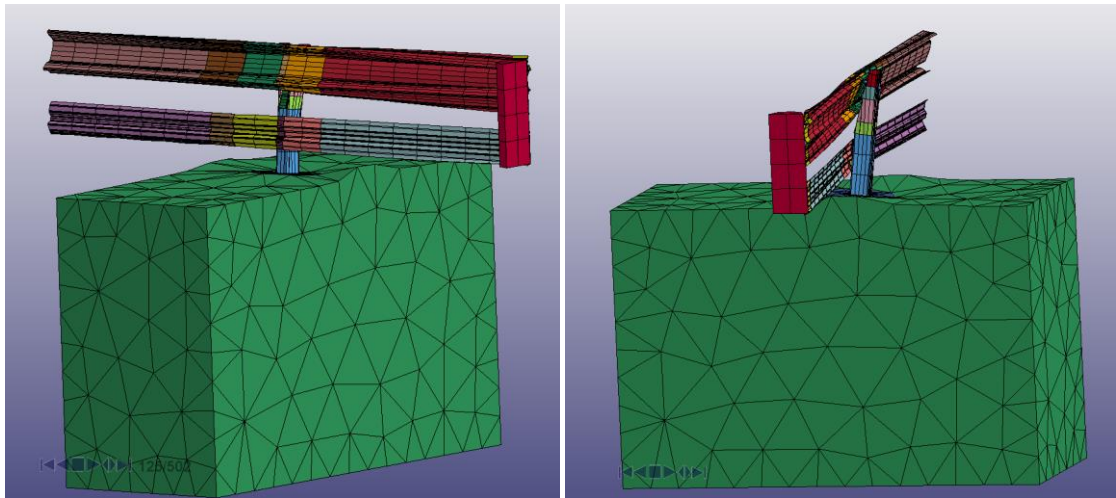


**Figure 3.23: Vehicle velocity - JSNH4/H2, TB11**

On this graph we can observe that maximum value of a vehicle velocity is 9,5006 m/s. This value corresponds to the requirements for crash test TB11 and has been set before performing numerical simulation. Then we can see how the velocity is decreasing in the course of an impact. At time step app. 0,125 ms velocity reaches 0 and then has negative values. This proves the fact that from time step 0,125 ms the vehicle begins moving to opposite direction, i.e. the safety barrier fulfills its purpose of catching the vehicle and redirecting it. It can be also confirmed by animation, where it is clearly seen that in certain time the vehicle begins to move away from the safety barrier.

Because at time step 0,125 ms velocity is equal to zero, we would take this time step to define what values the internal energy has at it.

The following figures illustrate safety barrier deformation at time step 0,125 ms.



**Figure 3.24: Safety barrier deformation at time step 0,125 ms - JSNH4/H2, TB11**

Other important information for our analysis is displacement of a barrier strip, a lower beam, distance spacers and a post of the safety barrier. It is logical to assume that the maximum values of displacement can be expected on the barrier strip, because in our numerical simulation the majority of a vehicle impact comes to this part of the safety barrier. Again due to specified boundary conditions we would mainly talk about displacement in y-direction, i.e. in the direction of a vehicle movement, and we would give the example of displacement in z-direction only to show that it is very small and can be neglected in our further analysis.

The next graph represents displacement of a barrier strip in y-direction. Because we have sliced the barrier strip into separate parts we have an individual curve for each of these parts. Figure 3.25 shows the numbering of individual parts and Figure 3.26 illustrates the above mentioned graph with corresponding curves for each part.

This is just an example, how it looks like and further on we would present the graphs showing the maximum displacement in y-direction instead of showing individual curves of displacement for each sliced part.

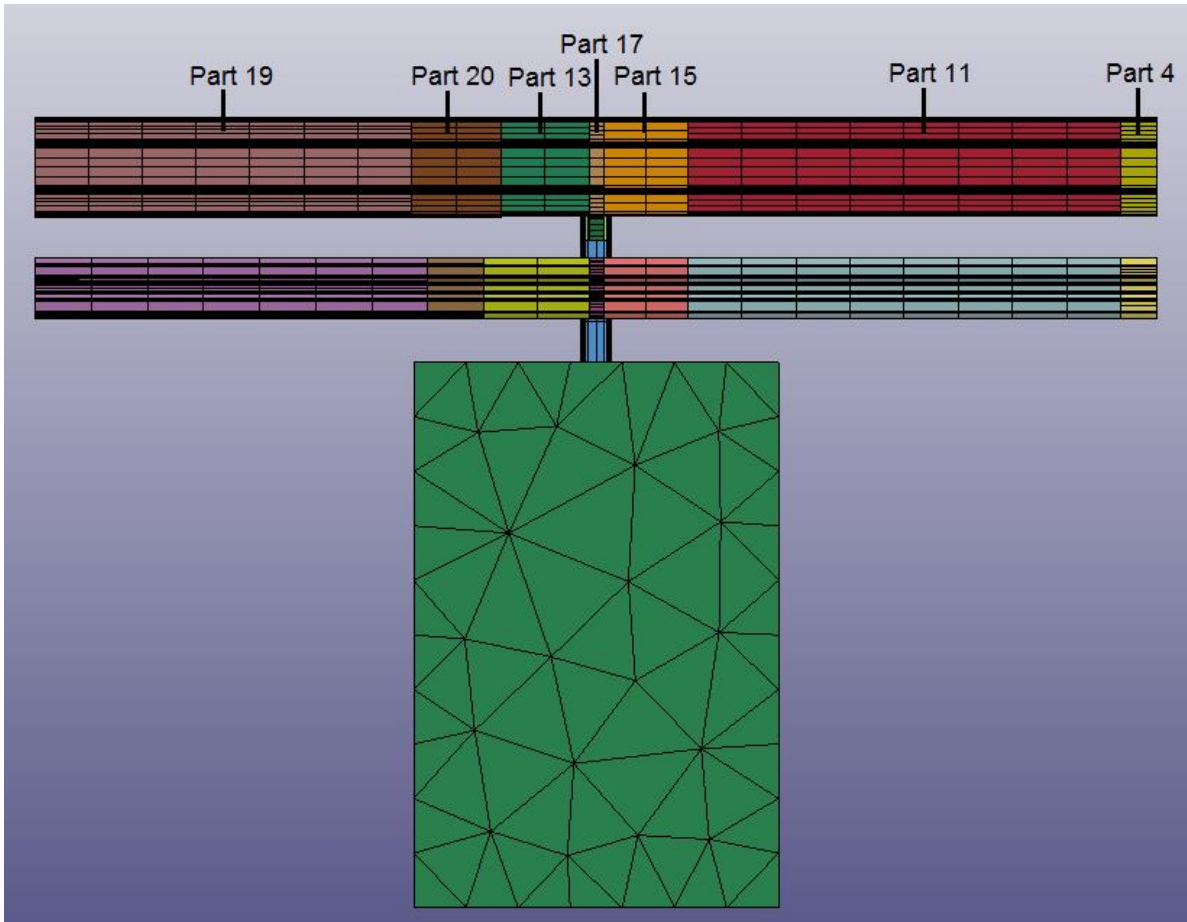


Figure 3.25: Numbering individual sliced parts of a barrier strip - JSNH4/H2, TB11

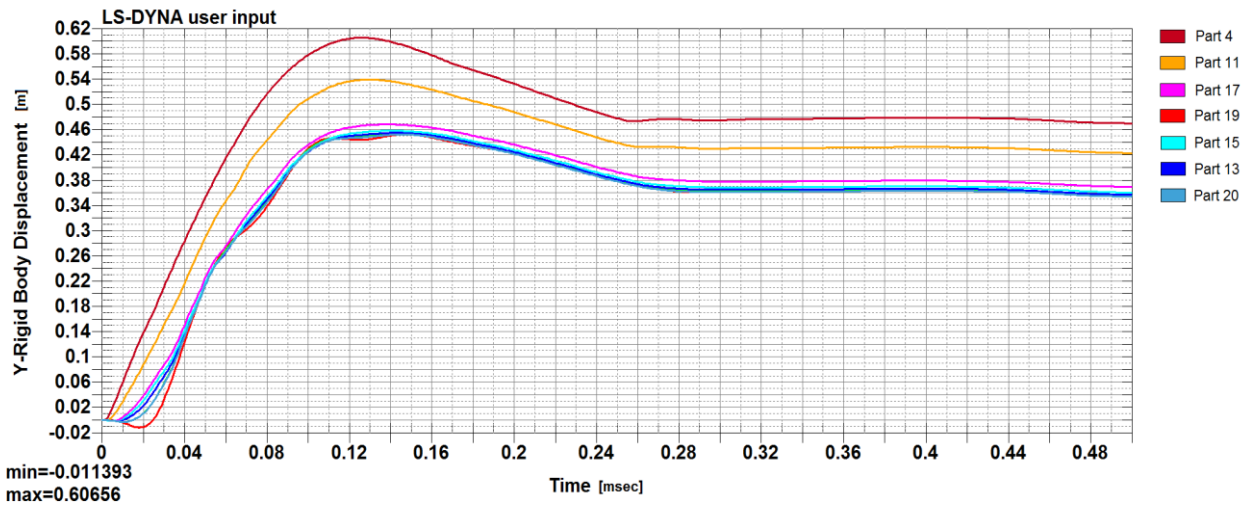
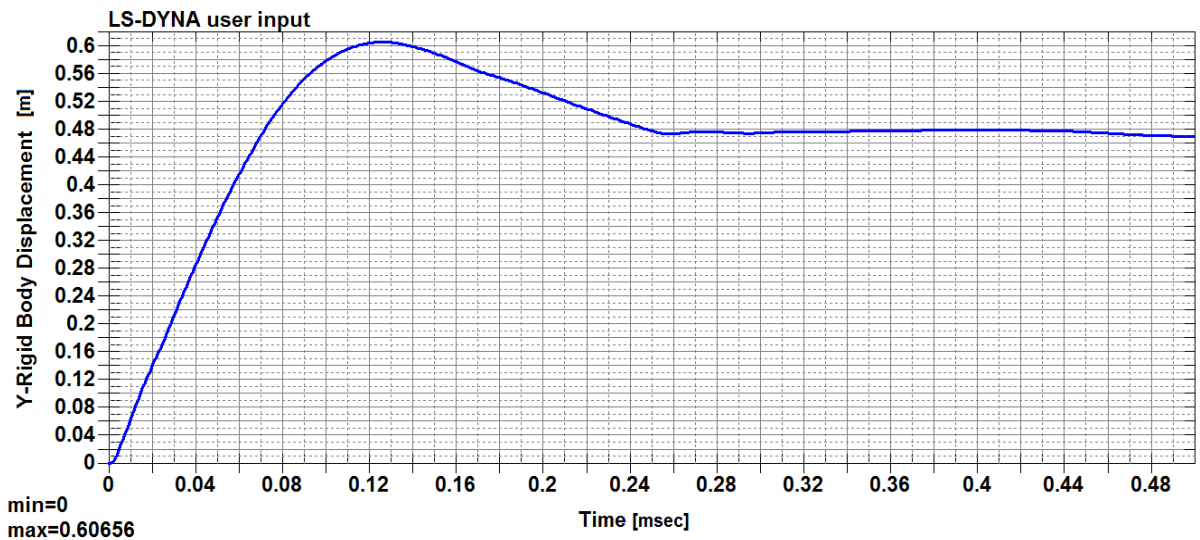


Figure 3.26: Barrier strip displacement in y-direction - JSNH4/H2, TB11

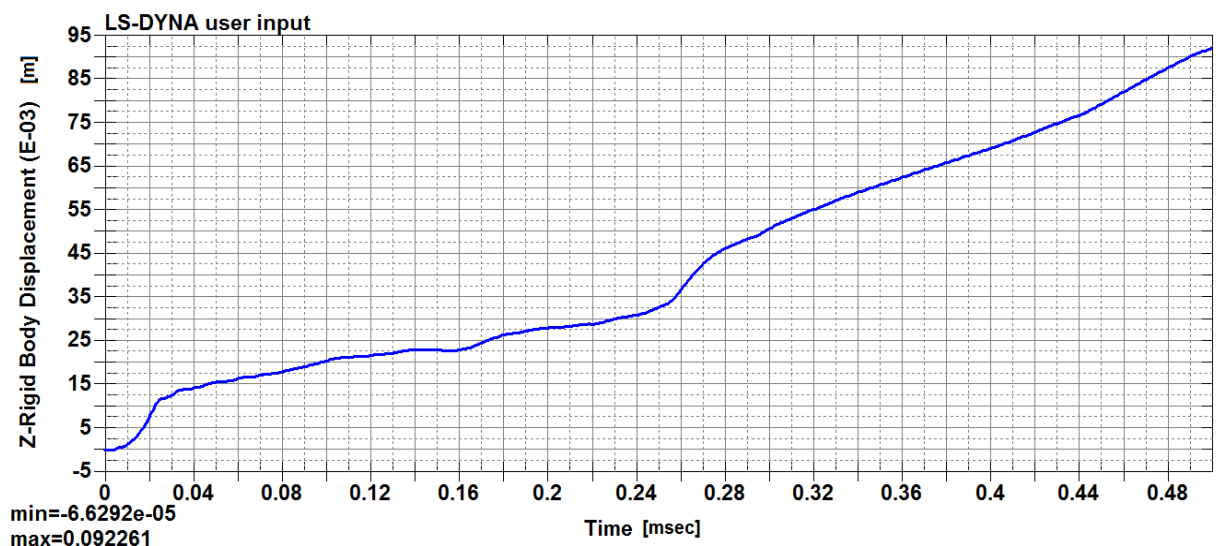
The most important is the maximum value, which refers to the part of the barrier strip where the vehicle collides. For this part we have drawn a separate graph presented below.



**Figure 3.27: Maximum barrier strip displacement in y-direction - JSNH4/H2, TB11**

We see that its maximum value is 0,60656 m at time step app. 0,125 ms. This value is in a very good accordance with the values of a dynamic deflection (1,750 m) and a working distance (1,850 m) specified in technical conditions of the manufacturer [4] and even much smaller.

Displacement in z-direction is shown in Figure 3.27.



**Figure 3.28: Barrier strip displacement in z-direction - JSNH4/H2, TB11**

We see that the values are indeed very small and we can easily ignore them for our further evaluation.

From Figure 3.28 we observe that a lower beam displacement is lower than that of a barrier strip and its maximum value reaches only 0,36569 m and it is in the area of a direct vehicle impact.

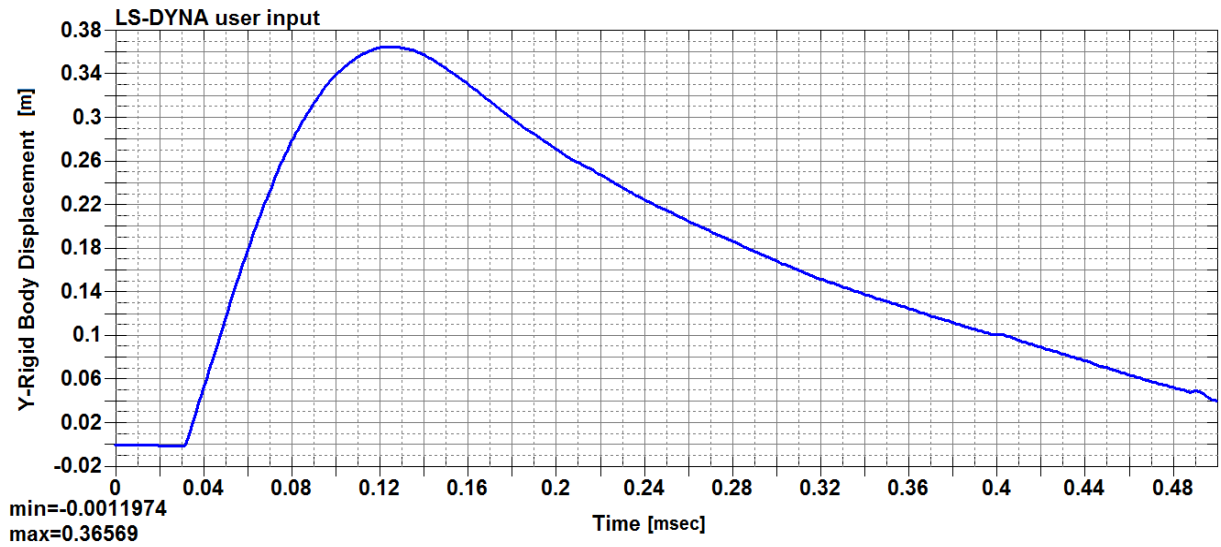


Figure 3.29: Lower beam displacement - JSNH4/H2, TB11

For distance spacers we have the following values of displacement:

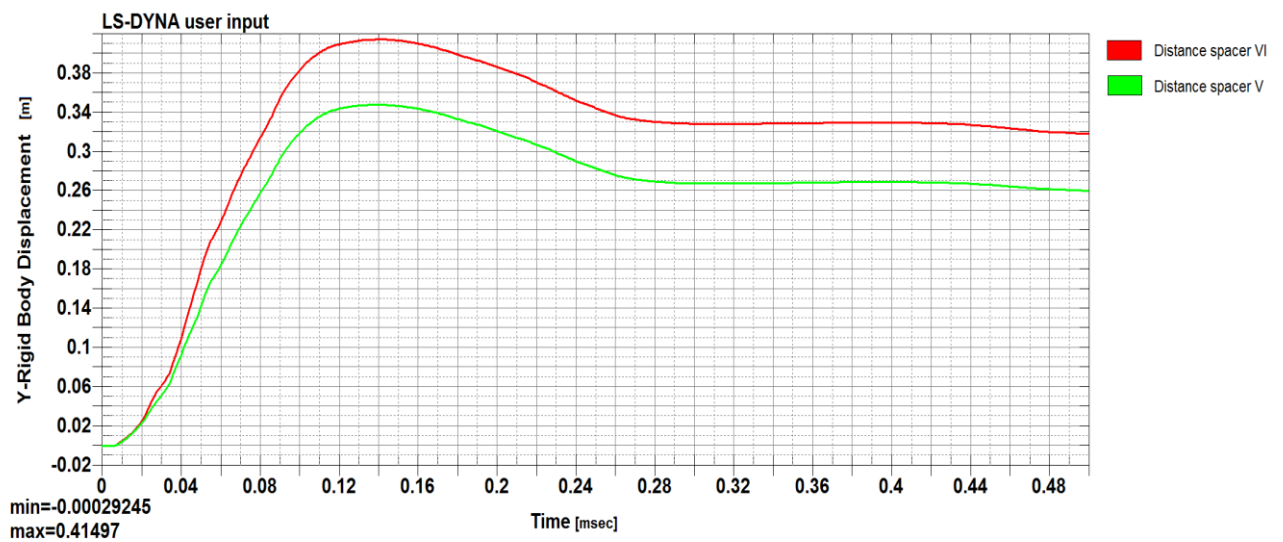
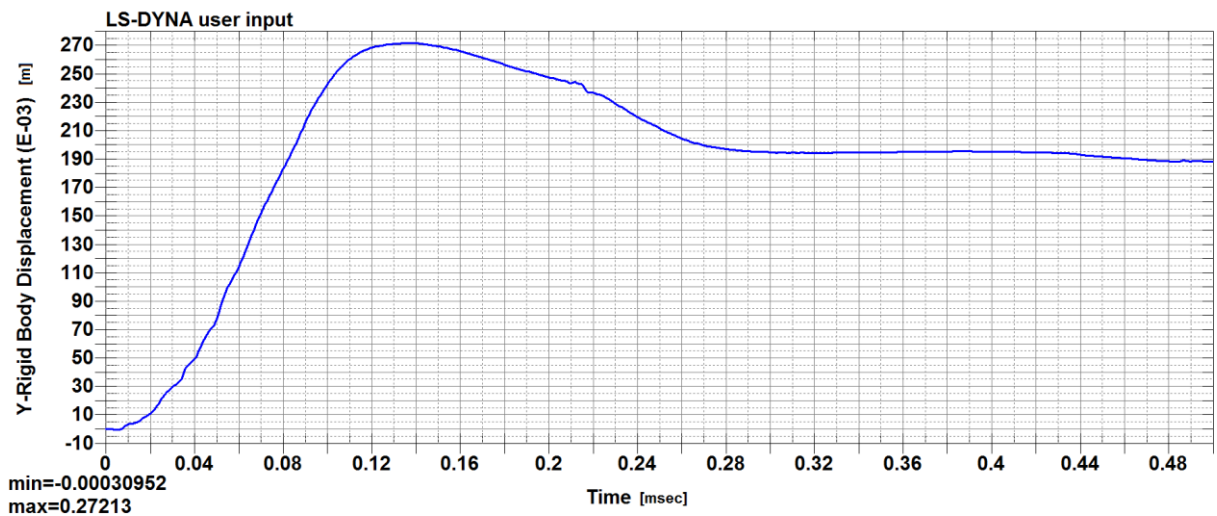


Figure 3.30: Distance spacer displacement - JSNH4/H2, TB11

Because we have two parts of a distance spacer, the lower one and the upper one, we have two curves of displacement. We need to notice that the upper part is deformed more than the lower one and has therefore the maximum value of displacement equal to 0,41497 m.



For a post the following values of displacement are valid:



**Figure 3.31: Post displacement - JSNH4/H2, TB11**

We see that the maximum value here is equal to 0,27213 m.

Resuming all mentioned above we see that our assumption has been proved and a barrier strip has the maximum value of displacement in comparison with all other parts, because it suffers the majority of impact forces after a vehicle crash during simulation. Moreover the maximum value of displacement (0,60656 m) does not exceed either a working width (1,850 m) or a dynamic deflection (1,750 m) specified for this type of the safety barrier in standards [4].

If we look at the graph representing the internal energy of our safety barrier obtained after a vehicle impact we see that its maximum value is equal to 29,718 kNm, which is 59,436 kNm for a symmetrical task. But we are not interested in the maximum value, but in a value at time step, when there is the maximum displacement, resp. when the velocity is zero. This time step is at app. 0,125 ms.

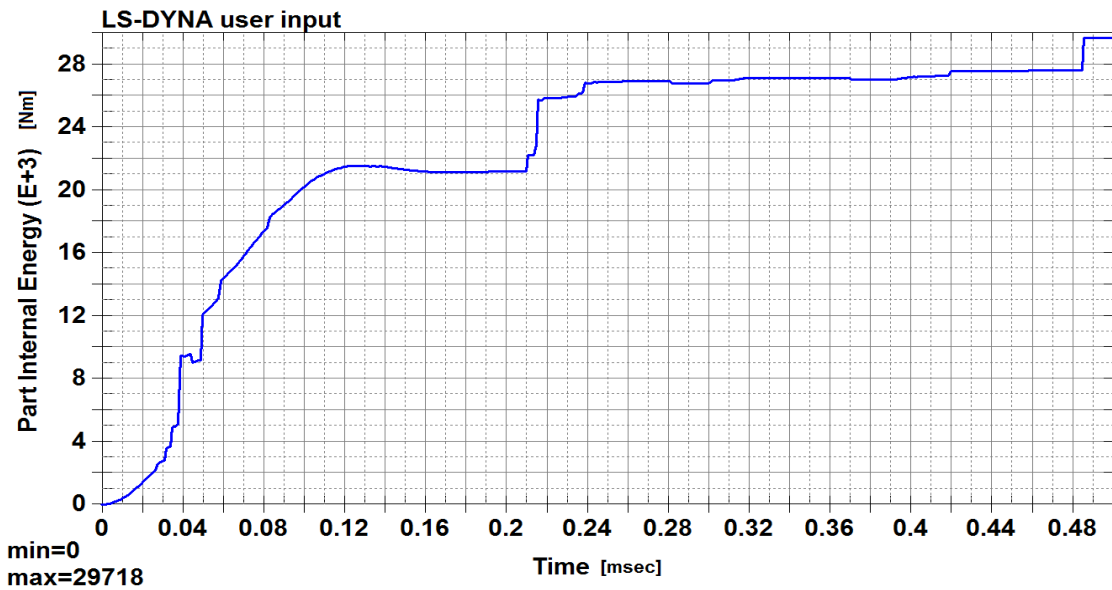


Figure 3.32: Internal energy - JSNH4/H2, TB11

At time step 0,125 ms the value of internal energy is 21,500 kNm, i.e. the total value for a symmetrical task is 43 kNm.

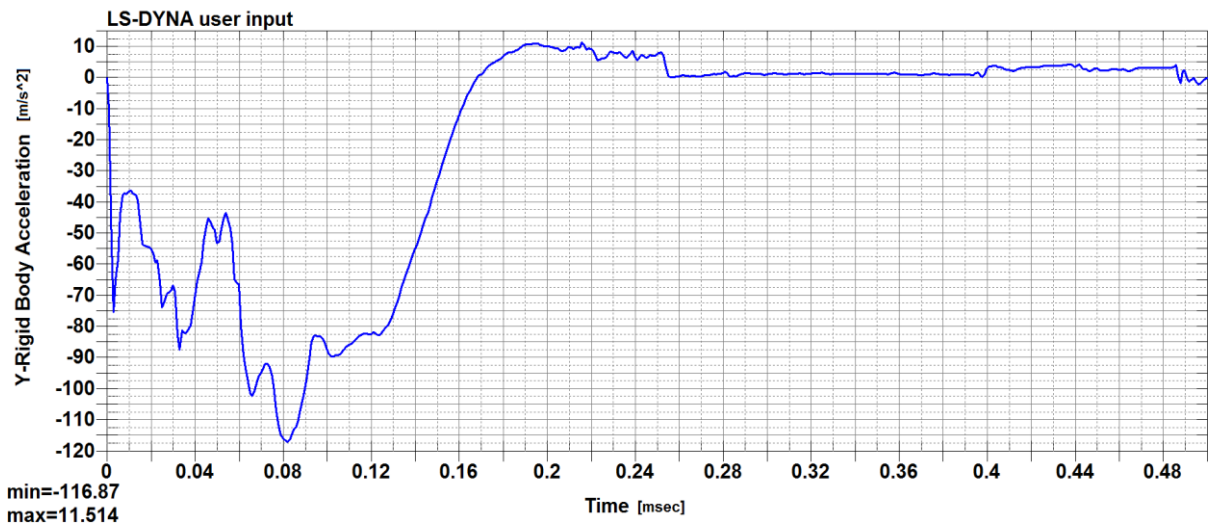
In both cases the value of internal energy is higher both the value of kinetic energy of a vehicle during simulation (36,569 kNm) and the value specified in standards for this type of a crash barrier test (40,600 kNm) (see table 2.1) [20]. It means that according to the criteria of consumed energy safety barrier JSNH4/H2 has successfully passed crash test TB11.

If we look at a graph of vehicle acceleration, we should observe that the maximum value of deceleration is  $-116,870 \text{ m/s}^2$ . At time step 0,125 ms it reaches app.  $-82,500 \text{ m/s}^2$ . If we take this range from  $-82,500 \text{ m/s}^2$  to  $-116,870 \text{ m/s}^2$  we will obtain the impact forces the vehicle can withstand during crash test TB11. The impact forces are calculated in the following way:

$$F = m \cdot a ,$$

where  $F$  is the impact force [kN],  $m$  is a mass of a vehicle [kg],  $a$  is a vehicle acceleration [ $\text{m/s}^2$ ].

Thus, for acceleration equal to  $-116,870 \text{ m/s}^2$  we will have the impact force equal to 105,183 kN, while for acceleration of  $-82,500 \text{ m/s}^2$  the impact force reaches the value of 74,250 kN.



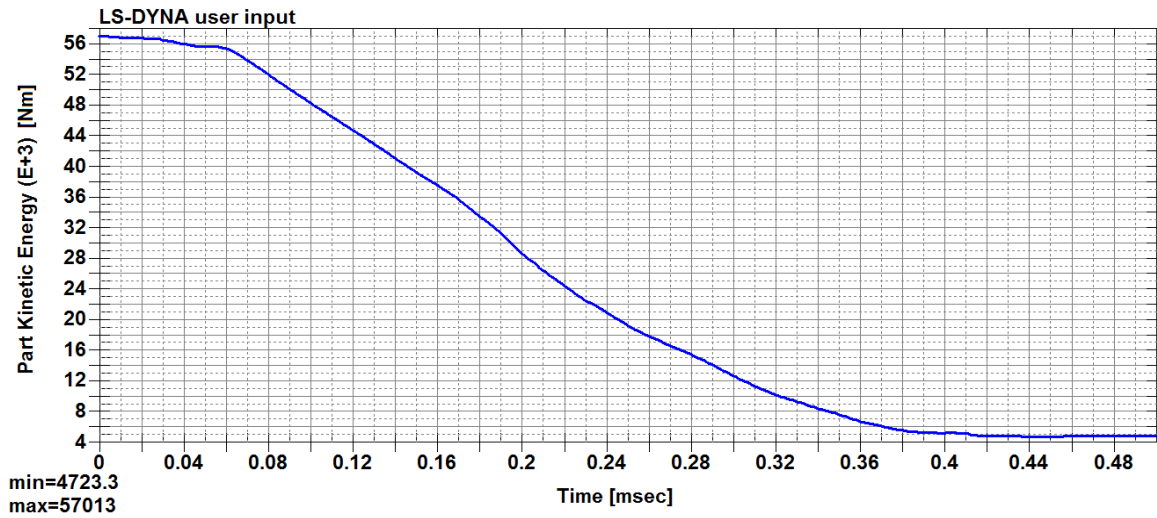
**Figure 3.33: Vehicle acceleration - JSNH4/H2, TB11**

According to TP 101 the alternative force a crash barrier could be loaded during TB11 is in the range from 15 kN to 35 kN for easily deformed safety barriers with a dynamic deflection from 1,5 m to 2,5 m and in the range from 35 kN to 80 kN for more rigid safety barriers with a dynamic deflection from 0,1 m to 0,5 m (see table 2.3) [48]. We have obtained much higher impact forces during numerical simulation of crash test TB11 and the safety barrier is proved to resist them.

The same analysis of JSNH4/H2 results is made for crash tests TB42 and TB51 and is presented below.

Crash test TB42 is fulfilled with a lorry of weight 10 000 kg, at crash speed 70 km/h, at crash angle 15° and kinetic energy 126,600 kNm [20].

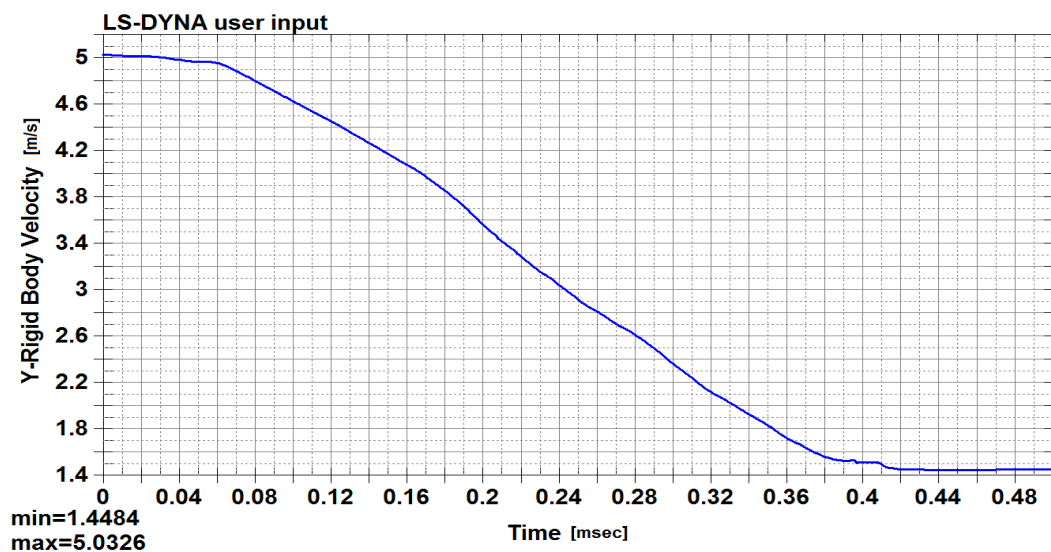
Kinetic energy of a vehicle is presented on the following graph:



**Figure 3.34: Kinetic energy of a vehicle - JSNH4/H2, TB42**

The maximum value of kinetic energy is 57,013 kNm that is 114,026 kNm while taking into account the symmetry of a task. The difference between this value and the one mentioned in standards is 12,574 kNm. This fact should be taken into consideration while speaking about the criteria of consumed energy.

A vehicle velocity in direction of y-axis is shown in Figure 3.41. The maximum value is 5,0326 m/s. This value is set before performing numerical simulation. We see that during our simulation the vehicle does not reach zero velocity. It is explained by the fact that during numerical simulation of this crash test the safety barrier has been fully destroyed.



**Figure 3.35: Vehicle velocity - JSNH4/H2, TB42**

As far as the displacement in y-direction is concerned we can see from the following figures that maximum displacement for a barrier strip is 1,5648 m, for a lower beam it is 1,3546 m, for a distance spacer it is 1,1727 m and for a post it is 1,4878 m. If we take the values of displacement at time step 0,250 ms when the safety barrier is not fully destroyed yet and can fulfill its functions (time step 0,250 ms is defined according to animation results), the values of displacement would be much smaller. Thus, for a barrier strip it is app. 1 m, for a lower beam it is app. 0,775 m, for a distance spacer it is app. 0,700 m and for a post it is app. 0,550 m.

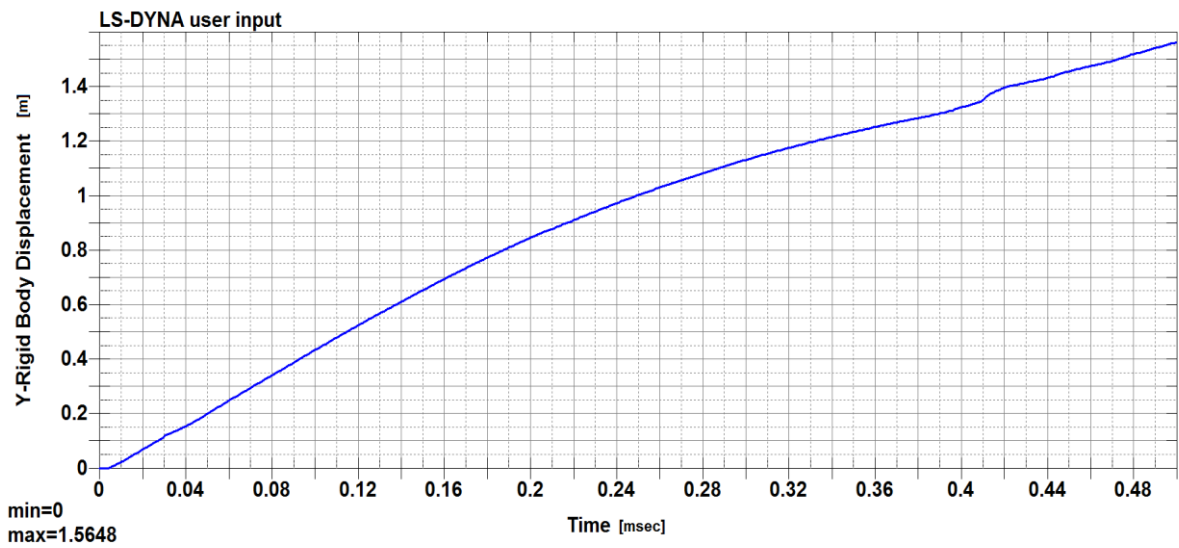


Figure 3.36: Barrier strip displacement - JSNH4/H2, TB42

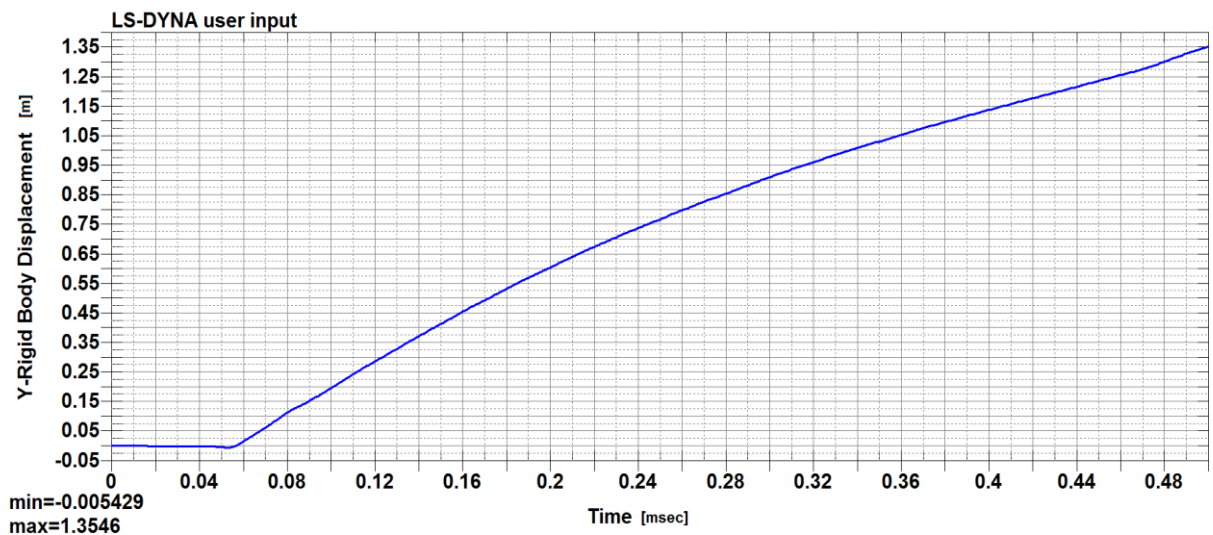


Figure 3.37: Lower beam displacement - JSNH4/H2, TB42

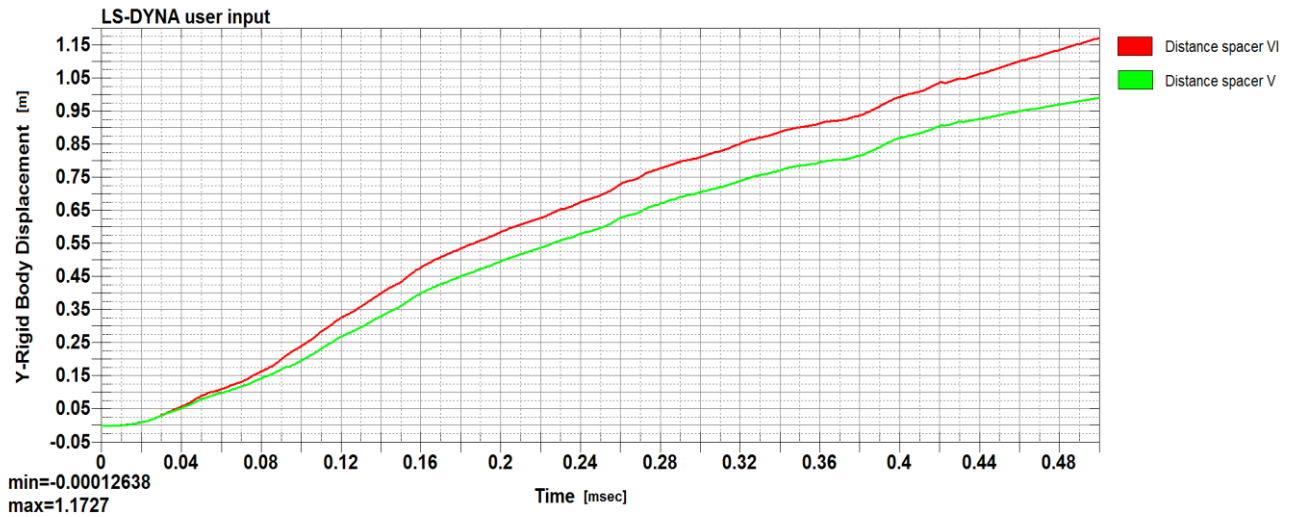


Figure 3.38: Distance spacer displacement - JSNH4/H2, TB42

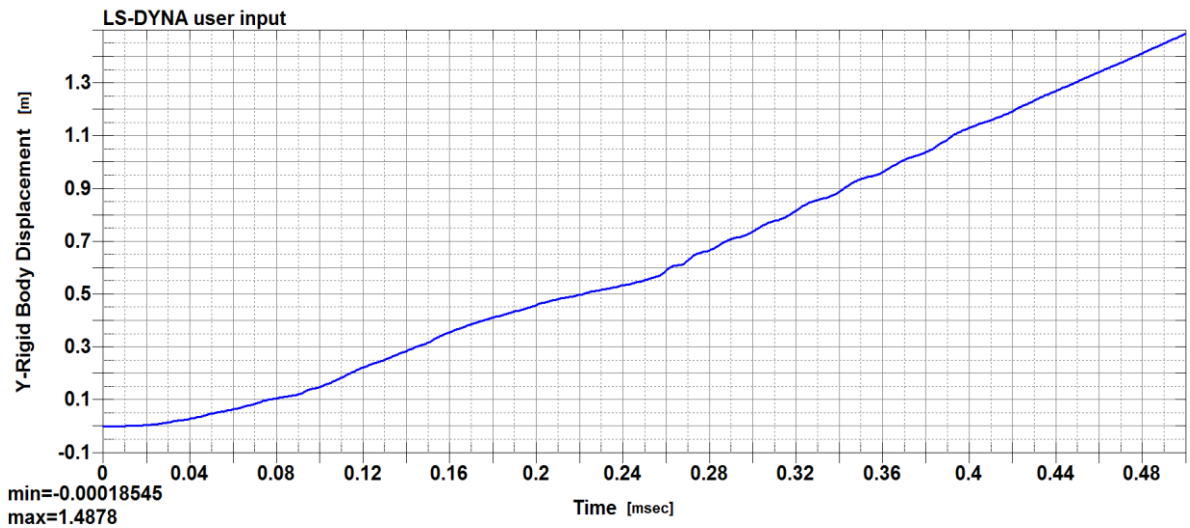
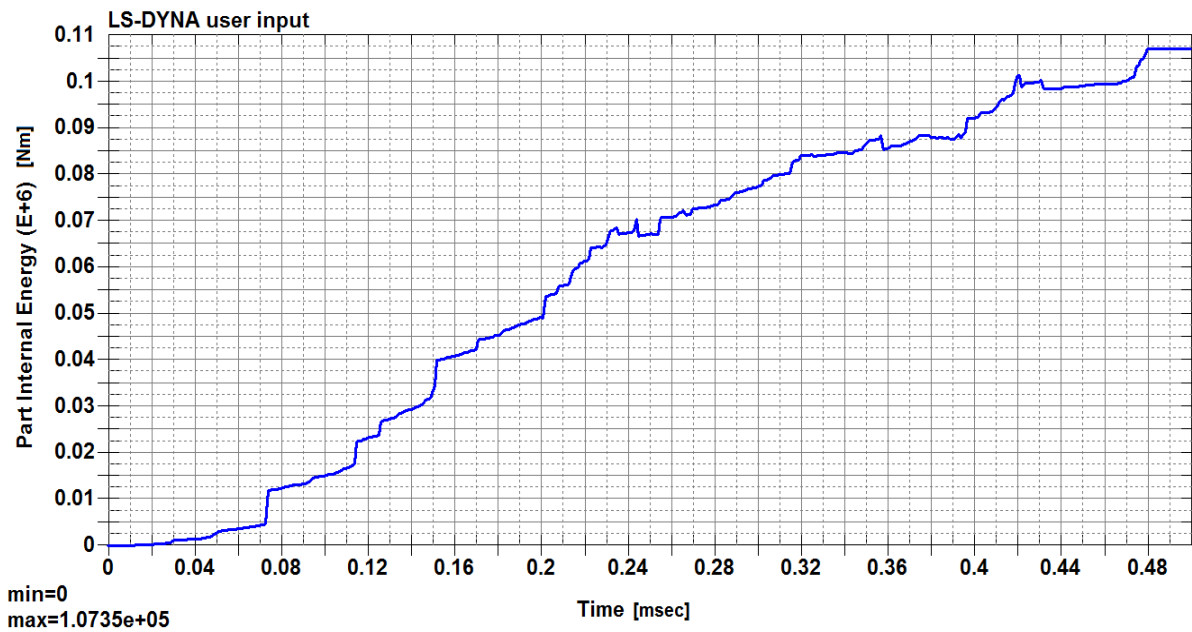


Figure 3.39: Post displacement - JSNH4/H2, TB42

We see that the maximum value of displacement 1,5648 m obtained during simulation of crash test TB42 does not exceed prescribed values of a dynamic deflection (1,750 m) and a working width (1,850 m) specified in technical conditions of the manufacturer [4].

The following graph illustrates the development of the internal energy of our construction.

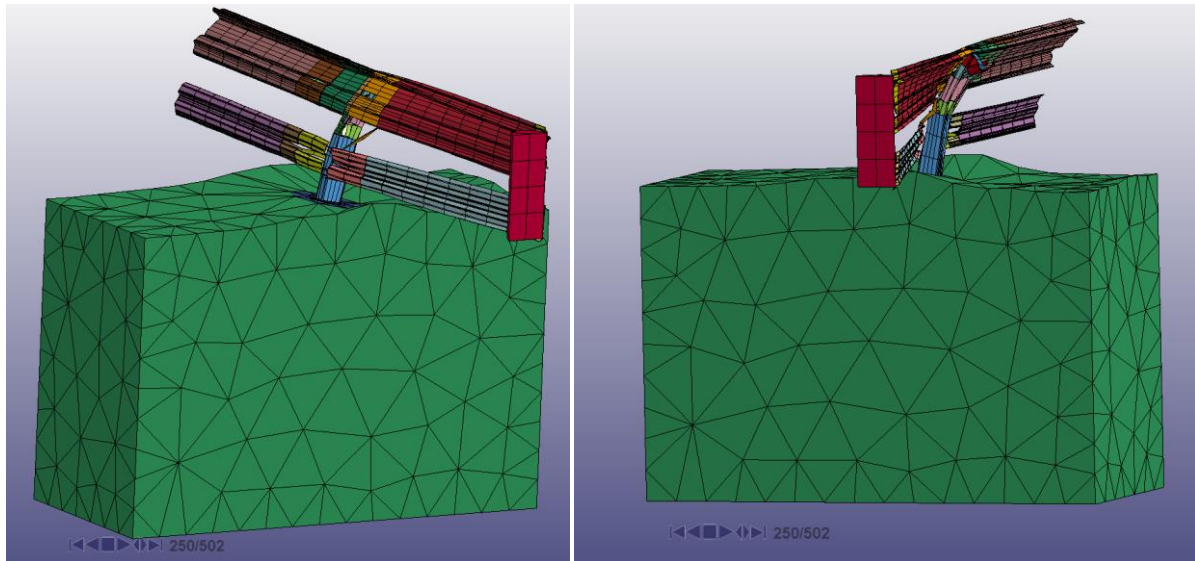


**Figure 3.40: Internal energy - JSNH4/H2, TB42**

Its maximum value is 107,350 kNm that is 214,700 kNm for a symmetrical task. But we cannot take this value, because it corresponds to a full destruction of the safety barrier. We need to find the value, when the safety barrier can still perform its functions. This value can be at time step 0,250 ms or a little bit higher according to animation results. Thus, at time step 0,250 ms the value of internal energy is 67,500 kNm that means that the total internal energy taking into consideration the symmetry of a task is 135 kNm.

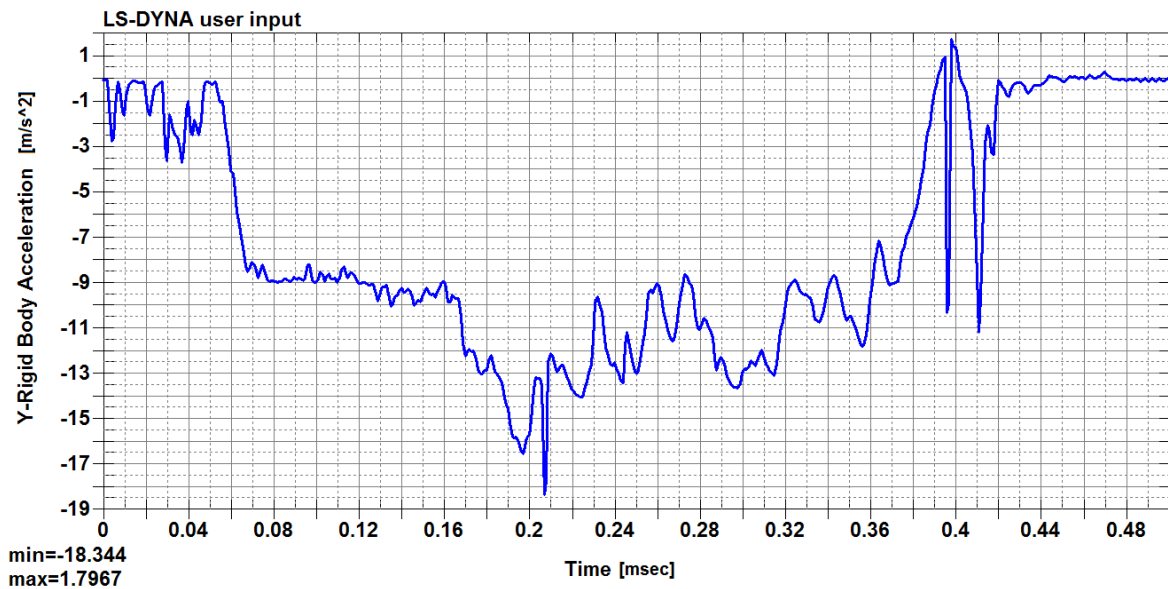
This value of internal energy is higher both a value of kinetic energy obtained during simulation (114,026 kNm) and a value specified in standards for this type of crash barrier test (126,600 kNm) (see table 2.1) [20]. It means that according to the criteria of consumed energy safety barrier JSNH4/H2 has successfully passed crash test TB42.

The following figures illustrate deformation of the safety barrier at time step 0,250 ms.



**Figure 3.41: Safety barrier deformation at time step 0,250 ms - JSNH4/H2, TB42**

A graph depicting vehicle acceleration in y-direction is presented in Figure 3.42. We can notice that the maximum value of acceleration reached during simulation of crash test TB42 is  $-18,344 \text{ m/s}^2$ . At time step 0,250 ms the acceleration is equal to  $-13 \text{ m/s}^2$ .



**Figure 3.42: Vehicle acceleration - JSNH4/H2, TB42**

Then the impact forces are 183,440 kN and 130 kN respectively. Both values are higher than those specified for alternative load forces for crash test TB42 in TP 101, where the alternative load force for deformable crash barriers with deflection 1,500 m - 2,500 m is in



the range from 45 kN to 80 kN and the alternative load force for more rigid barriers with deflection 0,100 m - 0,500 m is in the range from 100 kN to 140 kN (see table 2.3 ) [48].

Going on with our analysis we would evaluate the results obtained for crash test TB51, which is performed using a bus of weight 13 000 kg, at crash speed 70 km/h, at crash angle 20° and kinetic energy 287,500 kNm [20].

Kinetic energy of a vehicle is presented on the following graph.

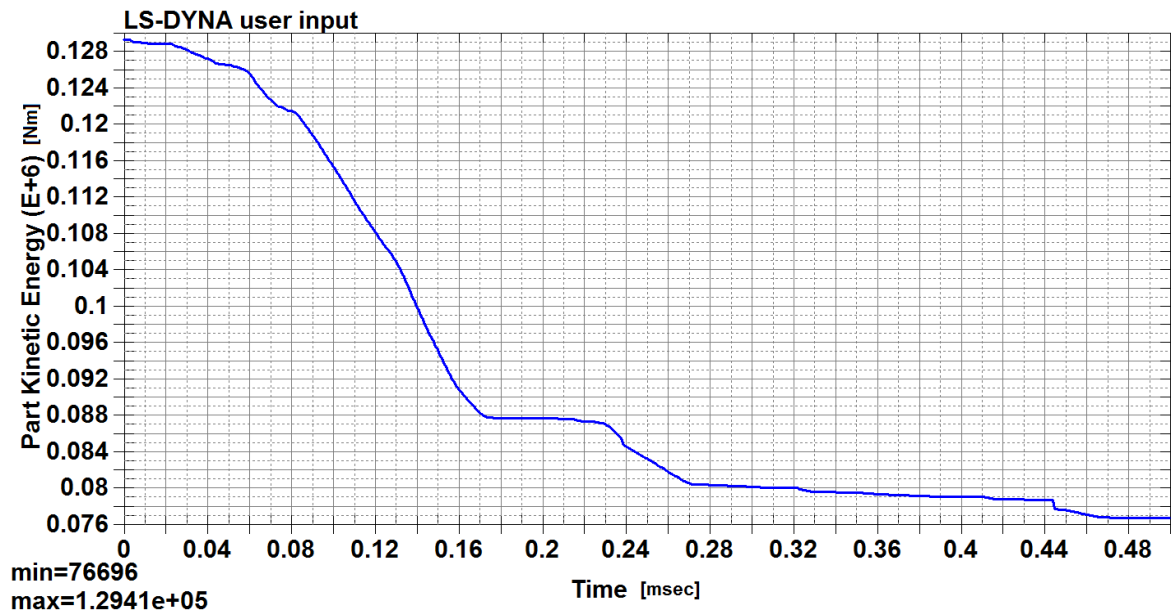


Figure 3.43: Kinetic energy of a vehicle - JSNH4/H2, TB51

We see that the maximum value of kinetic energy is equal to 129,410 kNm that is the total kinetic energy is 258,820 kNm for a symmetrical task. This value is smaller than kinetic energy specified in standards (see table 2.1). The difference is 28,680 kNm.

If we look at a vehicle velocity graph we see that the maximum value is at the beginning of simulation. It is predefined before running calculations and is equal to 6,6504 m/s.

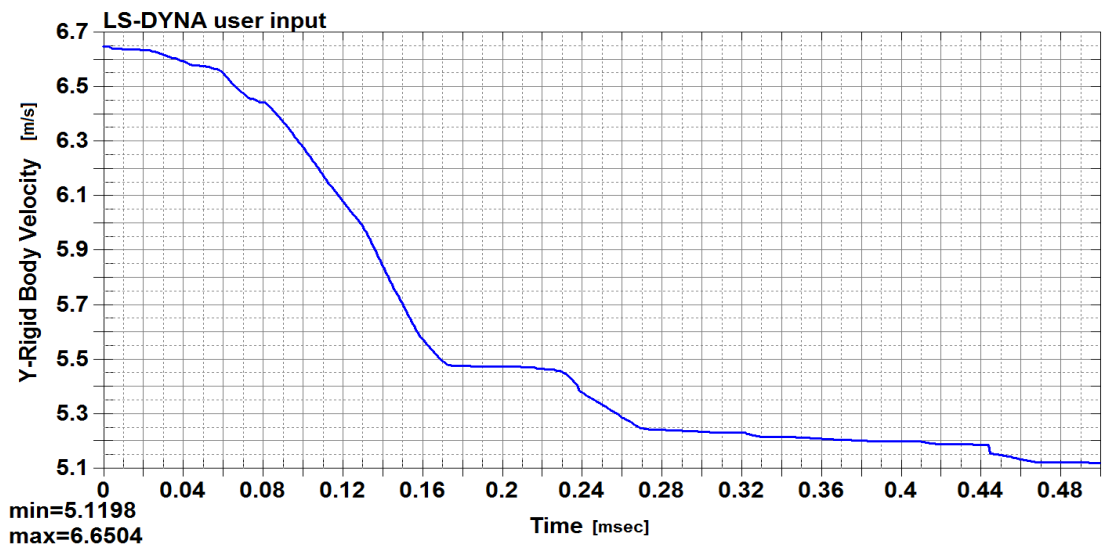


Figure 3.44: Vehicle velocity - JSNH4/H2, TB51

We can notice also that it never reaches zero, because the safety barrier is fully destroyed during simulation.

The figures below illustrate displacement in y-direction for a barrier strip, a lower beam, distance spacers and for a post. Thus, the maximum displacement for a barrier strip is 2,7405 m, for a lower beam it is 2,5032 m, for a distance spacer it is 2,4469 m and for the post it is 2,1846 m. These values are larger than the values of a working width (1,850 m) and a dynamic deflection (1,750 m) for this type of the safety barrier [4]. But if we take the values at certain time step, when the safety barrier still preserves its functions, i.e. at time step 0,160 ms, then we will obtain displacement of 1 m for a barrier strip, 0,700 m for a lower beam, 0,700 m for a distance spacer and 0,500 m for a post.

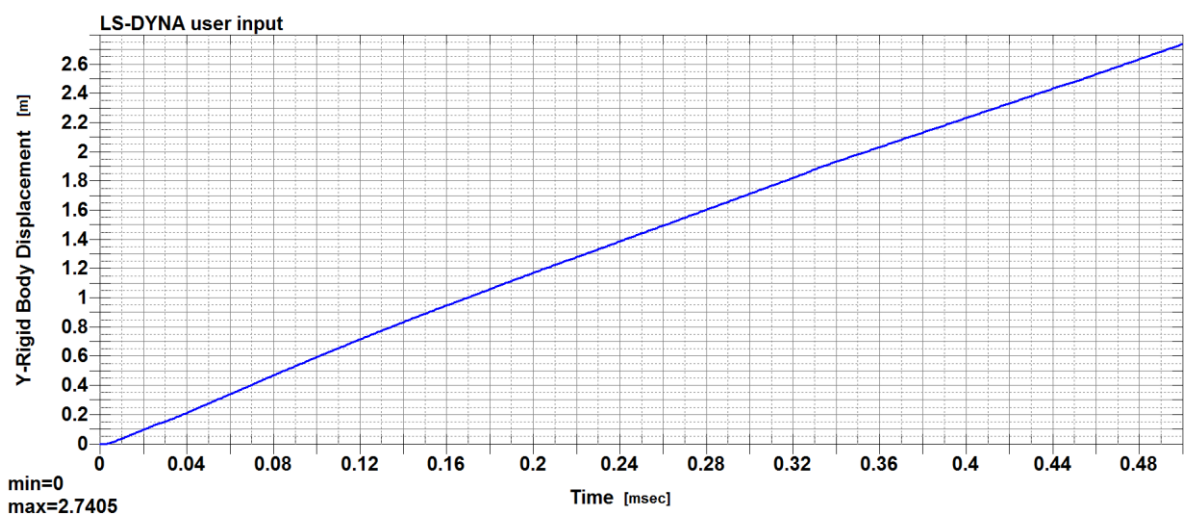


Figure 3.45: Barrier strip displacement - JSNH4/H2, TB51

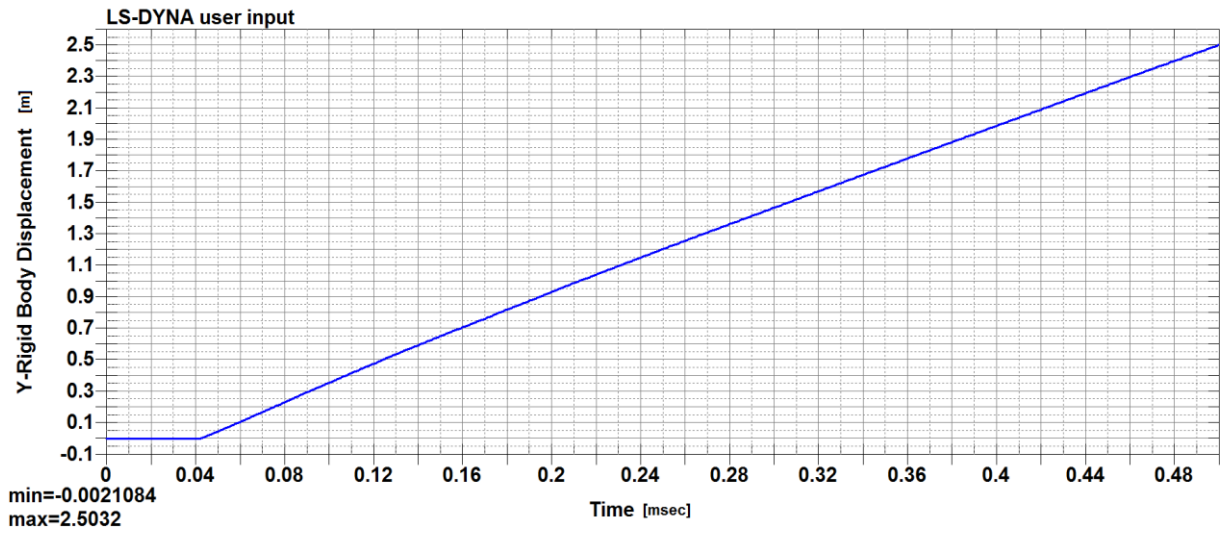


Figure 3.46: Lower beam displacement - JSNH4/H2, TB51

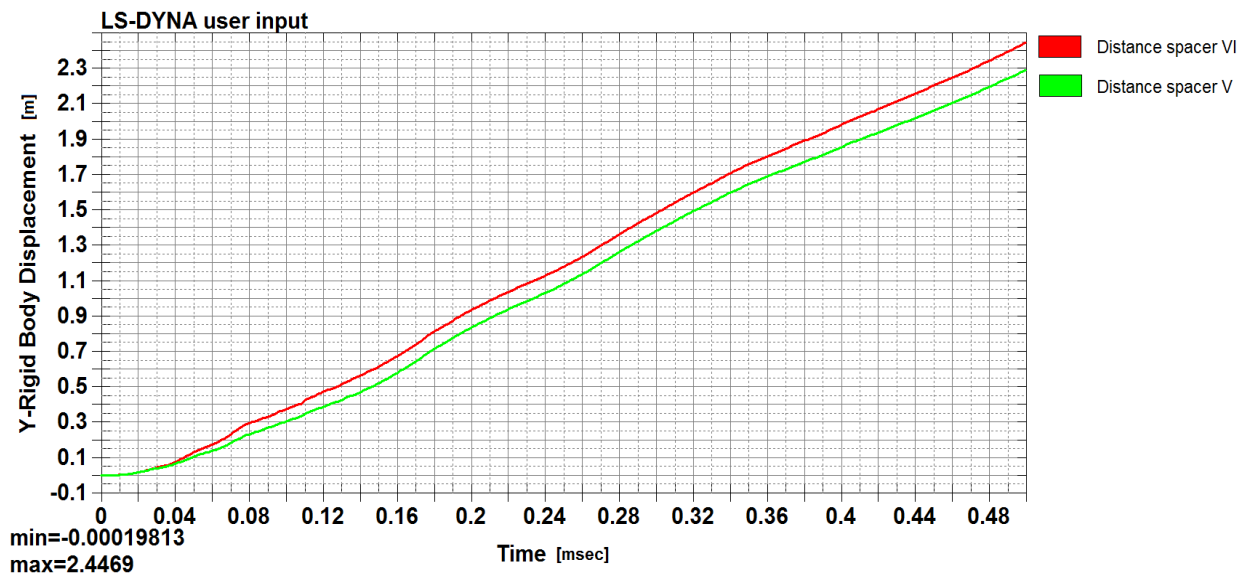
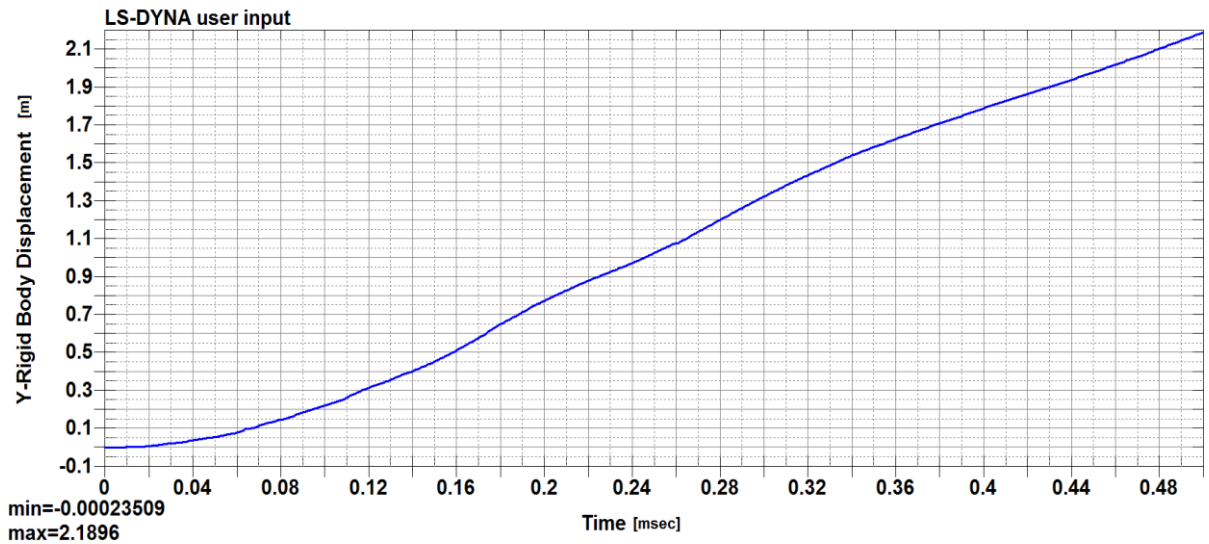
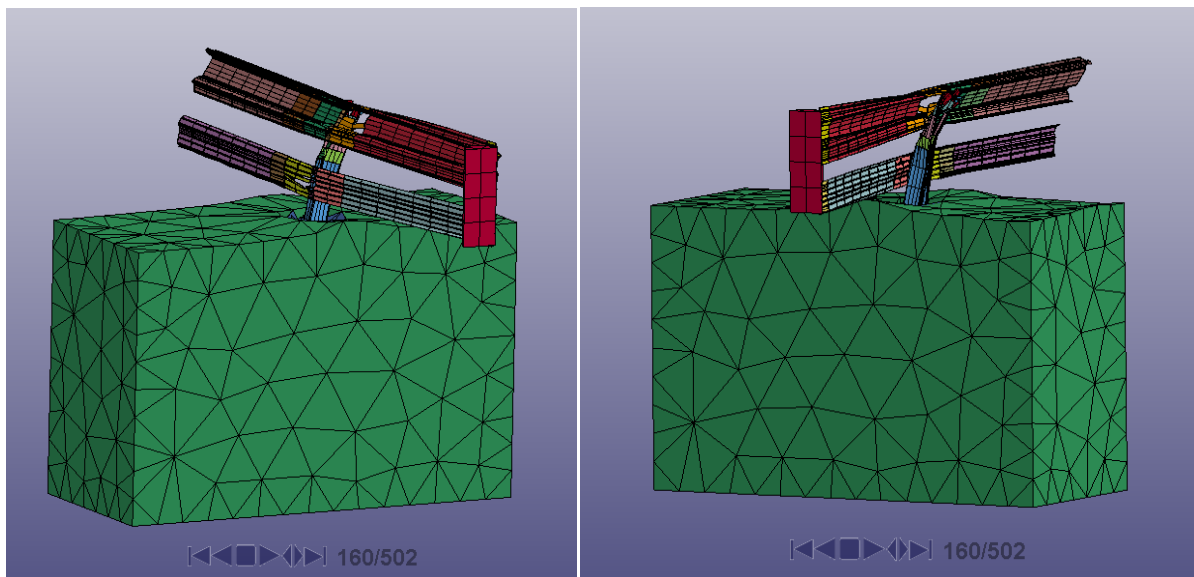


Figure 3.47: Distance spacer displacement - JSNH4/H2, TB51



**Figure 3.48: Post displacement - JSNH4/H2, TB51**

The following figures illustrate safety barrier destruction at time step 0,160 ms.



**Figure 3.49: Safety barrier deformation at time step 0,160 ms - JSNH4/H2, TB51**

The most important graph for our analysis is the one showing development of internal energy during time. We see that the maximum value it reaches is 116,620 kNm, it means 233,760 kNm for a symmetrical task. For time step 0,160 ms it is equal to 160 kNm. If we take the latter value for our further evaluation, we see that it does not correspond to kinetic energy either obtained during simulation (238,820 kNm) or to the one specified in standards (287,500 kNm) [20]. However, the maximum value of internal energy is not that far from those values. Nevertheless, we should state that according to the criteria of consumed

energy numerical simulation of crash test TB51 has failed and safety barrier model has not passed it.

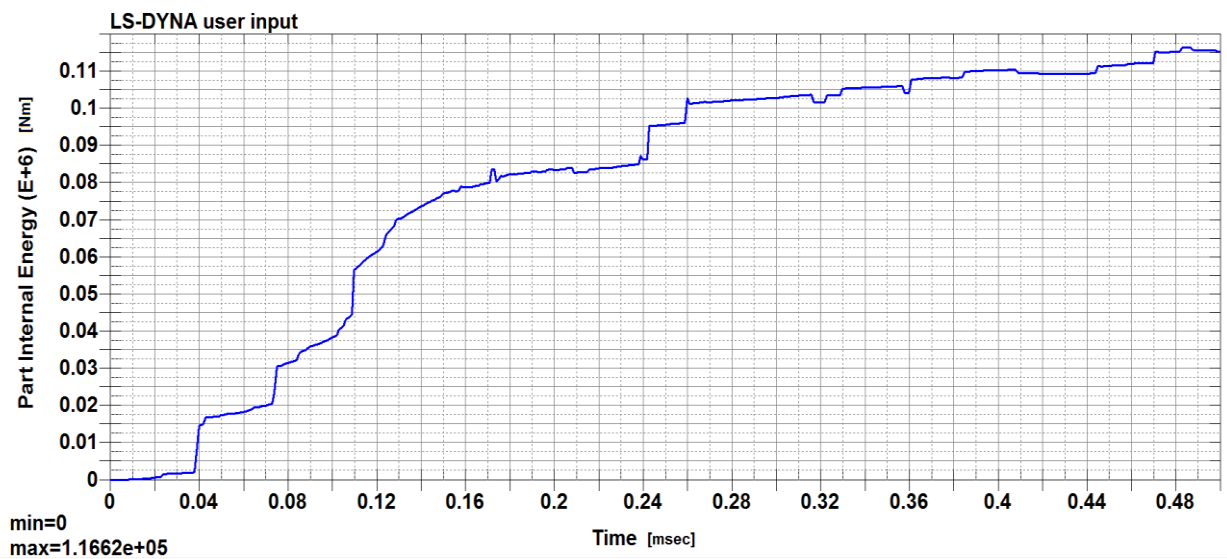


Figure 3.50: Internal energy - JSNH4/H2, TB51

Figure 3.51 shows vehicle acceleration obtained during simulation of crash test TB51.

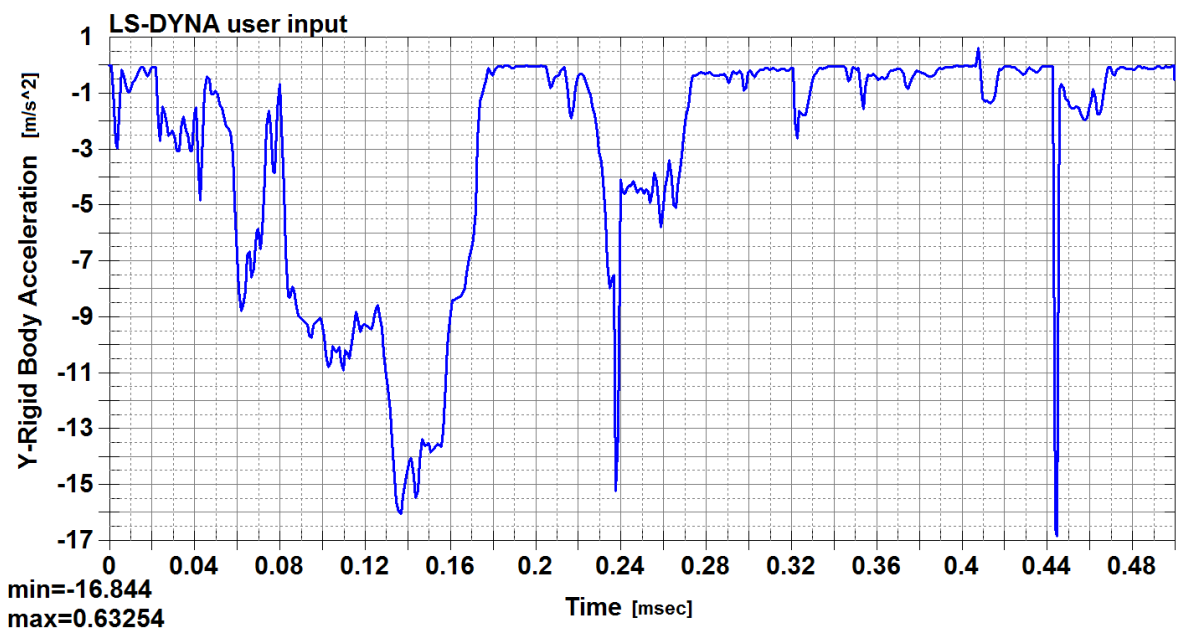


Figure 3.51: Vehicle acceleration - JSNH4/H2, TB51

The maximum value of acceleration is  $-16,844 \text{ m/s}^2$ . At time step 0,160 ms when the safety barrier is not fully destroyed and can perform its functions, it reaches  $-8 \text{ m/s}^2$ . The corresponding impact forces are 218,972 kN and 104 kN respectively. According to

TP 101 the alternative load force for this type of crash test should be from 90 kN to 170 kN for more flexible barriers with dynamic deflection of 1,500 m - 2,500 m and from 160 kN to 200 kN for more rigid barriers with dynamic deflection of 0,100 m - 0,500 m [48]. We see that the impact force at time step 0,160 ms is in the range specified by standards. The maximum impact force is, however, much higher.

Resuming described results for a safety barrier of type JSNH4/H2 we would underline that we have made numerical simulation of three crash tests: TB11, TB42 and TB51. On the basis of the criteria of consumed energy we could conclude that safety barrier JSNH4/H2 has passed successfully all crash tests except TB51, where the value of internal energy turned out to be small. However, for all crash test simulations the values of impact forces the vehicle is able to resist are high and sufficient to state that JSNH4/H2 corresponds to containment level H2.

The same analysis has been made for safety barrier JSAM-2/H2 and its detailed description is presented below.

The first numerical simulation performed for JSAM-2/H2 is a numerical simulation of crash test TB11.

If we look at a graph of vehicle kinetic energy, we would see that its value is gradually decreasing during an impact and at last reaches 1,7735 kNm. Its maximum value at the beginning of an impact is 18,288 kNm; it means 36,576 kNm for a symmetrical task.

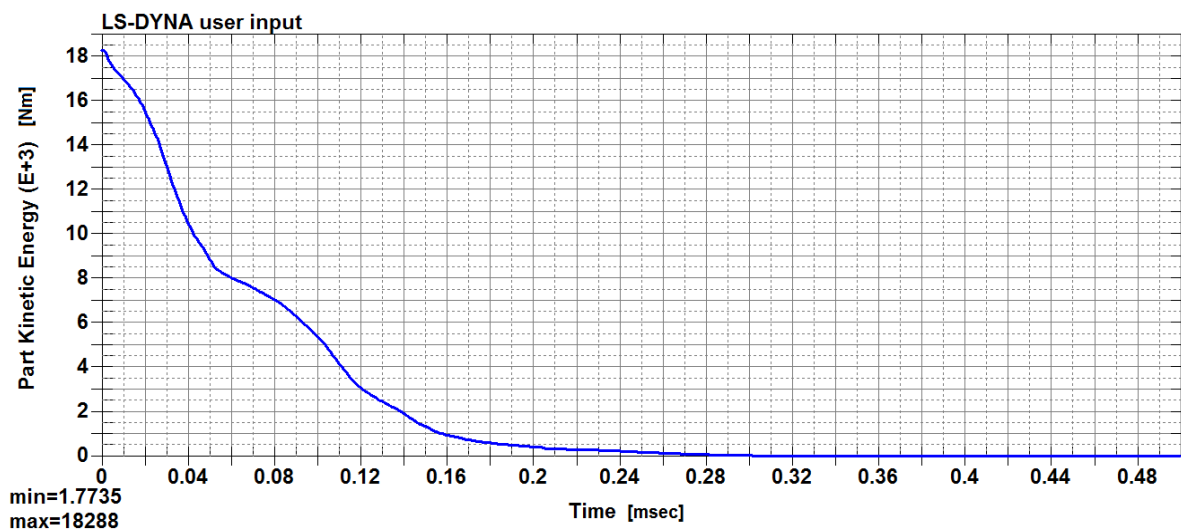


Figure 3.52: Kinetic energy of a vehicle - JSAM-2/H2, TB11

A vehicle velocity is decreasing as well and reaches almost zero. Its initial value of 9,5006 m/s is set before simulation and corresponds to a crash speed value specified in standards [20].

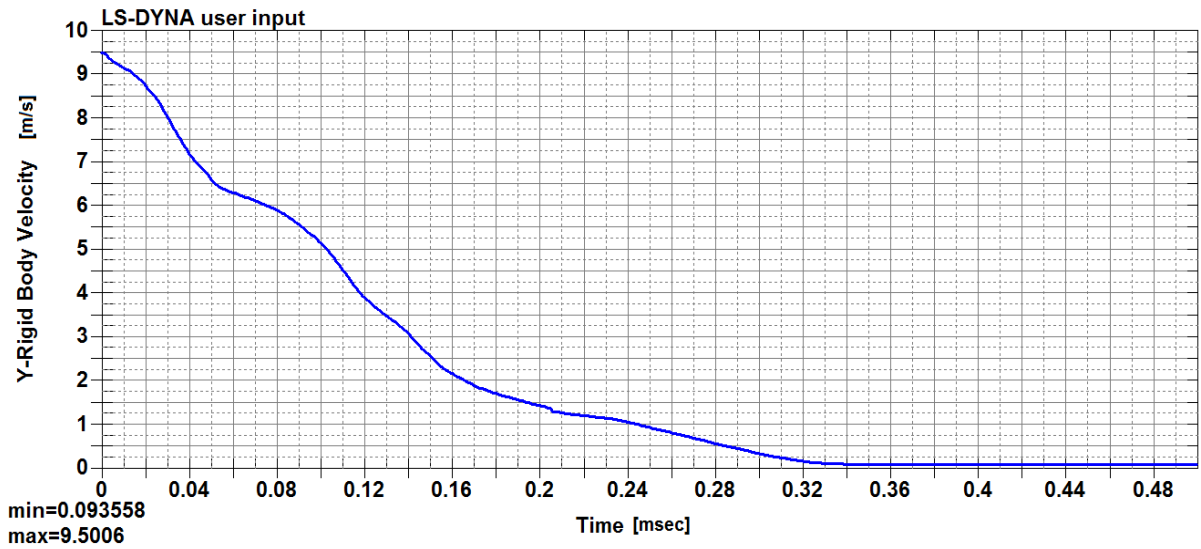


Figure 3.53: Vehicle velocity - JSAM-2/H2, TB11

The next graphs show displacement in y-direction for a barrier strip, a lower beam, distance spacers and a post.

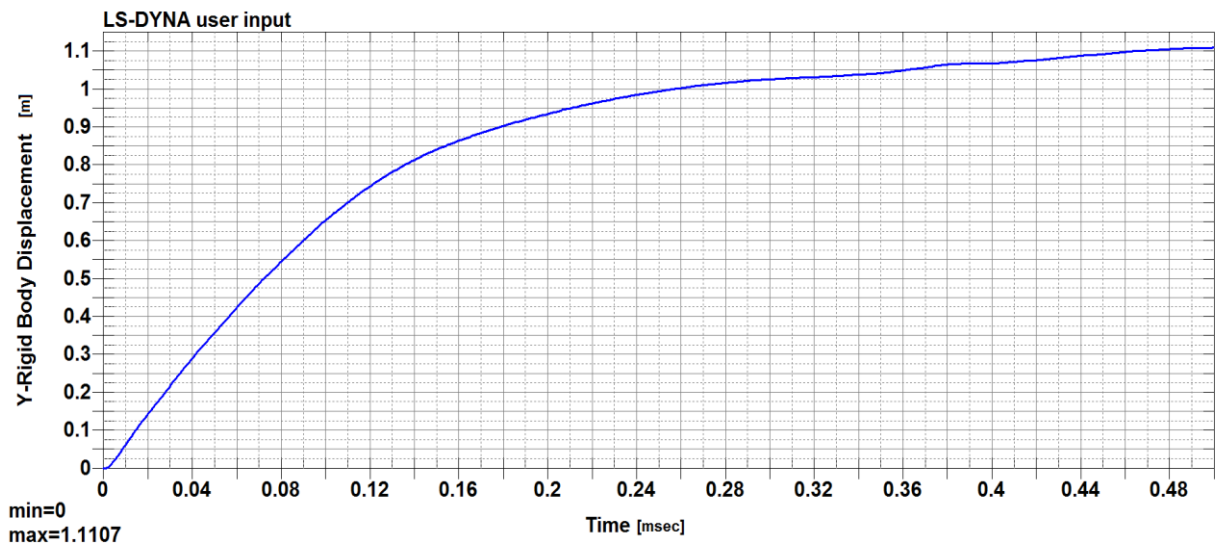


Figure 3.54: Barrier strip displacement - JSAM-2/H2, TB11

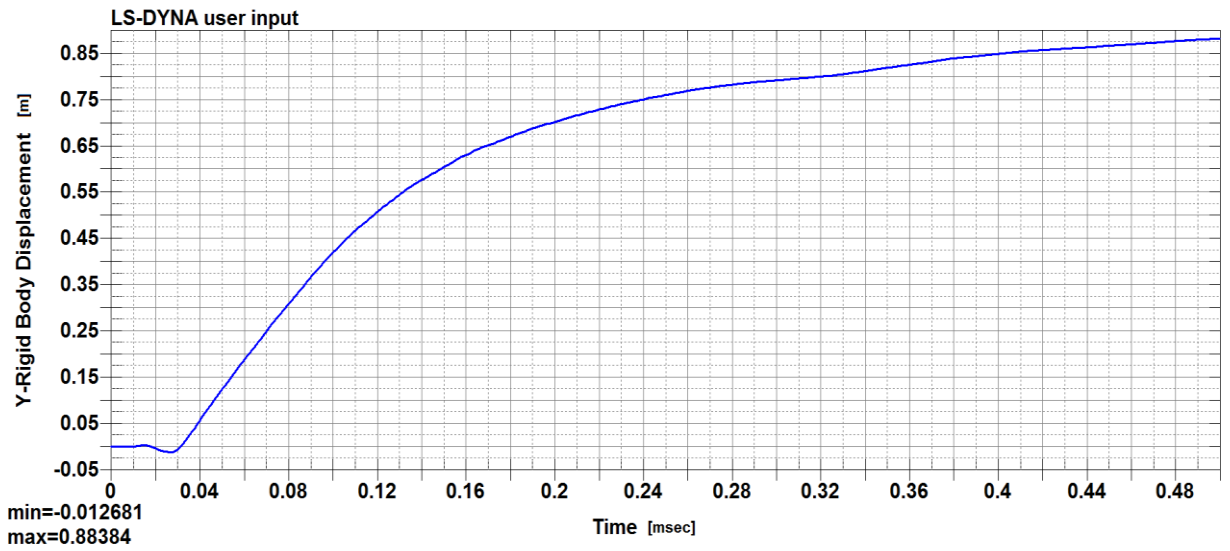


Figure 3.55: Lower beam displacement - JSAM-2/H2, TB11

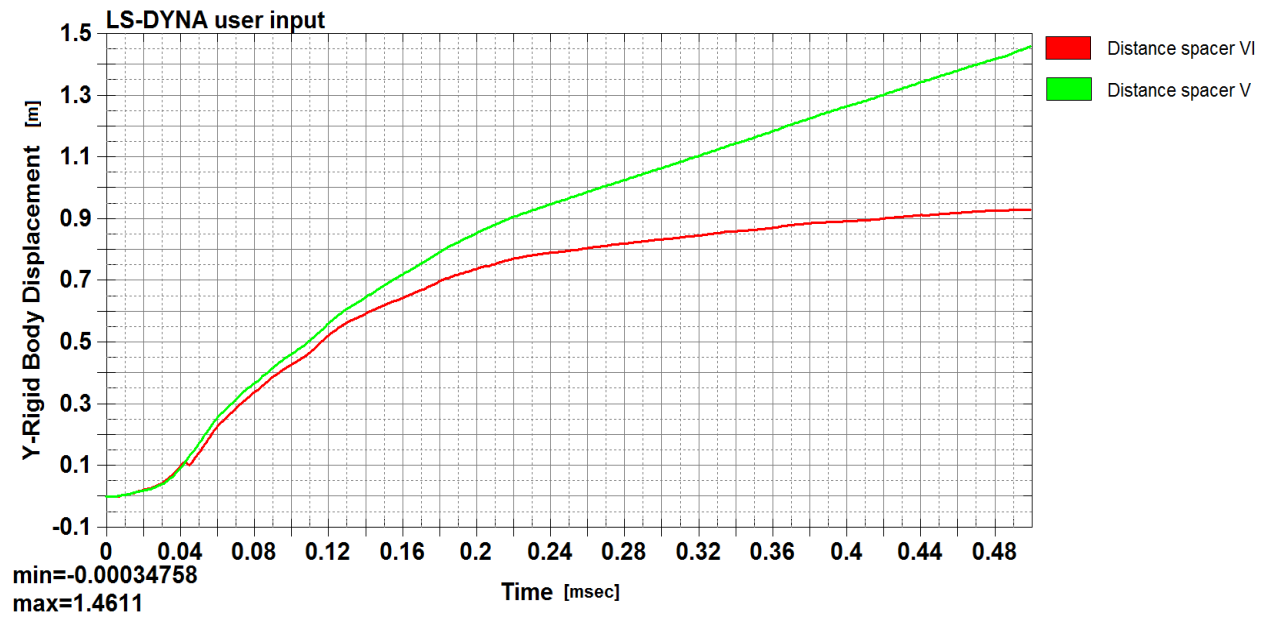
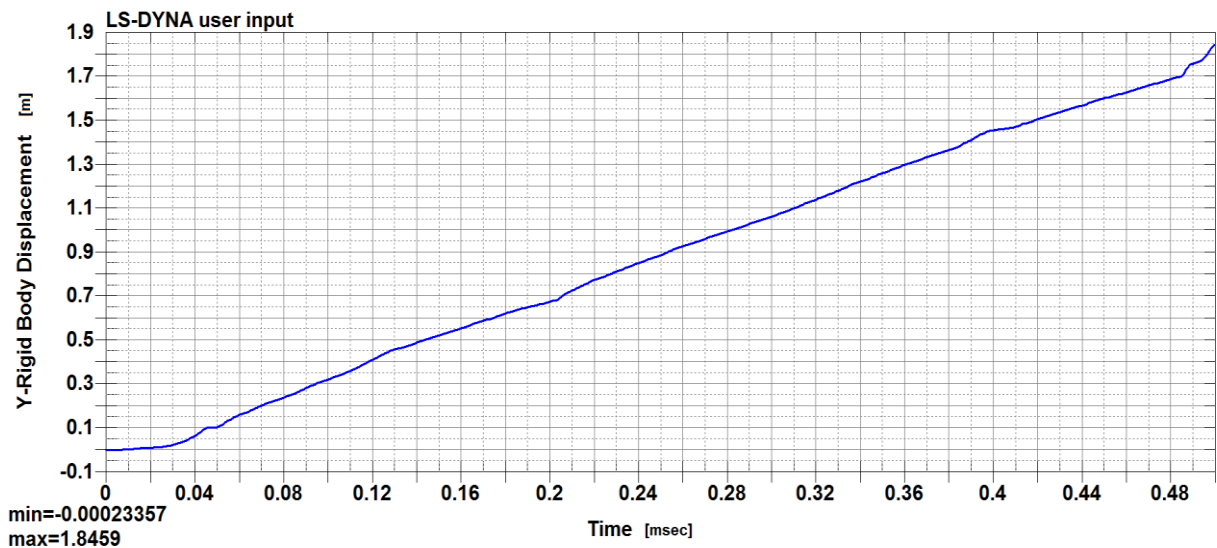


Figure 3.56: Distance spacer displacement - JSAM-2/H2, TB11





**Figure 3.57: Post displacement - JSAM-2/H2, TB11**

We see that the maximum value of displacement is the one of a post and it is equal to 1,8459 m. The values for other parts are the following:

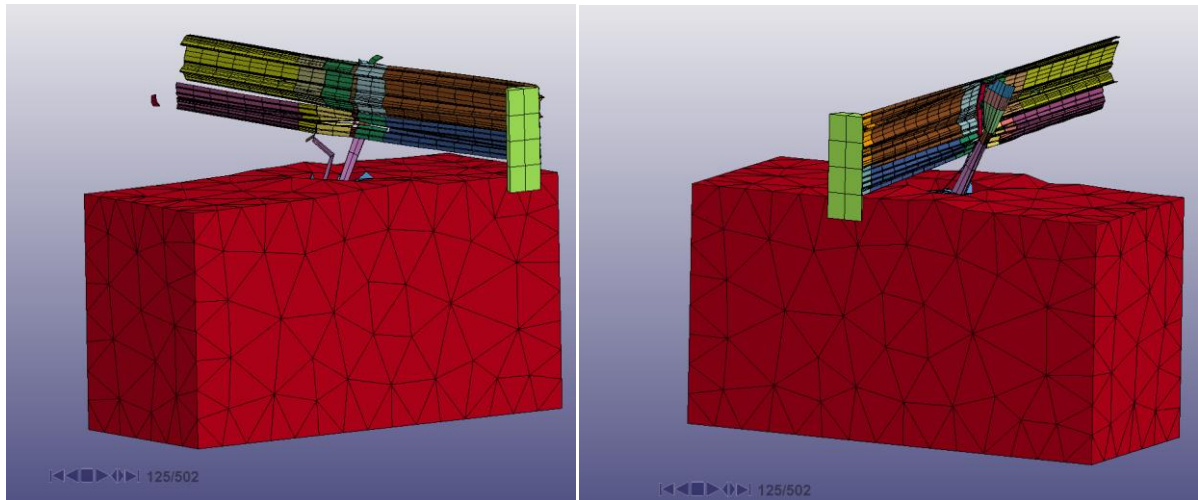
- a barrier strip - 1,1107 m,
- a lower beam - 0,88384 m,
- a distance spacer - 1,4611 m.

If we take the corresponding values at time step 0,125 ms as in an example with safety barrier JSNH4/H2 then we will obtain the following values:

- for a barrier strip it is app. 0,750 m,
- for a lower beam it is app. 0,525 m,
- for a distance spacer it is app. 0,590 m,
- for a post it is app. 0,460 m.

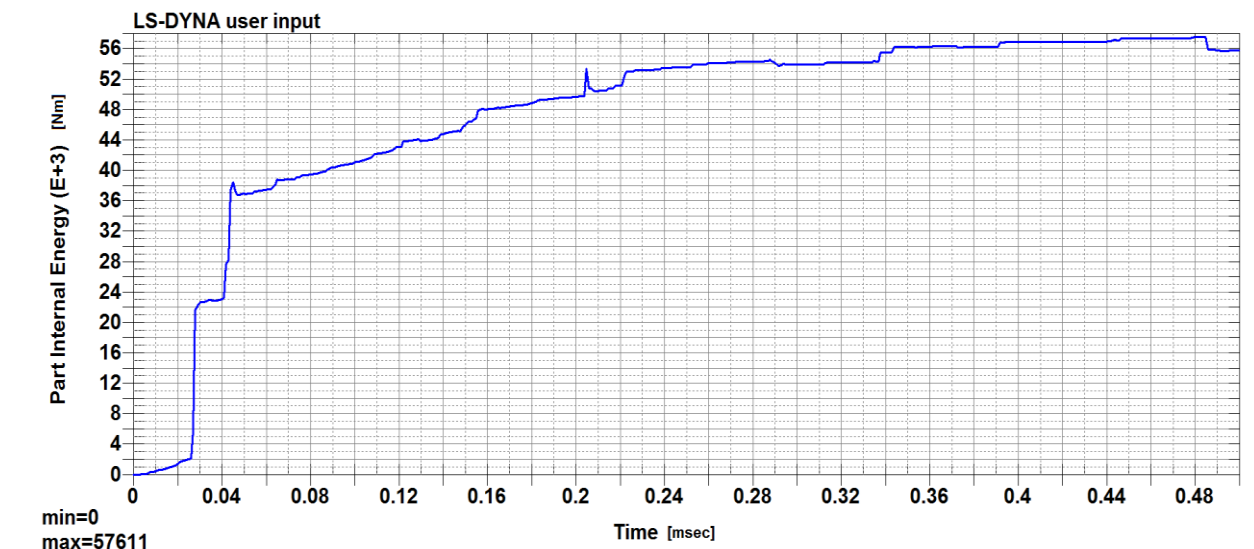
The values at time step 0,125 ms do not exceed the values for a working width (1,600 m) and a dynamic deflection (1,500 m) specified in technical conditions by the manufacturer [5].

The following figures illustrate safety barrier deformation at time step 0,125 ms.



**Figure 3.58: Safety barrier deformation at time step 0,125 ms - JSAM-2/H2, TB11**

The most interesting and speaking is a graph showing internal energy of our construction (see Figure 3.59).

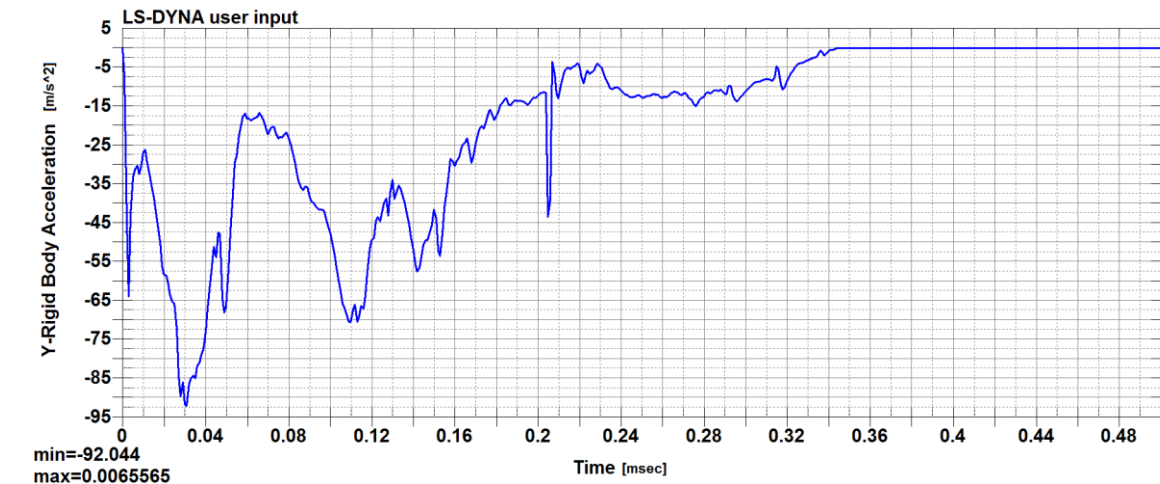


**Figure 3.59: Internal energy - JSAM-2/H2, TB11**

We see that the maximum value is 57,611 kNm, i.e. 115, 222 kNm for a symmetrical task. If we take the value of internal energy at time step 0,125 ms as we did for JSNH4/H2, we would find out that this value is equal to 44 kNm, i.e. 88 kNm for a symmetrical task. These values more than fully comply with the value specified in TP 114 (40,600 kNm) and with the value of kinetic energy obtained during simulation (36,576 kNm) [49]. Therefore, we can state that numerical simulation of crash test TB11 for JSAM-2/H2 is successfully performed

both according to the criteria of consumed energy and according to the maximum displacement value at certain time step.

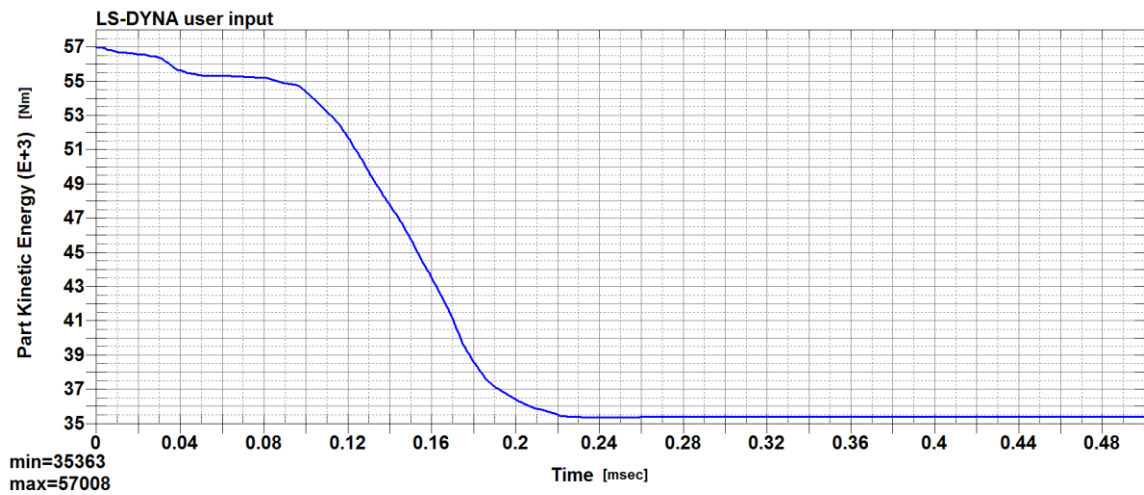
The next graph of our interest is the one illustrating vehicle acceleration.



**Figure 3.60: Vehicle acceleration - JSAM-2/H2, TB11**

From it we can see the maximum value of acceleration reached, which is 92,044  $\text{m/s}^2$ . At time step 0,125 ms it is equal to 42,500  $\text{m/s}^2$ . Therefore, the impact forces corresponding to these values of acceleration are 82,8396 kN and 38,250 kN respectively. Let us remind that TP 101 specifies the following alternative load forces corresponding to crash test TB11: 15 kN - 35 kN for a crash barrier with a dynamic deflection of 1,500 m - 2,500 m and 35 kN - 80 kN for a crash barrier with a dynamic deflection of 0,100 m - 0,500 m [48]. We see that the impact forces obtained during numerical simulation are sufficient or even higher than the alternative load forces described in TP 101.

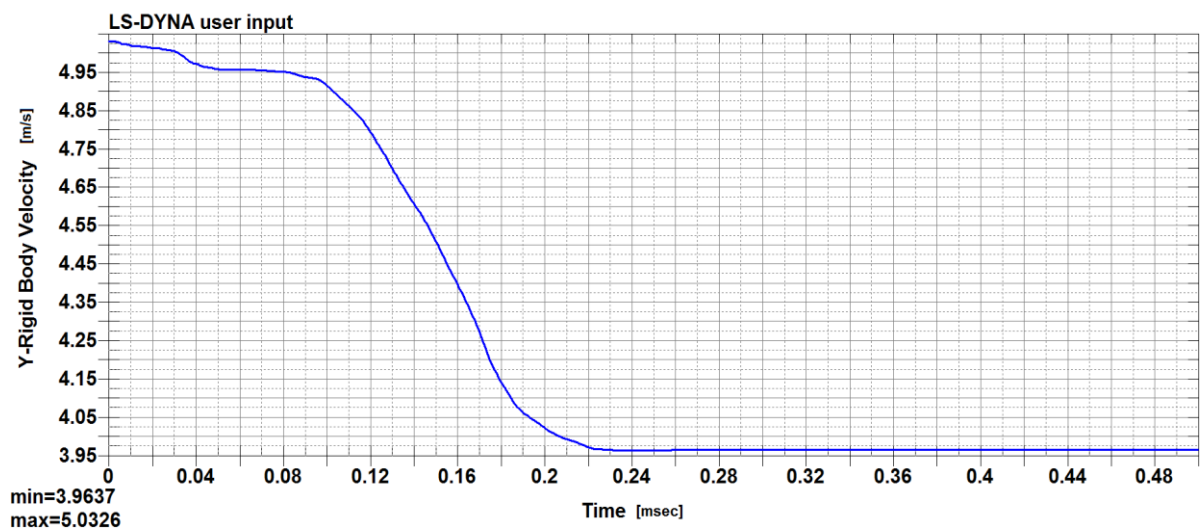
The graph depicting kinetic energy of a lorry resulted from numerical simulation of crash test TB42 is presented below.



**Figure 3.61: Kinetic energy of a vehicle - JSAM-2/H2, TB42**

We see that its maximum value is 57,008 kNm, i.e. 114,016 kNm for a symmetrical task. During an impact the safety barrier has managed to absorb only part of kinetic energy before its full destruction.

From the next graph we observe how the velocity of a vehicle is decreasing from its maximum value of 5,0326 m/s set before performing simulation to 3,9637 m/s.



**Figure 3.62: Vehicle velocity - JSAM-2/H2, TB42**

The following graphs present displacement in y-direction for a barrier strip, a lower beam, distance spacers and a post.

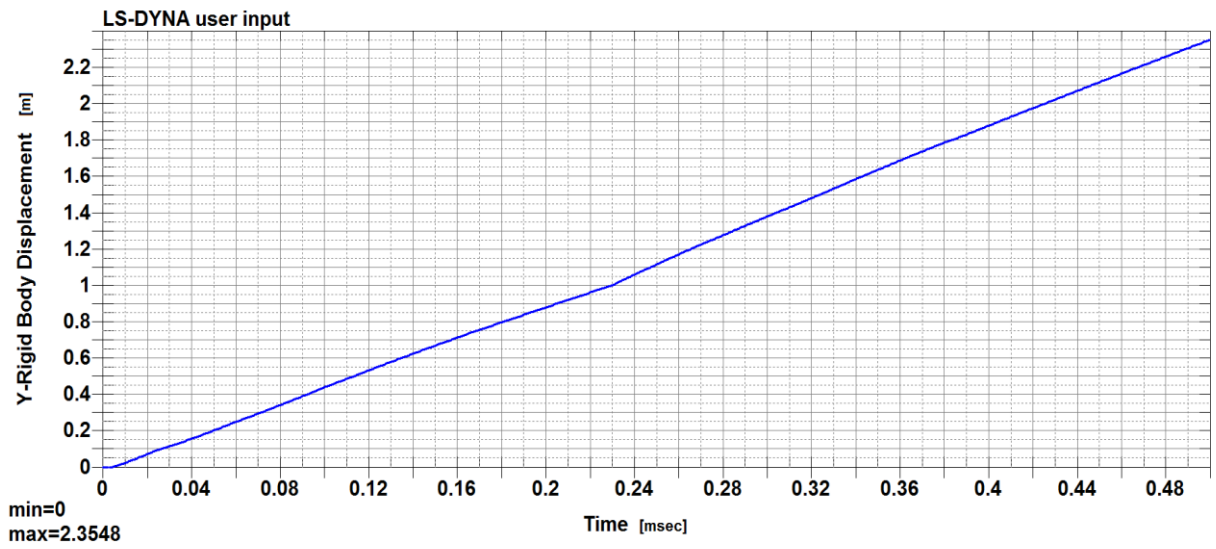


Figure 3.63: Barrier strip displacement - JSAM-2/H2, TB42

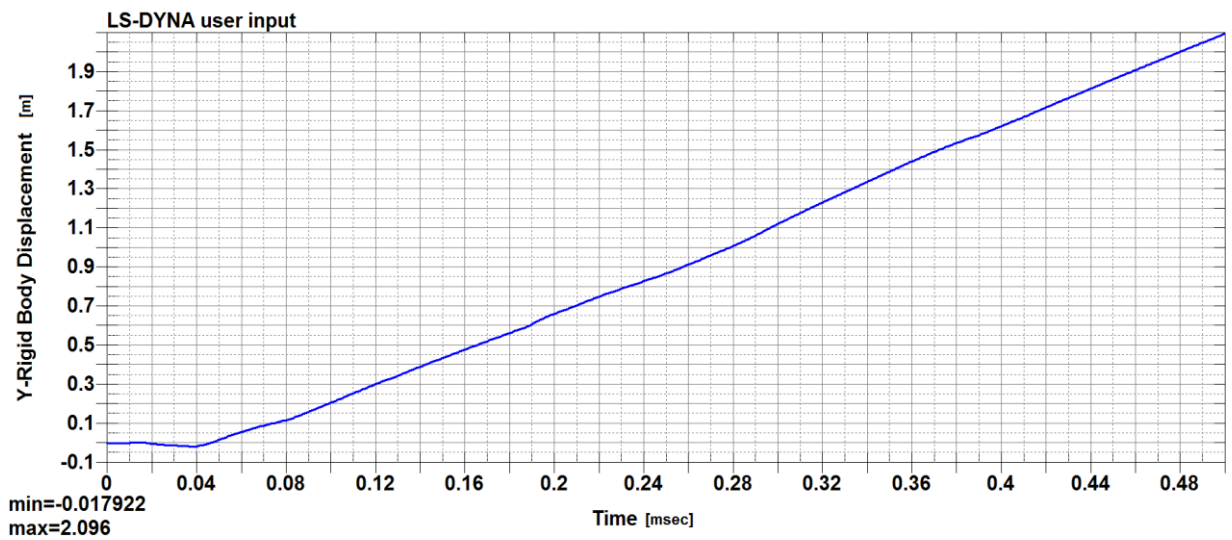


Figure 3.64: Lower beam displacement - JSAM-2/H2, TB42

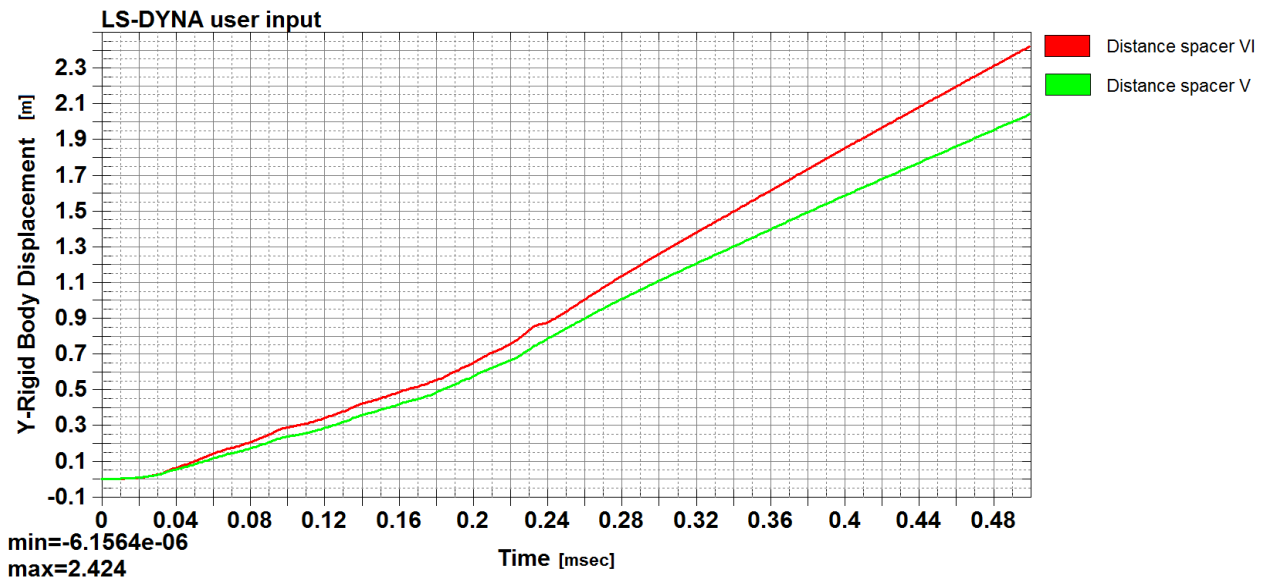


Figure 3.65: Distance spacer displacement - JSAM-2/H2, TB42

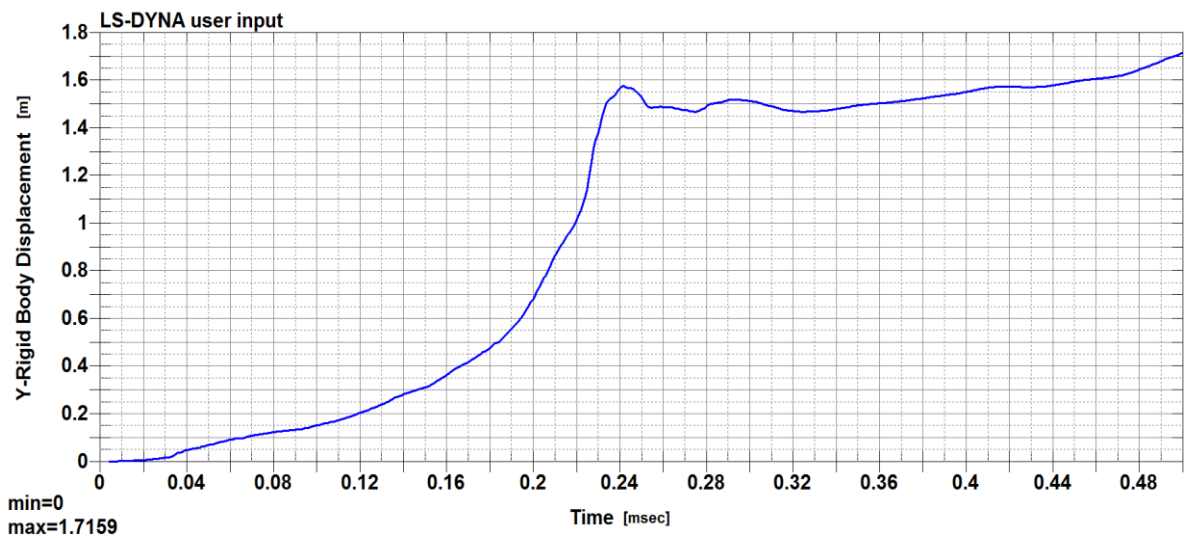


Figure 3.66: Post displacement - JSAM-2/H2, TB42

The maximum values of displacement are:

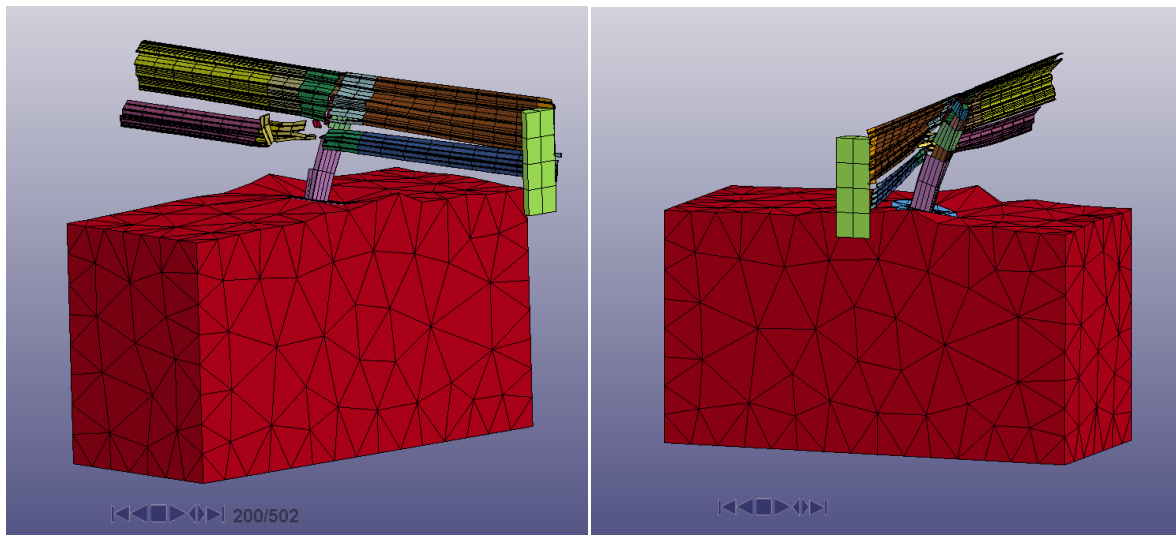
- a barrier strip - 2,3548 m,
- a lower beam - 2,096 m,
- a distance spacer - 2,424 m,
- a post - 1,7159 m.

If we take time step 0,200 ms when the safety barrier has not been fully destroyed yet, then the values of displacement will be:

- a barrier strip - 0,900 m,
- a lower beam - 0,670 m,
- a distance spacer - 0,650 m,
- a post - 0,700 m.

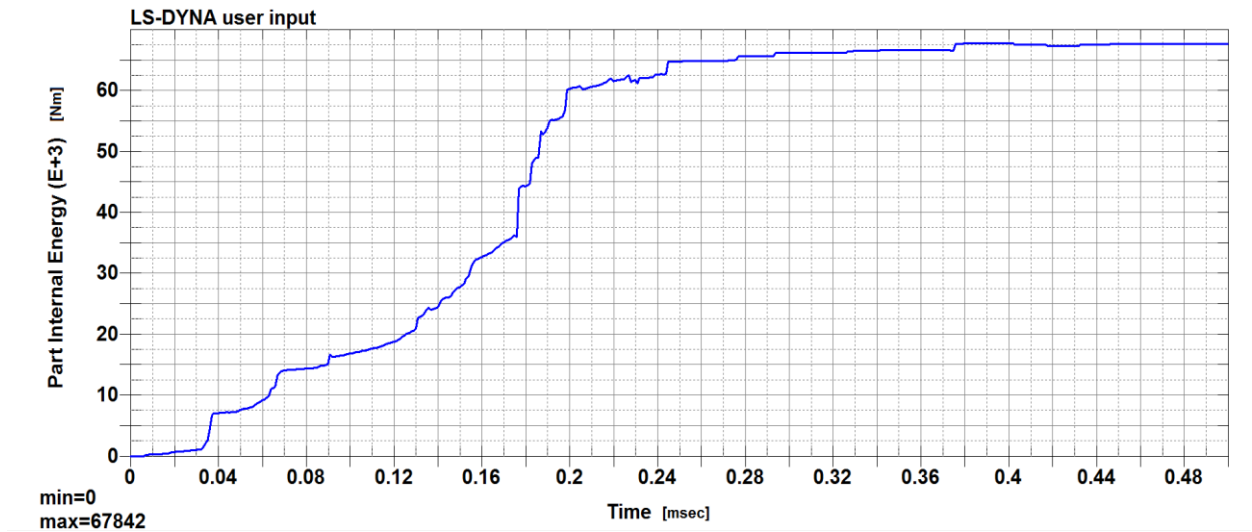
The values at time step 0,200 ms do not exceed the values of a working width (1,600 m) and a dynamic deflection (1,500 m) specified in technical conditions by the manufacturer [5].

The following figures illustrate deformation of the safety barrier at time step 0,200 ms.



**Figure 3.67: Safety barrier deformation at time step 0,200 ms - JSAM-2/H2, TB42**

The graph of internal energy of our construction is shown below.

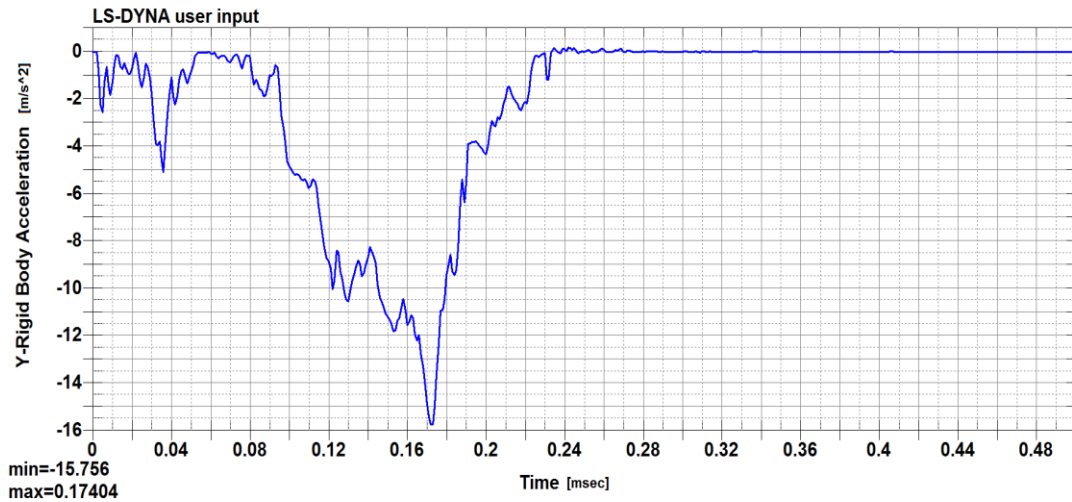


**Figure 3.68: Internal energy - JSAM-2/H2, TB42**

We see that its maximum value is 67,842 kNm, i.e. 135,684 kNm for a symmetrical task. We cannot take time step 0,250 ms as in an example with JSNH4/H2 for the same crash test, because at this time step a post and a lower beam are fully destroyed. In this case we can take time step 0,200 ms, where the post is not ruined yet. At this time step the value of internal energy is more than 60 kNm, i.e. more than 120 kNm for a symmetrical task. Though it is a little bit lower than specified in standards (126,600 kNm), however, taking into account that kinetic energy of a vehicle during simulation was lower as well and it was equal only to 114,016 kNm, we can conclude that according to the criteria of consumed energy safety barrier JSAM-2/H2 has passed crash test TB42 successfully [49].

The maximum achieved acceleration is  $-15,756 \text{ m/s}^2$  according to Figure 3.75. Acceleration at time step 0,200 ms is  $-4,500 \text{ m/s}^2$ .



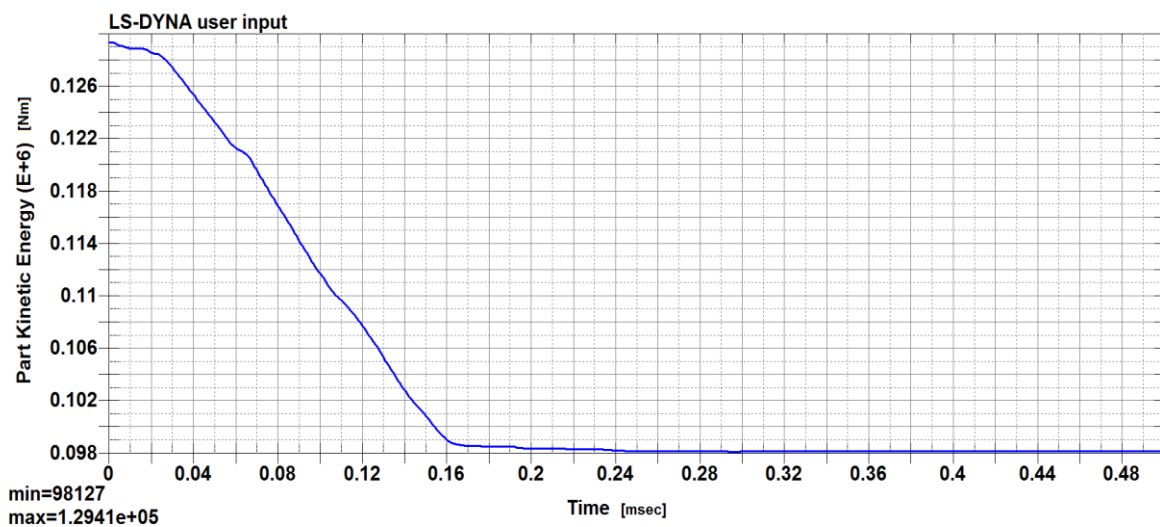


**Figure 3.69: Vehicle acceleration - JSAM-2/H2, TB42**

As in previous analysis we can calculate the impact forces. Thus, their values correspond to 157,56 kN for the maximum acceleration and 45 kN for acceleration at time step 0,200 ms. We see that 45 kN corresponds to below limit of the alternative load forces for TB42 specified in TP 101, where the values of alternative load forces for flexible barriers are in the range from 45 kN to 80 kN [48].

The results for crash test TB 51 are presented below.

During crash test TB51 kinetic energy of a vehicle was 129,41 kNm, i.e. 258,620 kNm for a symmetrical task. This value is lower than that specified in standards (287,500 kNm). We see that the safety barrier has not absorbed the whole energy of a vehicle and that during simulation it was fully destroyed.



**Figure 3.70: Kinetic energy of a vehicle - JSAM-2/H2, TB51**

A vehicle velocity does not reach zero as well and remains quite high, what indicates that the crash barrier did not either stop, catch or redirect the bus.

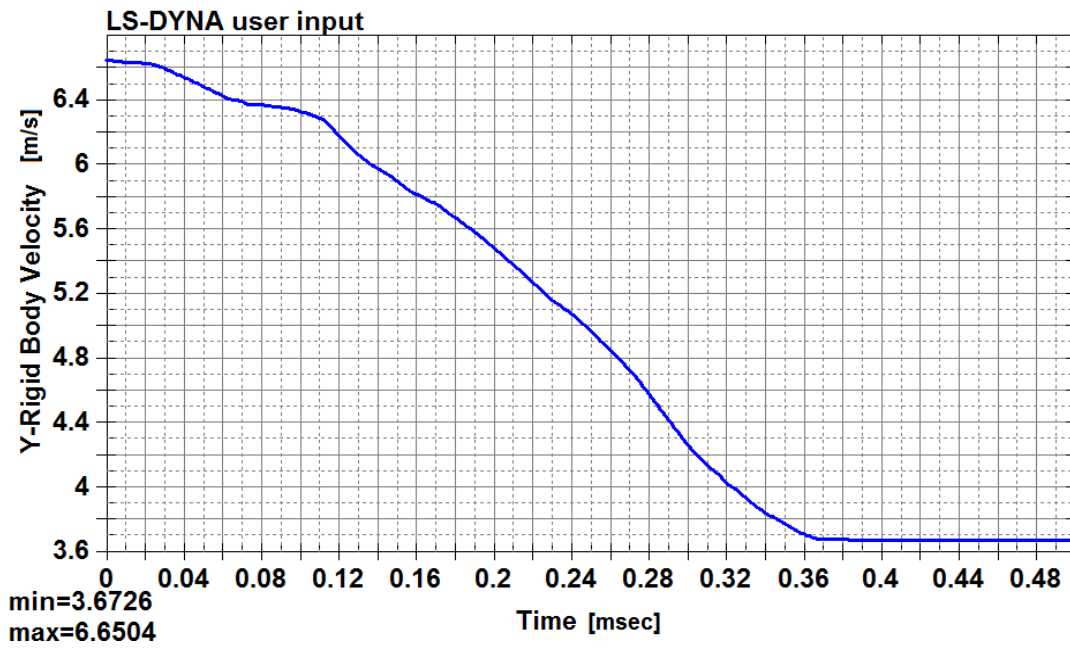


Figure 3.71: Vehicle velocity - JSAM-2/H2, TB51

The next graphs present displacement of corresponding parts in y-direction.

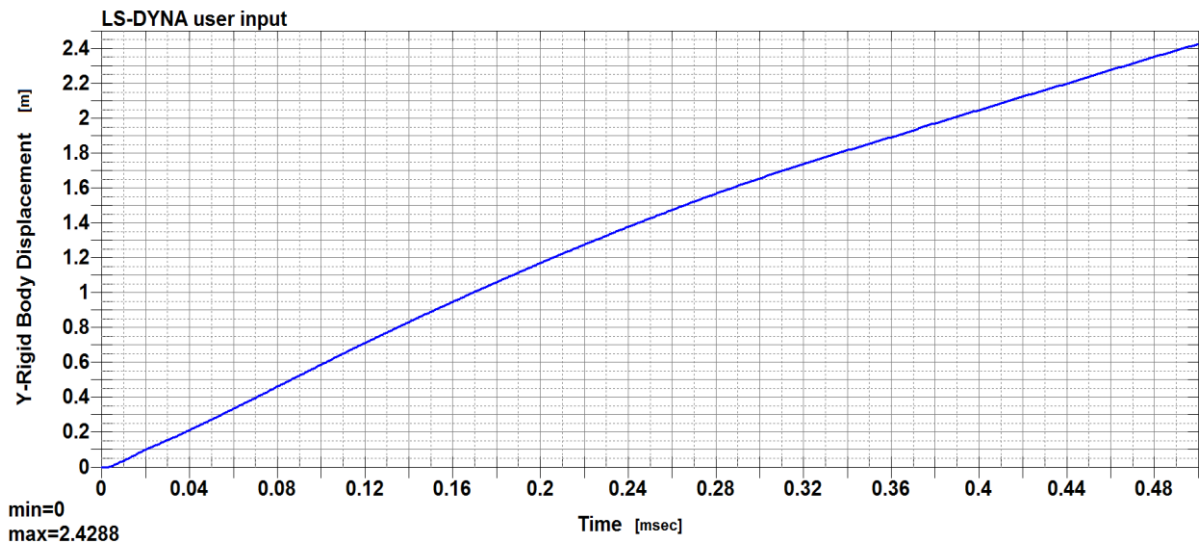


Figure 3.72: Barrier strip displacement - JSAM-2/H2, TB51

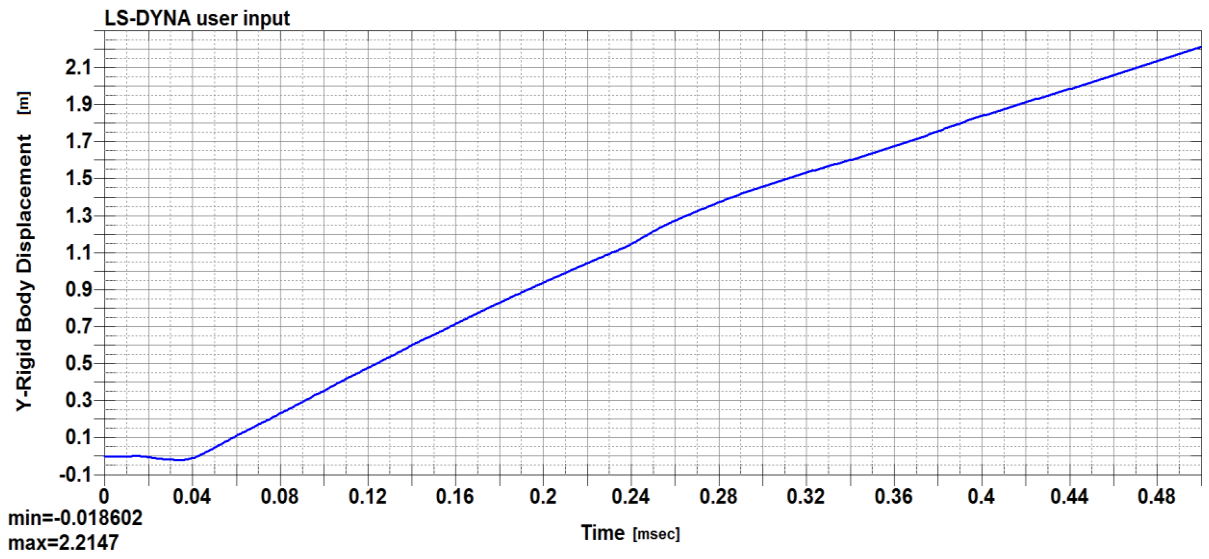


Figure 3.73: Lower beam displacement - JSAM-2/H2, TB51

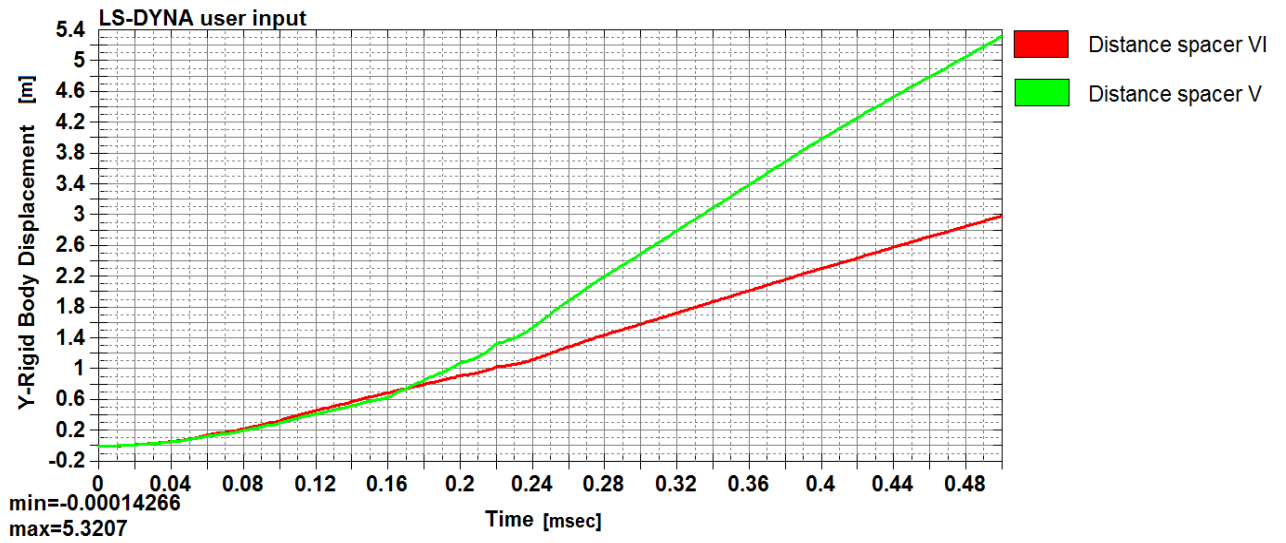
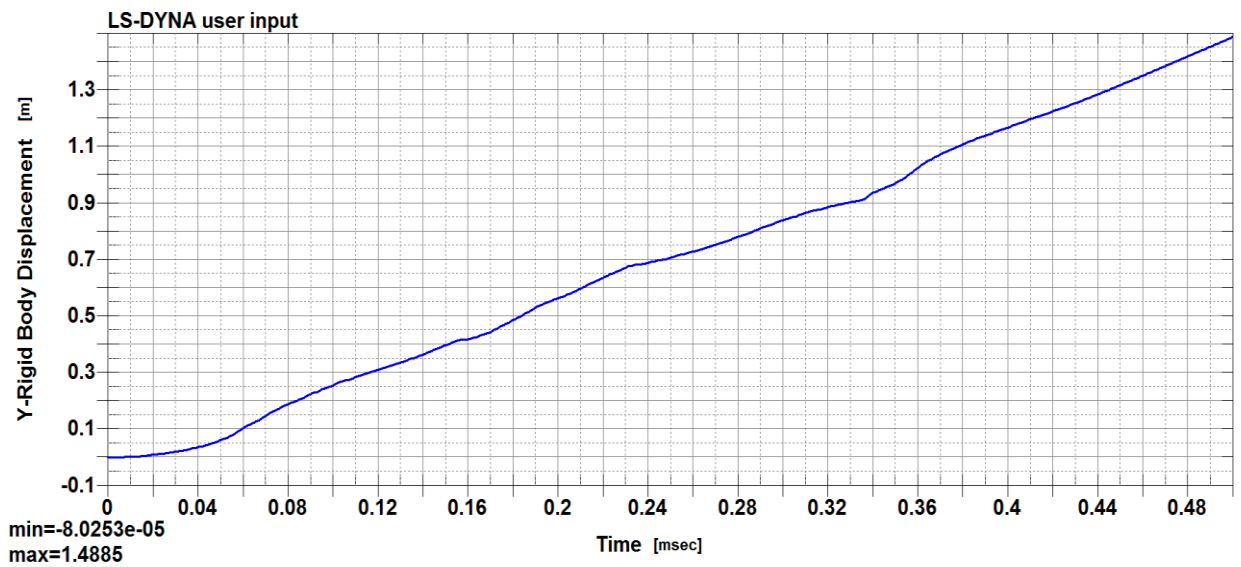


Figure 3.74: Distance spacer displacement - JSAM-2/H2, TB51



**Figure 3.75: Post displacement - JSAM-2/H2, TB51**

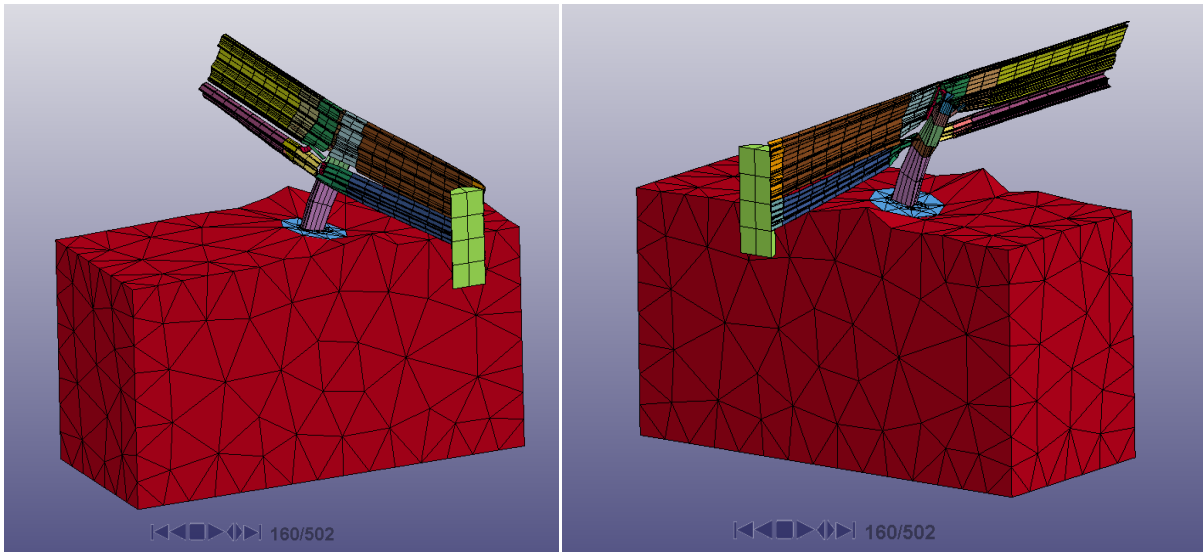
The maximum values of displacement are the following:

- a barrier strip - 2,4288 m,
- a lower beam - 2,2147 m,
- a distance spacer - 5,3207 m,
- a post - 1,4885 m.

For more objective notion of displacement of different parts of the safety barrier we need to consider some time step, when the safety barrier has not been fully destroyed. We can take, for example, time step 0,160 ms. Then the values of displacement are the following:

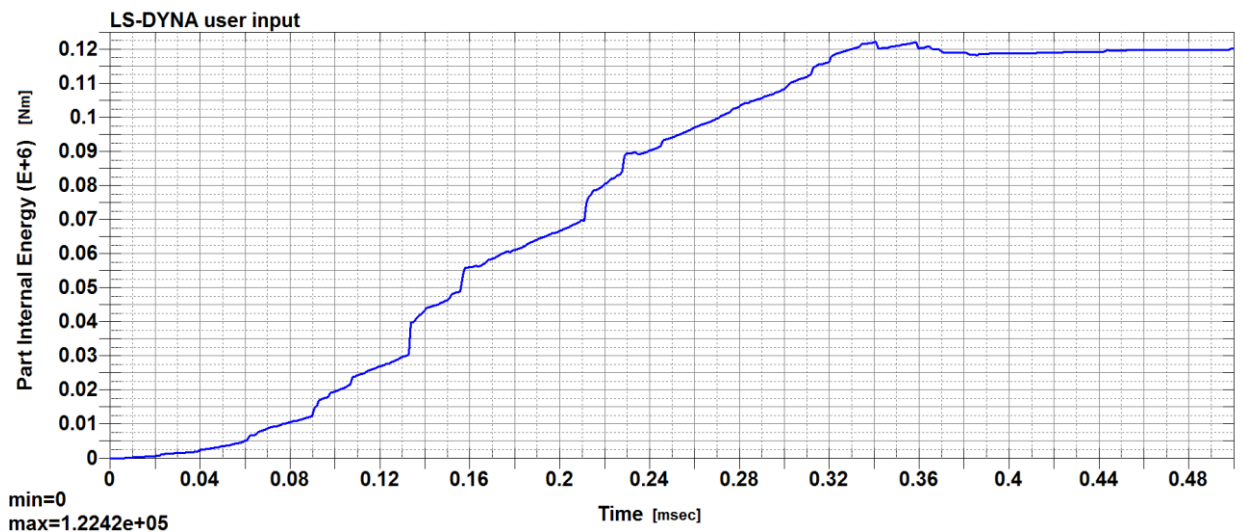
- a barrier strip - 0,950 m,
- a lower beam - 0,720 m,
- a distance spacer - 0,700 m,
- a post - 0,550 m.

The following figures illustrate a safety barrier deformation at time step 0,160 ms.



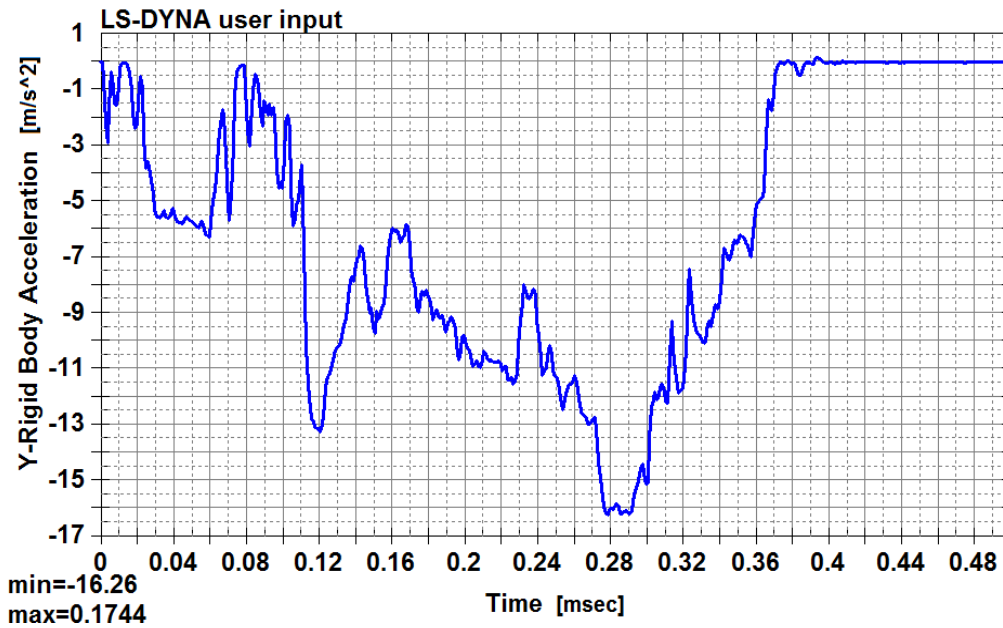
**Figure 3.76: Safety barrier deformation at time step 0,160 ms - JSAM-2/H2, TB51**

The next figure shows that internal energy of the construction reaches 122,420 kNm, i.e. 245,048 kNm for a symmetrical task. At time step 0,160 ms we have approximately 56 kNm, i.e. the total energy for a symmetrical task is 112 kNm. Though the value of maximum internal energy is quite high, however, at time step 0,160 ms it does not correspond either to kinetic energy of 287,500 kNm specified in standards or to kinetic energy obtained during simulation (258,620 kNm) [49]. Therefore, according to the criteria of consumed energy safety barrier JSAM-2/H2 has failed crash test TB51 simulated in LS-DYNA.



**Figure 3.77: Internal energy - JSAM-2/H2, TB51**

A graph for vehicle acceleration is presented below.



**Figure 3.78: Vehicle acceleration - JSAM-2/H2, TB51**

Again the maximum acceleration is  $-16,260 \text{ m/s}^2$ , while acceleration at time step 0,160 ms is  $-6 \text{ m/s}^2$ . The corresponding impact forces are 211,380 kN and 78 kN respectively. TP 101 specifies the following values of alternative load forces for flexible barriers: 90 kN -140 kN. We see that the impact forces achieved during numerical simulation of crash test TB51 are more or less in the range of alternative load forces specified in TP 101 [48].

Resuming all previous considerations about JSAM-2/H2 we can conclude that according to the criteria of consumed energy our model of safety barrier JSAM-2/H2 has successfully passed crash tests TB11 and TB42, but it has not succeeded in crash test TB51. However, the values of impact forces safety barrier can withstand are not lower than those specified in standards and therefore we can state that according to the impact forces the safety barrier has passed all tests and corresponds to containment level H2.

### 3.4. Comparison of obtained results for JSNH4/H2 and JSAM-2/H2

In this part we are nearing to the fulfillment of objectives of the present master's thesis, it means:

- firstly, we would compare the results obtained for JSNH4/H2 during numerical simulation in LS-DYNA with those got in the bachelor thesis while using a load force for simulation in ANSYS Workbench;
- secondly, for both models of safety barriers (JSNH4/H2 and JSAM-2/H2) we would compare parameters obtained during simulation with those specified in the manufacturer's documents;
- lastly, we would compare two types of safety barriers - JSNH4/H2 and JSAM-2/H2 - and underline the benefits the new type of a barrier is supposed to bring.

Let us remind that in the bachelor thesis we have created a model of JSNH4/H2 in ANSYS Workbench, defined contacts and boundary conditions and loaded it with the force equal to 120 kN for a symmetrical task. This force is much greater than that specified in TP 114, where taking into consideration a crash angle it will be equal to 68,400 kN [49]. The loading has been made gradually. The number of time steps was equal to 50. The initial force was equal to 0 N and for each time step it was increased for 1200 N. Calculation was stopped at the 27<sup>th</sup> time step, when the load force reached the value of 32,400 kN, i.e. the total value of impact force was 64,800 kN for a symmetrical task. According to TP 101 we have concluded that this type of safety barrier complies with the requirements for crash tests TB11 and TB42 [48]. But the value of internal energy obtained during simulation was too small and our conclusion was that according to the criteria of consumed energy this type of safety barrier did not fulfill the requirements for containment level H2. Besides we have concluded that the small value of internal energy could be caused by the fact that classic FEM calculation could not simulate further plastic deformation of a construction with a large deformation and neglects the dynamic impact forces. We have pointed out that it would be prosperous to use ANSYS LS-DYNA for dynamic simulation of an impact and for obtaining more accurate results.

Thus, in the present master's thesis we have performed numerical simulation in ANSYS LS-DYNA and we are able to compare obtained results.

As it was mentioned previously the values of internal energy we've obtained during simulation are compliant with the requirements for successful passing of crash tests TB11

and TB42. Moreover, the maximum value of internal energy (233,760 kNm) obtained during crash test TB51 is high enough to conclude that JSNH4/H2 successfully passed the test. However, this value corresponds to full destruction of the safety barrier under analysis. If we take the value of internal energy at certain time step - 160 kNm at 0,160 ms, - when the crash barrier is able to perform its functions, it turns to be small and insufficient. Due to this fact we have come to the conclusion that on the basis of the criteria of consumed energy our model has not succeeded in crash test TB51. On the other hands the values of impact forces are high enough to state that the safety barrier has passed all crash tests simulated during this work. The impact forces obtained are even much higher than the force achieved during simulation of static force in ANSYS Workbench (compare 64,800 kN got in ANSYS Workbench against even the minimum impact force for TB11, which is equal to 74,250 kN) and numerical simulation of all crash tests have had successful outputs in LS-DYNA, whereas in ANSYS Workbench the requirements only for TB11 and TB42 have been completely fulfilled [32]. We see that simulation of a dynamic impact gives more accurate and realistic results, because it takes into account shock and impact processes and other aspects, which are neglected during simulation of static force loading. Nevertheless, both methods if considering all details and setting properly all necessary parameters can give reliable and trustworthy preliminary information for evaluation of a safety barrier behavior during this or that crash test.

The same conclusion can be made in respect of safety barrier JSAM-2/H2. It means that according to impact forces this barrier can resist it is fully compliant with containment level H2. However, according to the criteria of consumed energy JSAM-2/H2 is proved to pass TB11 and TB42, and fail TB51, what corresponds to containment level H1.

The fact that numerical simulation of TB51 for both safety barriers was not successful, can be explained, for example, by simplification of the models (the impact was made at a right angle, simplified model of the ground and etc.), not precise material types used for deformation curves definition, not appropriate meshing and so on.

We see that to obtain more precise results we need to create more complex models, specify everything in more details and have more accurate inputs as far as materials, contacts and initial conditions are concerned.

Comparing two types of crash barriers we can notice that the impact forces the safety barrier can resist are higher for JSNH4/H2 for all crash tests (see table 3.18).



**Table 3.18: Comparison of JSNH4/H2 and JSAM-2/H2 - impact forces**

Crash test	Impact force [kN]	
	JSNH4/H2	JSAM-2/H2
<b>TB11</b>	From 74,250 kN to 105,183 kN	From 38,250 kN to 82,840 kN
<b>TB42</b>	From 130 kN to 183,440 kN	From 45 kN to 157,560 kN
<b>TB51</b>	From 104 kN to 218,978 kN	From 78 kN to 211,380 kN

It is explained by the fact that JSNH4/H2 has higher stiffness due to construction dimensions.

There is also a difference in the values of internal energy of two types, which is presented in the following table:

**Table 3.19: Comparison of JSNH4/H2 and JSAM-2/H2 - internal energy**

Crash test	Internal energy [kNm]	
	JSNH4/H2	JSAM-2/H2
<b>TB11</b>	43 kNm	88 kNm
<b>TB42</b>	135 kNm	120 kNm
<b>TB51</b>	max. 233,760 kNm	max. 245,050 kNm

The value of internal energy in TB11 for JSAM-2/H2 is app. twice higher than that for JSNH4/H2. From this we can conclude that JSAM-2/H2 better absorbs kinetic energy of a vehicle during an impact and therefore it is safer for passengers [6]. This fact is also proved by ASI index specified in technical documentation, which is lower for JSAM-2/H2: 1,1 against 1,186 [4], [5].

Similarly the value of internal energy obtained during TB51 is higher for JSAM-2/H2 in comparison with JSNH4/H2. However, it is a little bit lower during TB42.

As a conclusion we could say that both safety barriers have passed crash tests TB11 and TB42 according to the criteria of consumed energy and therefore the models correspond to containment level H1. According to the impact forces the barriers are able to withstand both types have passed all three crash tests - TB11, TB42, TB51 - and thus correspond to containment level H2 specified in technical documentation of the manufacturer. Moreover,

performing the same functions JSAM-2/H2 is proved to have several advantages over JSNH4/H2. Among them is better energy absorption and therefore higher safety for vehicle occupants. Another advantage is its weight, which is less up to 32 % in comparison with JSNH4/H2 (29 kg against 42,670 kg) [5], [6]. Decrease in weight is resulted in decrease in material consumption, less expenses and less influence on environment. Besides due to it being lighter there are certain benefits in terms of installation and maintenance [6].

## 4. Conclusion

In the present master's thesis numerical simulation of a vehicle impact on safety barriers has been performed and evaluated. Two types of safety barriers produced by Czech manufacturer ArcelorMittal have been selected. The chosen safety barriers are JSNH4/H2 and JSAM-2/H2.

On the basis of requirements specified in corresponding standards, technical conditions and technical documents of ArcelorMittal, geometrical models of safety barriers have been created in ANSYS Workbench, after which the discretization has been performed. After creating numerical models materials and contacts definition, boundary conditions and parameters specifications for crash tests TB11, TB42 and TB51 have been made in LS-DYNA PrePost. The last step was to run calculations in ANSYS LS-DYNA.

A non-linear behavior of a material has been preserved using non-linear steel characteristics. A plastic behavior of certain parts of a construction has been performed in such a way that we have defined deformation curves for steel S235JR and S355J0. We have had to replace S355MC by S355J0 and not to use S420MC, which is used for a post of JSAM-2/H2, because there were not found stress-strain diagrams for these types of steel due to reasons specified in previous chapters. S355J0 is from the same grade as S355MC, which is used for a post of JSNH4/H2 and for a barrier strip and a lower beam of JSAM-2/H2 and which differs from S355MC mainly in yield strength.

Numerical simulation has been fulfilled for three crash tests TB11, TB42 and TB51 for both models. In the result we have internal energy, displacement, vehicle acceleration and other useful information, on the basis of which we can evaluate calculation.

Thus, for JSNH4/H2 in TB11 we have obtained 43 kNm for internal energy and the range of impact forces the safety barrier is able to resist is 74,250 kN - 105,183 kN. For the same crash test JSAM-2/H2 has internal energy of 88 kNm and impact forces in the range of 38,250 kN - 82,840 kN. During TB42 the internal energy for JSNH4/H2 was equal to 135 kNm and for JSAM-2/H2 it was 120 kNm. The impact forces for this type of test correspond to 130 kN - 83,440 kN for JSNH4/H2 and 45 kN - 157,560 kN for JSAM-2/H2. Crash test TB51 has been failed by both safety barriers, because the value of internal energy obtained at certain time step was too small: 160 kNm for JSNH4/H2 and 112 kNm for JSAM-2/H2, though its maximum values corresponding to full destruction of the barriers - 233,760 kNm for JSNH4/H2 and 245,050 kNm for JSAM-2/H2 - can be counted as being

sufficient for passing TB51. However, crash test TB51 can be considered as successful one according to the impact forces achieved: 104 kN - 218,972 kN for JSNH4/H2 and 78 kN - 211,380 kN for JSAM-2/H2. Thus, we have concluded that according to the impact forces both types correspond to containment level H2. However, according to the criteria of consumed energy they fulfill the requirements only for containment level H1.

Further on we have compared two types of barriers and though both types can perform the same functions equally well, however, safety barrier JSAM-2/H2 absorbs energy better. Taking into account that JSAM-2/H2 has other advantages in terms of its small weight and material properties, we can state that JSAM-2/H2 is a good designer solution, which in respect of catching and redirecting vehicle fulfills purposes it has been constructed for as good as JSNH4/H2 does, but besides it is lighter, safer for passengers and has other advantages due to costs and influence on the environment.

Resuming all facts we can conclude that ANSYS Workbench and ANSYS LS-DYNA are proved to be very good tools for stress assessment of different constructions - resistance against plastic deformation. Though in standards it is indicated that the safety barriers should be tested in real crash tests, however, preparation and financing of such tests is a challenging task. ANSYS having excellent tools for simulating similar tests can be used for preliminary calculations, which would help avoid possible mistakes and waste of time. Besides it would reduce costs, and what is the most important - increase the efficiency of the preparation of experimental tests and improve the final results.

# Bibliography

- [1] Agrozet ZS. *Otevírací svodidlo GATE-GUARD 16 QC* [online]. [cit.15.03.2015]. Available at <http://www.agrozetzs.eu/mobilni-ocelove-svodidlo-gate-guard16.html>
- [2] Agrozet ZS. *Tlumiče nárazů* [online]. [cit. 15.03.2015]. Available at <http://www.agrozetzs.eu/>
- [3] ANSYS, Inc. *ANSYS Workbench User's Guide*. Release 12.1 [online]. November 2009. [cit. 05.02.2013]. Available at [http://orange.engr.ucdavis.edu/Documentation12.1/121/wb2\\_help.pdf](http://orange.engr.ucdavis.edu/Documentation12.1/121/wb2_help.pdf)
- [4] ArcelorMittal Ostrava a. s. *Jednostranné svodidlo JSNH4/H2* [online]. [cit. 15.11.2012]. Available at: <http://www.arcelormittal.cz/index.html>
- [5] ArcelorMittal Ostrava a. s. *Jednostranné svodidlo JSAM-2/H2* [online]. Available at: [http://www.doznac.cz/wp-content/uploads/6\\_JSAM-2-H2.pdf](http://www.doznac.cz/wp-content/uploads/6_JSAM-2-H2.pdf)
- [6] ArcelorMittal Europe. *Flat Products. Update*. Zákaznický časopis: May 2014 [online]. Available at [http://flateurope.arcelormittal.com/repository2/About/CZ\\_Update\\_May14.pdf](http://flateurope.arcelormittal.com/repository2/About/CZ_Update_May14.pdf)
- [7] ArcelorMittal. *Hutnické listy: odborný časopis pro metalurgii a materiálové inženýrství*. Ročník LXI, 2008 [online]. Available at [www.hutnickelisty.cz](http://www.hutnickelisty.cz)
- [8] ArcelorMittal a. s. *Safety barriers brochure*: May 2014 [online]. Available at <http://industry.arcelormittal.com/news/may/safetybarriersbrochure>
- [9] ArcelorMittal Ostrava a. s. *Ocelové svodidlo ArcelorMittal. Profil svodnice AM. Montážní návod č. 1/2014*. February, 2014 [online]. Available at <http://www.arcelormittal.cz/pdf/OceloveSvodidloAM-MontazniNavod-1-2014.pdf>
- [10] ArcelorMittal Ostrava a. s. *Ocelové svodidlo ArcelorMittal. Profil svodnice NH4. Montážní návod č. 2/2014*. February, 2014 [online]. Available at [http://www.arcelormittal.cz/pdf/Montazni\\_navod\\_NH4SK09.pdf](http://www.arcelormittal.cz/pdf/Montazni_navod_NH4SK09.pdf)
- [11] Barnat W., Bogusz P., Dziejulski P., Gieleta R., Kiczko A., Klasztorny M., Niezgoda T., Ochelski S. *Experimental validation of the numerical model of a car impact on a road barrier*. Journal of KONES Powertrain and Transport, Vol. 17, No. 1, 2010 [online]. Available at <http://www.kones.eu/ep/2010/vol17/no1/2.pdf>

- [12] Bligh R. P., Briaud J.-L., Kim K. M., Abu-Odeh A. *Design of roadside barrier systems placed on MSE retaining walls*. NCHRP: National cooperative highway research program, Report 663. Transportation research board of the national academies: Washington, D.C. 2010 [online]. Available at [www.trb.org](http://www.trb.org)
- [13] Bonin G., Cantisani G., Loprencipe G.. *Computational 3D models of vehicle's crash on road safety systems*. Universita di Roma "La Sapienza", Rome, Italy [online]. Available at <http://road-transport-technology.org/Proceedings/8%20-%20ISHVWD/COMPUTATIONAL%203D%20MODELS%20OF%20VEHICLES%20CRASH%20ON%20ROAD%20SAFETY%20SYSTEMS%20-%20Bonin.pdf>
- [14] Borkowski W., Hryciów Z., Rybak P., Wysocki J., Wiśniewski A.. *Studies on the effectiveness of the innovative road safety system*. Journal of KONES Powertrain and Transport, Vol. 21, No. 2, 2014 [online]. Available at [http://webcache.googleusercontent.com/search?q=cache:M1oIEqjGxqYJ:yadda.icm.edu.pl/yadda/element/bwmeta1.element.baztech-dc015947-71aa-4ce2-96f0-2def6c52b4b2/c/Journal\\_of\\_KONES\\_2014\\_No.\\_2\\_Vol.\\_21\\_ISSN\\_1231-4005\\_BORKOWSKI.pdf+&cd=3&hl=en&ct=clnk&gl=cz](http://webcache.googleusercontent.com/search?q=cache:M1oIEqjGxqYJ:yadda.icm.edu.pl/yadda/element/bwmeta1.element.baztech-dc015947-71aa-4ce2-96f0-2def6c52b4b2/c/Journal_of_KONES_2014_No._2_Vol._21_ISSN_1231-4005_BORKOWSKI.pdf+&cd=3&hl=en&ct=clnk&gl=cz)
- [15] Borovinšek M., Vesenjāk M., Ulbin M., Ren Z. *Simulating the impact of a truck on a road-safety barrier*. Strojniški vestnik: Journal of Mechanical Engineering 52(2006)2 [online]. Available at <http://www.sv-jme.eu/archive/sv-jme-volume-2006/sv-jme-52-2-2006/>
- [16] B2B Metal: online metal marketplace. *S235JR steel grade, mechanical properties, chemical composition, grade equivalent* [online]. [cit. 12.12.2014]. Available at <http://www.b2bmetal.eu/en/pages/index/index/id/141/>
- [17] B2B Metal: online metal marketplace. *S355J0 steel grade, mechanical properties, chemical composition, grade equivalent* [online]. [cit. 12.12.2014]. Available at <http://www.b2bmetal.eu/en/pages/index/index/id/141/>
- [18] Consolazio G. R., Chung H. J., Gurley K. R. *Impact simulation and full scale crash testing of a low profile concrete work zone barrier*. Department of civil and coastal engineering. University of Florida: USA, 2002 [online]. Available at [www.sciencedirect.com](http://www.sciencedirect.com)
- [19] Consolazio G. R., Chung J. H. *Vehicle impact simulation for curb and barrier design. Volumi I - Impact simulation procedures*. Center for advanced infrastructure & transportation, Civil & Environmental engineering: Rutgers, The state university, Piscataway, NJ 08854-8014, October 1998

- [20] ČSN EN 1317-2 *Silniční záchytné systémy. Část 2: Svodidla a mostní svodidla. Funkční třídy, kritéria přijatelnosti nárazových zkoušek a zkušební metody*. ICS 13.200; 93.080.30, February, 2011.
- [21] ČSN EN 1317-5+A1 *Silniční záchytné systémy. Část 5: Požadavky na výrobky a posuzování shody záchytných systémů pro vozidla*. ICS 13.200; 93.080.30, Listopad 2008.
- [22] Doporučený standard technický. Skupina: silniční stavby. *Silniční záchytné systémy* [online]. DOS T soubor 5: č.10 2002. [cit. 13.11.2012]. Dostupné z: [www.profesis.cz](http://www.profesis.cz)
- [23] Drozda J. *Methodology of validation of FE Model for simulations of real crash tests*. Katedra ocelových a dřevěných konstrukcí FSv ČVUT. Nadace Františka Faltuse. Sborník semináře doktorandů katedry ocelových a dřevěných konstrukcí: Praha, 2014 [online]. Available at <http://www.ocel-drevo.fsv.cvut.cz/NFF/docs/sborniky/NFF-sbornik14.pdf>
- [24] Drozda J., Rotter R. *Využití numerické analýzy pro návrh a ověření mostních svodidel*. Centre for Effective and Sustainable Transport Infrastructure, WP3, 3.8b, 2014 [online]. Available at [http://www.cesti.cz/technicke\\_listy/tl2014/2014\\_WP3\\_TL3\\_8b.pdf](http://www.cesti.cz/technicke_listy/tl2014/2014_WP3_TL3_8b.pdf)
- [25] Dumitrache P. *Numerical simulation of the behaviour of the safety barriers and experimental validation*. Dunarea de Jos University Galaji, Engineering faculty Braila: Romania, 2010 [online]. Available at [http://das.tuwien.ac.at/fileadmin/mediapool-das/Diverse/Publications/BoA\\_Siofok/files/p047.pdf](http://das.tuwien.ac.at/fileadmin/mediapool-das/Diverse/Publications/BoA_Siofok/files/p047.pdf)
- [26] European steel and alloy grades. *S355MC(1.0976)* [online]. [cit. 05.02.2013]. Dostupné z: [http://www.steelnumber.com/en/steel\\_composition\\_eu.php?name\\_id=206](http://www.steelnumber.com/en/steel_composition_eu.php?name_id=206)
- [27] European steel and alloy grades. *S420MC(1.0980)* [online]. [cit. 12.12.2014]. [http://www.steelnumber.com/en/steel\\_composition\\_eu.php?name\\_id=207](http://www.steelnumber.com/en/steel_composition_eu.php?name_id=207)
- [28] Fracasso hellas. *Impact Severity index* [online]. [cit. 20.11.2014]. Available at [www.fracassohellas.gr/wordpress/wp.../11/Impact-Severity-Index.pdf](http://www.fracassohellas.gr/wordpress/wp.../11/Impact-Severity-Index.pdf)
- [29] Gruber K., Herrmann M., Pitzer M. *Computer simulation of side impact using different mobile barriers*. DOI 10.4271/910323. 1991 [online]. Available at <http://papers.sae.org/910323/>

- [30] Hao H., Deeks J. A., Wu C.. *Numerical Simulations of the performance of steel guardrails under vehicle impact*. Transactions of Tianjin University: October 2008 [online]. Available at <http://link.springer.com/article/10.1007%2Fs12209-008-0054-2#page-1>
- [31] Hong K.-E., Thai H.-T., Kim S.-E. *Numerical simulation of composite safety barrier under vehicle impact*. Dept. of Civil & Environmental Engineering, Sejong University: Korea, 2010 [online]. Available at [http://wjoe.hebeu.edu.cn/sup.2.2010/HIJ/Hong,%20Kab-Eui%20\(Sejong%20U.,%20Seoul,%20S.%20Korea\)%20%20255.pdf](http://wjoe.hebeu.edu.cn/sup.2.2010/HIJ/Hong,%20Kab-Eui%20(Sejong%20U.,%20Seoul,%20S.%20Korea)%20%20255.pdf)
- [32] Likhonina R. N. *Strength and deformation behavior of barriers (bachelor thesis)*. ČVUT, Prague, 2013
- [33] LS-DYNA. *User's manual*. LSTC: Livermore Software Technology Corporation, 2011 [online]. Available at <http://www.lstc.com/products/ls-dyna>
- [34] LS-DYNA. *Keyword user's manual*. Volume I. Livermore software technology corporation (LSTC): Michigan, May 2007 [online]. Available at [http://www.lstc.com/pdf/ls-dyna\\_971\\_manual\\_k.pdf](http://www.lstc.com/pdf/ls-dyna_971_manual_k.pdf)
- [35] MABA PREFA Spol. s.r.o. *Dočasná svodidla DB 50SL a DB 65S* [online]. [cit. 15.03.2015]. Available at <http://www.mabaprefa.cz/prefabrikaty/vyrobky-a-sluzby/silnicni-dopravni-stavitelstvi/docasna-svodidla-db-50sl-a-db-65s/245/>
- [36] Mongiardini M., Ray M. H., Grzebieta R., Bambach M. *Verification and validation of models used in computer simulations of roadside barrier crashes*. Transport and road safety research, University of New South Wales - Australia, RoadSafe LLC - Maine, USA, 2013 [online]. Available at <http://acrs.org.au/files/arsrpe/Paper%2081%20-%20Mongiardini%20-%20Safety%20Perf%20Road%20Features.pdf>
- [37] Proznak. *Dopravní značení, vybavení komunikací, lanová svodidla* [online]. [cit. 15.03.2015]. Available at <http://www.proznak.cz/cze/index.php?pageid=detail.php?item=5-0000-0000>
- [38] Radimský, M. *Bezpečnostní zařízení na pozemních komunikacích*. Vysoké učení technické v Brně: Fakulta stavební [online]. Available at [www.fce.vutbr.cz/PKO/juza.p/vyuka/1.ppt](http://www.fce.vutbr.cz/PKO/juza.p/vyuka/1.ppt)



- [39] Ray H. M., et al. *Procedures for Verification and Validation of Computer Simulations Used for Roadside Safety Applications*. NCHRP Document 179: Washington, D.C. 2010 [online]. Available at [http://onlinepubs.trb.org/onlinepubs/nchrp/nchrp\\_w179.pdf](http://onlinepubs.trb.org/onlinepubs/nchrp/nchrp_w179.pdf)
- [40] Rochovanský, D. *Historie výroby ocelových svodidel v ČR* [online]. ISSN 1803-8441, 2009. [cit. 13.11.2012]. Dostupné z: <http://www.silnice-zeleznice.cz/clanek/historie-vyroby-ocelovych-svodidel-v-ceske-republice/>
- [41] Saferoad compan: FLOP dopravní značení. *Technické podmínky dřevooceľových svodidel* [online]. [cit. 15.03.2015]. Available at <http://www.flop-dz.cz/vyroba-a-prodej-svodidla-drevooceľova-svodidla-technicke-podminky/>
- [42] SOMARO: dopravní značení. *Oceľová svodidla* [online]. [cit. 15.03.2015]. Available at [http://www.somaro.cz/cs-stranky-ocelova\\_svodidla.html](http://www.somaro.cz/cs-stranky-ocelova_svodidla.html)
- [43] Stavební noviny. *ArcelorMittal zavádí do výroby nové typy svodidel* [online], 2011. [cit. 21.04.2013]. Dostupné z <http://tvstav.cz/clanek/1658-arcelormittal-zavadi-do-vyroby-nove-typy-svodidel>
- [44] Sura J. *České dálnice změni vizáž, dostanou moderní svodidla za miliardu*. iDNES.cz, March 2013 [online]. Available at [http://ekonomika.idnes.cz/dalnice-a-nova-svodidla-07q-/ekonomika.aspx?c=A130307\\_195506\\_ekonomika\\_ert](http://ekonomika.idnes.cz/dalnice-a-nova-svodidla-07q-/ekonomika.aspx?c=A130307_195506_ekonomika_ert)
- [45] Svodidla s.r.o. *Betonová svodidla* [online]. Available at [www.svodidla.cz](http://www.svodidla.cz)
- [46] Šebková I. *Nová svodidla ochrání motokáře*. Policie České Republiky, 2013 [online]. Available at <http://www.policie.cz/clanek/nova-svodidla-ochrani-motorkare.aspx>
- [47] Technické kvalitativní podmínky staveb pozemních komunikací. *Kapitola 11: Svodidla, zábradlí a tlumiče nárazů*. Č.j. 205/10-910-IPK/1. Praha: Ministerstvo dopravy, Odbor silniční infrastruktury, January, 2010.
- [48] TP 101 *Výpočet svodidel*. Č.j. 26514/97-120. Praha: Ministerstvo dopravy a spojů, Odbor pozemních komunikací, Dopravoprojekt, 1998.
- [49] TP 114. *Svodidla na pozemních komunikačních: Zatížení. Stanovení úrovně zadrženi na PK. Navrhování „jiných“ svodidel. Zkoušení a uvádění svodidel na trh*. Č.j. 148/10-910-IPK/1. Praha: Ministerstvo dopravy, Odbor silniční infrastruktury, Dopravoprojekt Brno, a.s., 2010.

- [50] TP 128 *Ocelové svodidlo NH4*. Praha: Ministerstvo dopravy, Dopravoprojekt Brno, a.s., 1999
- [51] TP 129 *Zkoušení a schvalování svodidel*. Praha: Ministerstvo dopravy, Dopravoprojekt Brno, a.s., 2009
- [52] TP 167 *Ocelová svodidla Arcelormittal: Prostorové uspořádání*. Č.j. 24/2012-120-TN/1. Praha: Ministerstvo dopravy, ArcelorMittal Ostrava, 2013
- [53] TP 167 *Ocelová svodidla Arcelormittal: Prostorové uspořádání. Dodatek č. 2/2013*. Č.j. 50/2013-120-TN/1. Praha: Ministerstvo dopravy, ArcelorMittal Ostrava, 2012
- [54] TP 203 *Ocelová svodidla (svodnicového typu)*. Č.j. 151/10-910-IPK/1. Praha: Ministerstvo dopravy, Odbor silniční infrastruktury. February, 2010.
- [55] Thiyahuddin M. I. M., Thambiratnam D., Gu Y. T., Gover R. *Safety enhancement of water-filled road safety barrier using interaction of composite materials*. International Journal of Technology: ISSN 2086-9614, 2013 [online]. Available at <http://www.google.kz/url?sa=t&rct=j&q=&esrc=s&source=web&cd=257&cad=rja&uact=8&ved=0CE0QFjAJOPcB&url=http%3A%2F%2Fwww.ijtech.eng.ui.ac.id%2Findex.php%2Fjournal%2Farticle%2Fdownload%2F119%2F150&ei=p-nYVJ6nlcOfyAOKloKwBA&usg=AFQjCNGtynK5HfMmQaZ6UxN4xd7IY32kow&bvm=bv.85464276,d.bGQ>
- [56] Ulker M. B. C., Rahman M. S. *Traffic barriers under vehicular impact from computer simulation to design guidelines*. Comp.-Aided Civil and Infrastructure Engineering 23(6): 2008 [online]. Available at [http://www.google.kz/url?sa=t&rct=j&q=&esrc=s&source=web&cd=121&cad=rja&uact=8&ved=0CDAQFjADOHU&url=http%3A%2F%2Fakademik.itu.edu.tr%2Fmbulker%2FDosyaGetir%2F69574%2FUlker%2520et%2520al%25202008.pdf&ei=7-rYVIXZJuSnygPbmYDQCg&usg=AFQjCNGkHNQ7wKFSLR\\_TE7Jrc0dh3otV3Q&bvm=bv.85464276,d.bGQ](http://www.google.kz/url?sa=t&rct=j&q=&esrc=s&source=web&cd=121&cad=rja&uact=8&ved=0CDAQFjADOHU&url=http%3A%2F%2Fakademik.itu.edu.tr%2Fmbulker%2FDosyaGetir%2F69574%2FUlker%2520et%2520al%25202008.pdf&ei=7-rYVIXZJuSnygPbmYDQCg&usg=AFQjCNGkHNQ7wKFSLR_TE7Jrc0dh3otV3Q&bvm=bv.85464276,d.bGQ)
- [57] Ústav mechaniky těles, mechatroniky a biomechaniky. *Metoda konečných prvků* [online]. [cit. 13.11.2012]. Dostupné z: [www.umt.fme.vutbr.cz/~jbursa/MKP4.doc](http://www.umt.fme.vutbr.cz/~jbursa/MKP4.doc)
- [58] Volkwein A. *Numerical simulation of flexible rockfall protection systems*. Proceedings of the International Conference on Computing in Civil Engineering: Cancun, Mexico, July 2005 [online]. Available at <http://www.pubs.asce.org/WWWdisplay.cgi?0523123>

- [59] Wu C., Hao H., Deeks J. A. *Vehicle impact response analysis of two-rail steel RHS traffic barrier*. Taylor and Francis Group: ISBN 90 5809 659 9, London, 2005 [online]. Available at [https://books.google.kz/books?id=vgprkYFib4AC&pg=PA975&lpg=PA975&dq=Numerical+simulation+of+impact+with+the+barriers&source=bl&ots=1bo6n71SSk&sig=rSK1YgymDNocEYv2kb8GEIhJgms&hl=en&sa=X&ei=PYnYVLg9x9\\_LA\\_nagTg&ved=0CDoQ6AEwBQ#v=onepage&q=Numerical%20simulation%20of%20impact%20with%20the%20barriers&f=false](https://books.google.kz/books?id=vgprkYFib4AC&pg=PA975&lpg=PA975&dq=Numerical+simulation+of+impact+with+the+barriers&source=bl&ots=1bo6n71SSk&sig=rSK1YgymDNocEYv2kb8GEIhJgms&hl=en&sa=X&ei=PYnYVLg9x9_LA_nagTg&ved=0CDoQ6AEwBQ#v=onepage&q=Numerical%20simulation%20of%20impact%20with%20the%20barriers&f=false)
- [60] Zienkiewicz O. C., Taylor R. L., Fox D. *The finite element method for solid and structural mechanics*. Science Direct, 7th seventh edition, ISBN: 978-1-85617-634-7 [online]. Available at <http://www.sciencedirect.com/science/book/9781856176347>
- [61] Zike S., Kalkins K., Ozolins O. *Experimental verification of simulation model of impact response tests for unsaturated polyester/GF and PP/GF composites*. CMMS Journal: 2011 [online]. Available at [http://www.cmms.agh.edu.pl/abstract.php?p\\_id=317](http://www.cmms.agh.edu.pl/abstract.php?p_id=317)

# List of terminology

**Acceleration severity index (ASI)** is an index characterizing the intensity of the impact and is regarded as the most important rate of impact on occupants [28].

**"Approved" safety barriers** are products of road restraint systems, which are produced for repeat use on the roads and tested in the full-scale crash tests [20]. They are subject to standards ČSN EN 1317-1, ČSN EN 1317-2 and harmonized ČSN EN 1317-5.

**Cable crash barrier** means a complete construction consisted of wire cables, steel posts and concrete anchorage blocks with anchor carcass (terminal and intermediate) [22].

**Concrete barrier** means a complete concrete construction composed from prefabricated segments and connecting parts (steel cables, connecting rods or loose locks) or a concrete monolithic construction [22].

**Containment level** is a parameter defined as a verified magnitude of a vehicle side impact, which a crash barrier is able to resist to without a vehicle overcoming it, whilst, on the other hand, ensuring a desired value of impact severity and vehicle behavior acceptability [20].

**Deformation work** is a work needed for deformation of the construction.

**Double-sided safety barrier** is a barrier designed for vehicle impacts from both sides.

**Dynamic deflection  $D_m$**  is the maximum dynamic lateral displacement of any point of the front part of a restraint system defined in ČSN EN 1317-2 [20].

**FEM** is a numerical method, which simulate loading, deformation and resonance development as well as other physical phenomena.

**Flexible (deformable) barrier** is a barrier, which is greatly deformed during an impact.

**Meshing** means dividing the model into finite number of elements.

**Opening barrier** is a special type of a crash barrier, which is usually installed in the central dividing strip, where it is necessary to ensure the fast opening without using mechanical means [22].

**"Other" safety barriers** refer to unit production according to the project documentation [20]. They are not tested in the full-scale crash tests and are allowed to be used only in justified cases.

**Parapet** is a complete construction consisted of the same components as the crash barriers, but which is also equipped with a steel handrail, infill, eventually wires [22].

**Post-impact head deceleration (PHD)** describes the head deceleration after an impact and has to be less than 20 g (acceleration of gravity) [28].

**Rigid (non-deformable) barrier** is a crash barrier, which deformation is very small after an impact and can be neglected.

**Road safety restraint system** is a system installed on the roads for ensuring a certain containment level of a vehicle, specified impact severity and corresponding working width [22].

**Safety barrier** is a type of road restraint systems installed on the roadside and in the central dividing strips.

**Single-sided safety barrier** is a barrier designed for vehicle impacts from one side.

**Temporary barrier** is a barrier frequently used during maintenance of the roads of category D, R, MR and roads of the 1<sup>st</sup> and 2<sup>nd</sup> classes [22].

**Steel safety barrier** means a complete steel construction consisted of barrier strips, lower beams (depending on type), posts, spacers, connecting straps, bolts, washers, fasteners and etc [22].

**Theoretical head impact velocity (THIV)** describes the theoretical speed of the head, colliding with an obstacle during an impact. It has to be less than 33 km/h [28].

**Vehicle deflection  $V_{I_m}$**  is its maximum dynamic lateral position from the front of not deformed barrier [20]. It is defined in accordance with ČSN EN 1317-2.

**Vehicle attenuator** means a complete construction composed of deformable elements (steel or plastic), which are assembled parallel or wedge. The function of this system is to reduce vehicle energy before an impact with a solid barrier [22].

**Vehicle cockpit deformation index (VCDI)** describes deformation of vehicle cockpit after an impact.

**Wooden steel crash barrier** means a complete construction consisted of combined barrier strips, combined posts, connectors and fasteners, etc [22].

**Working width  $W_m$**  is the maximum lateral distance between any part of a crash barrier on its front part before an impact and the maximum dynamic position of any part of a crash barrier during an impact [20]. It is defined in accordance with ČSN EN 1317-2.

# List of figures

Figure 2.1: Example of a steel safety barrier.....	19
Figure 2.2: Example of a cable safety barrier.....	20
Figure 2.3: Example of a wooden steel safety barrier.....	21
Figure 2.4: Example of a concrete safety barrier.....	22
Figure 2.5: Example of a parapet.....	23
Figure 2.6: Example of a vehicle atenuátor.....	23
Figure 2.7: Example of a temporary safety barrier.....	24
Figure 2.8: Example of an opening safety barrier.....	25
Figure 2.9: A crash barrier on connections, exits and junctions.....	44
Figure 2.10: Example of a steel barrier placement on the road.....	44
Figure 2.11: Single-sided crash barrier placement on a roadside.....	45
Figure 2.12: Single-sided crash barrier installation in a central dividing strip.....	45
Figure 2.13: Double-sided crash barrier installation in a central dividing strip.....	45
Figure 2.14: Safety barrier JSNH4/H2.....	52
Figure 2.15: Height of JSNH4/H2.....	54
Figure 2.16: JSNH4/H2 installation on the roadside verge.....	54
Figure 2.17: Example of JSNH4/H2 installation in a central dividing strip.....	55
Figure 2.18: Barrier trip of JSNH4/H2.....	55
Figure 2.19: Barrier strip interconnection.....	56
Figure 2.20: Orientation of NH4.....	56
Figure 2.21: Spacer and post interconnection.....	57
Figure 2.22: Barrier strip connection with a spacer.....	57

Figure 2.23: Lower beam interconnection.....	58
Figure 2.24: Lower beam and post interconnection.....	58
Figure 2.25: JSNH4/H2 safety barrier model.....	59
Figure 2.26: Safety barrier JSAM-2/H2.....	62
Figure 2.27: Barrier strip interconnection.....	64
Figure 2.28: Spacer parts interconnection.....	64
Figure 2.29: Barrier strip and distance spacer interconnection.....	65
Figure 2.30: Lower beam of JSAM-2/H2.....	65
Figure 2.31: Lower beam interconnection.....	66
Figure 2.32: Lower beam and post interconnection.....	66
Figure 2.33: JSAM-2/H2 safety barrier model.....	67
Figure 3.1: Simulation process.....	71
Figure 3.2: System's inputs and outputs.....	72
Figure 3.3: Structure of the system.....	72
Figure 3.4: Geometrical model of JSNH4/H2.....	75
Figure 3.5: Geometrical model of JSNH4/H2 - side and top view.....	75
Figure 3.6: Geometrical model of JSAM-2/H2.....	76
Figure 3.7: Geometrical model of JSAM-2/H2 - side and top view.....	76
Figure 3.8: "Imaginary" contact between the upper part of a distance spacer and a sliced part of a post.....	77
Figure 3.9: "Imaginary" contact between a barrier strip and the lower part of a distance spacer.....	77
Figure 3.10: "Imaginary" contact between a barrier strip and a post.....	78
Figure 3.11: JSNH4/H2 meshing.....	80



Figure 3.12: JSNH4/H2 meshing - front and side view.....	80
Figure 3.13: JSAM-2/H2 meshing.....	81
Figure 3.14: JSAM-2/H2 meshing - front and side view.....	81
Figure 3.15: Boundary conditions for JSNH4/H2.....	85
Figure 3.16: Boundary conditions for JSAM-2/H2.....	85
Figure 3.17: JSNH4/H2 in LS-DYNA PrePost.....	87
Figure 3.18: JSAM-2/H2 in LS-DYNA PrePost.....	87
Figure 3.19: S235JR stress-strain curve.....	95
Figure 3.20: S355J0 stress-strain curve.....	97
Figure 3.21: Comparison of S235JR and S355J0.....	98
Figure 3.22: Kinetic energy of a vehicle - JSNH4/H2, TB11.....	104
Figure 3.23: Vehicle velocity - JSNH4/H2, TB11.....	105
Figure 3.24: Safety barrier deformation at time step 0,125 ms - JSNH4/H2, TB11.....	106
Figure 3.25: Numbering individual sliced parts of a barrier strip.....	108
Figure 3.26: Barrier strip displacement in y-direction - JSNH4/H2, TB11.....	108
Figure 3.27: Maximum barrier strip displacement in y- direction - JSNH4/H2, TB11.....	109
Figure 3.28: Barrier strip displacement in z-direction - JSNH4/H2, TB11.....	109
Figure 3.29: Lower beam displacement - JSNH4/H2, TB11.....	110
Figure 3.30: Distance spacer displacement - JSNH4/H2, TB11.....	110
Figure 3.31: Post displacement - JSNH4/H2, TB11.....	111
Figure 3.32: Internal energy - JSNH4/H2, TB11.....	112
Figure 3.33: Vehicle acceleration - JSNH4/H2, TB11.....	113
Figure 3.34: Kinetic energy of a vehicle - JSNH4/H2, TB42.....	114
Figure 3.35: Vehicle velocity - JSNH4/H2, TB42.....	114

Figure 3.36: Barrier strip displacement - JSNH4/H2, TB42.....	115
Figure 3.37: Lower beam displacement - JSNH4/H2, TB42.....	115
Figure 3.38: Distance spacer displacement - JSNH4/H2, TB42.....	116
Figure 3.39: Post displacement - JSNH4/H2, TB42.....	116
Figure 3.40: Internal energy - JSNH4/H2, TB42.....	117
Figure 3.41: Safety barrier deformation at time step 0,250 ms - JSNH4/H2, TB42.....	118
Figure 3.42: Vehicle acceleration - JSNH4/H2, TB42.....	118
Figure 3.43: Kinetic energy - JSNH4/H2, TB51.....	119
Figure 3.44: Vehicle velocity - JSNH4/H2, TB51.....	120
Figure 3.45: Barrier strip displacement - JSNH4/H2, TB51.....	120
Figure 3.46: Lower beam displacement - JSNH4/H2, TB51.....	121
Figure 3.47: Distance spacer displacement - JSNH4/H2, TB51.....	121
Figure 3.48: Post displacement - JSNH4/H2, TB51.....	122
Figure 3.49: Safety barrier deformation at time step 0,160 ms - JSNH4/H2, TB51.....	122
Figure 3.50: Internal energy - JSNH4/H2, TB51.....	123
Figure 3.51: Vehicle acceleration - JSNH4/H2, TB51.....	123
Figure 3.52: Kinetic energy of a vehicle - JSAM-2/H2, TB11.....	124
Figure 3.53: Vehicle velocity - JSAM-2/H2, TB11.....	125
Figure 3.54: Barrier strip displacement - JSAM-2/H2, TB11.....	125
Figure 3.55: Lower beam displacement - JSAM-2/H2, TB11.....	126
Figure 3.56: Distance spacer displacement - JSAM-2/H2, TB11.....	126
Figure 3.57: Post displacement - JSAM-2/H2, TB11.....	127
Figure 3.58: Safety barrier deformation at time step 0,125 ms - JSAM-2/H2, TB11.....	128
Figure 3.59: Internal energy - JSAM-2/H2, TB11.....	128

Figure 3.60: Vehicle acceleration - JSAM-2/H2, TB11.....	129
Figure 3.61: Kinetic energy of a vehicle - JSAM-2/H2, TB42.....	129
Figure 3.62: Vehicle velocity - JSAM-2/H2, TB42.....	130
Figure 3.63: Barrier strip displacement - JSAM-2/H2, TB42.....	130
Figure 3.64: Lower beam displacement - JSAM-2/H2, TB42.....	131
Figure 3.65: Distance spacer displacement - JSAM-2/H2, TB42.....	132
Figure 3.66: Post displacement - JSAM-2/H2, TB42.....	132
Figure 3.67: Safety barrier deformation at time step 0,200 ms- JSAM-2/H2, TB42.....	133
Figure 3.68: Internal energy - JSAM-2/H2, TB42.....	134
Figure 3.69: Vehicle acceleration - JSAM-2/H2, TB42.....	135
Figure 3.70: Kinetic energy of a vehicle - JSAM-2/H2, TB51.....	135
Figure 3.71: Vehicle velocity - JSAM-2/H2, TB51.....	136
Figure 3.72: Barrier strip displacement - JSAM-2/H2, TB51.....	136
Figure 3.73: Lower beam displacement - JSAM-2/H2, TB51.....	137
Figure 3.74: Distance spacer displacement - JSAM-2/H2, TB51.....	137
Figure 3.75: Post displacement - JSAM-2/H2, TB51.....	138
Figure 3.76: Safety barrier deformation at time step 0,160 ms - JSAM-2/H2, TB51.....	139
Figure 3.77: Internal energy - JSAM-2/H2, TB51.....	139
Figure 3.78: Vehicle acceleration - JSAM-2/H2, TB51.....	140

# List of tables

Table 2.1: Design load of „approved“ crash barriers.....	26
Table 2.2: Design load of „other“ crash barriers.....	27
Table 2.3: Comparison of crash test intensity (efficiency) and alternative loads on bridges.....	28
Table 2.4: Safety barrier containment level.....	30
Table 2.5: Minimum threshold levels for the road restraint systems.....	31
Table 2.6: Impact severity levels.....	32
Table 2.7: Levels of normalized working width.....	33
Table 2.8: Levels of normalized vehicle deflection.....	33
Table 2.9: Determining a containment level for road sections according to a risk degree and protection of their environment.....	39
Table 2.10: Determining containment levels for road sections on the basis of road types.....	40
Table 2.11: Containment levels of JSNH4/H2.....	53
Table 2.12: Distance of the front part of a crash barrier from a solid obstacle.....	53
Table 2.13: Basic components of JSNH4/H2.....	59
Table 2.14: Chemical composition of S235JR.....	60
Table 2.15: Mechanical properties of S235JR.....	61
Table 2.16: Chemical composition of S355MC.....	61
Table 2.17: Mechanical properties of S355MC.....	61
Table 2.18: Containment levels of JSAM-2/H2.....	63
Table 2.19: Distance of the front part of a crash barrier JSAM-2/H2 from a solid obstacle.....	63
Table 2.20: Basic components of JSAM-2/H2.....	67

Table 2.21: Chemical composition of S420MC.....	68
Table 2.22: Mechanical properties of S420MC.....	68
Table 2.23: Comparison of JSNH4/H2 and JSAM-2/H2.....	69
Table 3.1: Contact regions.....	78
Table 3.2: Meshing properties for JSNH4/H2 model.....	79
Table 3.3: Meshing properties for JSAM-2/H2 model.....	79
Table 3.4: Parameters of the whole construction - JSNH4/H2.....	82
Table 3.5: Parameters of the whole construction - JSAM-2/H2.....	82
Table 3.6: Properties of separate parts of JSNH4/H2.....	83
Table 3.7: Properties of separate parts of JSAM-2/H2.....	84
Table 3.8: Parameters for tied nodes to surface offset contacts.....	90
Table 3.9: Parameters for automatic single surface contact.....	92
Table 3.10: Plastic deformation of S235JR steel.....	96
Table 3.11: Properties of steel S235JR.....	96
Table 3.12: Plastic deformation of steel S355J0.....	97
Table 3.13: Properties of steel S355J0.....	98
Table 3.14: Parameters for specification of vehicle material type.....	99
Table 3.15: Parameters for ground material specification.....	100
Table 3.16: Material properties for a concrete cap.....	102
Table 3.17: Calculated velocity for different crash tests.....	102
Table 3.18: Comparison of JSNH4/H2 and JSAM-2/H2 - impact forces.....	143
Table 3.19: Comparison of JSNH4/H2 and JSAM-2/H2 - internal energy.....	143